IMPACT OF GENOTYPE AND TOBACCO ADDITIVES ON CLEARANCE OF NNAL, AN IMPORTANT TOBACCO CARCINOGEN

By

SHANNON MARIE JAMES KOZLOVICH

A dissertation submitted in partial fulfillment of
the requirements for the degree of

DOCTOR OF PHILOSOPHY

WASHINGTON STATE UNIVERSITY
College of Pharmacy and Pharmaceutical Sciences

JULY 2019

To the Faculty of Washington State University:

The members of the Committee appointed to examine the dissertation of SHANNON MARIE JAMES KOZLOVICH find it satisfactory and recommend that it be accepted.

Philip Lazarus, Ph.D., Chair

Gang Chen, Ph.D.

Michael Court, Ph.D.

Shobhan Gaddameedhi, Ph.D.

Kathryn Meier, Ph.D.

ACKNOWLEDGMENT

Achieving a doctoral degree is not a solitary act; teamwork, community, and mentorship all have a part to play. There have been joys and losses since I began this academic journey, each of these became a part of who I am and who I am becoming. Spokane Community College was my first foray into the academic field. Dr. Mike Miller and Jaye Hopkins were instrumental in helping me see that becoming a scientist was a possibility for my life. I will be forever grateful for their guidance, mentorship and support as I was just beginning my academic journey. From there I went on to Whitworth University where I was awarded large academic scholarships and was given my first opportunities to work in a research lab; it was also where I first discovered both the power and limitations of student voices on university campuses. The ASPET funded SURF program at WSU Health Sciences, where I was first placed in the lab of Dr. Lazarus, introduced me to the research opportunities available in Spokane. I began my PhD program with a cohort of trainees that quickly formed into a collective of support that carried me through my first couple of years in this program; Panshak, Maha, Sheena, Yadira, and Shamema have been my support, my family, and my rock when I needed them most.

I was raised by a family of strong women activists; raised to question everything (except your mom). I have thrown myself behind causes with passion, voice, and attitude as needed. Never was this truer than when I began to advocate for the desperately needed changes to STEM culture being called for nation-wide. When I was offered a position to serve my campus community as the Director of Legislative Affairs for our student body government I took the opportunity to learn how to effectively push for change with policy makers and develop collaborations with like-minded community organizations. I want to thank Dr. Jim Mohr, Katie Gilsdorf, Pat McQuitty,

and Dr. Daryll DeWald for the support, the time, and the care they all gave to each of the causes Priyanka Bushana (advocacy partner) and I brought to the forefront. Even when we have not seen eye to eye on issues, you were all there to support me with what I wanted to run with.

For most of my degree I was mentored daily by Dr. Gang Chen, who allowed me to talk through troubleshooting experiments and nurtured my scientific curiosity in a way that kept me focused on the goal and the central question of each project. Since I started at WSU as a SURF student Dr. Kay Meier has been a constant supporter and mentor. Thank you for your belief in my abilities, the encouragement at the times I needed it most, and for the award nominations. I want to additionally acknowledge and thank my entire doctoral committee (page ii) as well as Dr. Connie Remsberg and Dr. Grant Trobridge for their mentorship in science communication and developing my scientific presentations.

Dr. Philip Lazarus, none of this could have been possible without you; without your lab and your mentorship. I would not be the scientist I am right now, nor the scientist I will become without your guidance, time, instruction, and high standards. I have a deep appreciation for you. Thank you for your support, for taking a chance on the menthol project, for allowing me the latitude to fail and figure out how to overcome failure.

IMPACT OF GENOTYPE AND TOBACCO ADDITIVES ON CLEARANCE OF NNAL, AN IMPORTANT TOBACCO CARCINOGEN

Abstract

by Shannon Marie James Kozlovich, Ph.D.
Washington State University
July 2019

Chair: Philip Lazarus

Tobacco remains the leading cause of preventable, premature death in adults world-wide. Among the most potent carcinogens in tobacco are the tobacco-specific nitrosamines, with 4-(methylnitrosamino)-1-(3-pyridyl)-1-butanone (NNK) the most potent as well as one of the most abundant. *In vivo* NNK is extensively metabolized to the equally carcinogenic 4-(methylnitrosamino)-1-(3-pyridyl)-1-butanol (NNAL). Of the two NNAL enantiomers, (*S*)-NNAL appears to be more carcinogenic than its (*R*)- counterpart within rodent models. Menthol, which creates mint flavor and scent, is often added to tobacco in both menthol and non-menthol cigarettes and has been shown to decrease the detoxification of NNAL. Due to the differential carcinogenic potential of the NNAL enantiomers, it is increasingly important to identify UGT enzyme targets the specific NNAL enantiomers for glucuronidation, to understand the UGTs involved in tissue-specific NNAL detoxification, and to characterize the mechanism of menthols inhibition of the NNAL detoxification pathway. To examine these, each of the six UGTs (1A4, 1A9, 1A10, 2B7,

2B10, 2B17) known to detoxify racemic NNAL were tested against pure NNAL enantiomers, targeted upper aerodigestive tissues were examined for stereo-selective NNAL-Gluc formation with racemic NNAL as a substrate, and urinary metabolites of NNAL and menthol were analyzed. In a screening of cells expressing individual UGT enzymes, all NNAL glucuronidating UGTs exhibited some level of stereo-specific preference for individual NNAL enantiomers, with UGTs 1A10 and 2B17 forming primarily (*R*)-NNAL-*O*-Gluc. Kinetic analysis indicated that 2B17 exhibited at least a 9-fold lower K_M than UGT1A10. All tissue types preferentially formed (*R*)-NNAL-*O*-Gluc in the presence of racemic-NNAL; only esophagus exhibited any detectable formation of (*S*)-NNAL-*O*-Gluc. Levels of urinary NNAL-*N*-Gluc significantly ($p<0.05$) decreased among subjects with high levels of total urinary menthol, indicating that the presence of menthol could lead to NNAL being retained in the body longer, which could increase the opportunity for NNAL to damage DNA and lead to the development of tobacco-related cancers. These data demonstrate that variations in the expression or activity of specific UGTs may affect the clearance of specific NNAL enantiomers known to induce tobacco-related cancers.

TABLE OF CONTENTS

Page

LIST OF TABLES

Page

CHAPTER ONE

LIST OF FIGURES

Page

LIST OF ABBREVIATIONS

(*R*)-NNAL	(*R*)-4-(methylnitrosamino)-1-(3-pyridyl)-1-butanol
(*R*)-NNAL-*N*-Gluc	(*R*)-4-(methylnitrosamino)-1-(3-pyridyl)-1-butanol *N*- β-D-glucuronide
(*R*)-NNAL-*O*-Gluc	(*R*)-4-(methylnitrosamino)-1-(3-pyridyl)-1-butanol *O*- β-D-glucuronide
(*S*)-NNAL	(*S*)-4-(methylnitrosamino)-1-(3-pyridyl)-1-butanol
(*S*)-NNAL-*N*-Gluc	(*S*)-4-(methylnitrosamino)-1-(3-pyridyl)-1-butanol *N*- β-D-glucuronide
(*S*)-NNAL-*O*-Gluc	(*S*)-4-(methylnitrosamino)-1-(3-pyridyl)-1-butanol *O*- β-D-glucuronide
ACN	acetonitrile
AhR	Ah receptors
AKR	aldo-keto reductase
B[*a*]P	benzo[*a*]pyrene
BCA	bicinchoninic acid
CBR1	carbonyl reductase type 1
CDC	Centers for Disease Control
CHTN	Cooperative Human Tissue Network
COPD	chronic obstructive pulmonary disease
CYP	cytochrome P450
EH	epoxide hydrolase
ENDS	Electronic nicotine delivery systems
ER	endoplasmic reticulum
FBS	fetal bovine serum
FDA	Food and Drug Administration
GRAS	generally regarded as safe
GST	glutathione-S-transferase
HIM	human intestinal microsomes
HLM	human liver microsomes
HS	hydroxymethyl synthase
HSD	hydroxysteroid dehydrogenase
IARC	International Agency for Research on Cancer
IPO	4-ipomeanol
IPTG	isopropyl β-D-1-thiogalactopyranoside
LC	liquid chromatography
LXR	liver X receptor
MeOH	methanol
MG	menthol glucuronide
miRNA	microRNA
MO	monooxygenase

MRM	multiple reaction monitoring mode
MS	mass spectrometer
NAB	N-nitrosoanabasine
NAT	N-nitrosoanatabine
NCTHD	National Conference on Tobacco Health Disparities
NDRI	National Disease Research Institute
NHIS	National Health Interview Survey
NNAL	4-(methylnitrosamino)-1-(3-pyridyl)-1-butanol
NNK	4-(methylnitrosamino)-1-(3-pyridyl)-1-butanone
NNN	N-nitrosonornicotine
NNN-*N*-Gluc	N-nitrosonornicotine glucuronide
NQO1	NADPH quinone oxido-reductase 1
NSDUH	National Survey on Drug Use and Health
PAH	polycyclic aromatic hydrocarbon
PBS	phosphate-buffered saline
PXR	pregnane X receptor
rac-NNAL	racemic NNAL
RPLP0	ribosomal protein lateral stalk subunit P0
S9	9,000 *g* supernatant
SCCS	Southern Community Cohort Study
SLT	smokeless tobacco
SULT	sulfotransferase
TPSAC	Tobacco Product Scientific Advisory Committee
TSNA	tobacco specific nitrosamine
UDPGA	UDP-glucuronic acid
UGT	uridine diphosphate glucuronosyltransferase
WHO	World Health Organization

Dedication

This dissertation is dedicated to

Those who have been an integral part of my journey

My mom, Debbie Kozlovich

My spouse, Justin Parks

My son, Dakota Coon

CHAPTER ONE

INTRODUCTION

Introduction

Tobacco has been linked to lung cancer for over a century,[4] and remains the leading cause of preventable premature death in adults world-wide.[5] In the United States, tobacco smokers have a mortality rate three times higher than individuals who have never smoked.[6] Tobacco smoke contains more than 7000 chemicals, 250 of which are known to be harmful including nearly 70 chemicals known to cause cancer.[7] Many of these chemicals, both carcinogenic and non-carcinogenic, undergo glucuronidation as a part of their metabolic pathway and furthermore, this pathway is often the detoxification step for tobacco carcinogens. Chemicals in tobacco known to cause cancer are frequently referred to as pro-carcinogens, as they go through metabolic activation once they enter the body. Activation pathways tend to be more extensively studied when compared to detoxification pathways, but findings have shown that decreases in glucuronidation are linked to increased tobacco-related cancer risk.

Glucuronidation is a conjugation reaction that is mediated by glucuronosyltransferase (UGT) enzymes. UGT enzymes catalyze the transfer of glucuronic acid moiety to a nucleophilic functional group from a uridine diphosphate glucuronic acid (UDPGA) cofactor. Acceptor functional groups for glucuronidation reactions can be hydroxyl (aliphatic or phenolic), carboxylic acid, amines, thiol groups, and even acidic carbon atoms.[8] The human UGT superfamily of enzymes consists of 21 functional enzymes which are responsible for the glucuronidation of drugs, non-drug xenobiotics, and various endogenous compounds.[1, 9] The UGTs are expressed in all of

the tobacco-related cancer tissues within the body and they play a primary role in the detoxification of many tobacco carcinogens, including polycyclic aromatic hydrocarbons (PAH) and tobacco specific nitrosamines (TSNA) as well as being involved in the clearance of flavor compounds such as menthol.

Tobacco Use

Market Share

Some 19% of the US population (~47.4 million people) used some form of tobacco product in 2017.[10] While the smoking rate in the US has been steadily falling since the Centers for Disease Control and Prevention (CDC) started tracking the adult smoking rate in 1970, US consumers still spend an estimated 100 billion dollars a year on tobacco products. This includes the purchase of 249 billion cigarettes, 11.9 billion large cigars, 0.6 billion small cigars, and 129.4 million pounds of smokeless tobacco.[11-14] Tobacco product descriptions are summarized in Table 1.1. In 2017 there were four companies who controlled 92% of the cigarette market: Philip Morris USA, Reynolds America Inc., ITG Brands, and Liggett.[11, 15] Meanwhile, 98% of the smokeless tobacco market is controlled by three companies: Altria Group Inc. [who purchased the fastest growing electronic cigarette company, JUUL, in 2018], British American Tobacco, and Swedish Match.[14] In addition to domestic tobacco sales, in 2000 US tobacco companies exported 182.5 thousand metric tons of tobacco leaves and 864 billion cigarettes, which is nearly 20% of total cigarettes sold worldwide.[16] To maintain market share and sales levels tobacco companies spent 9.6 billion dollars on US advertising in 2016, roughly 26 million dollars a day or more than 1 million dollars an hour.[14, 15]

Table 1.1. Types of tobacco products available in the US.

Tobacco Product	Description	Related Diseases
Smokeless Tobacco [17, 18]	A type of tobacco that is not burned.	Oral cancer, esophageal cancer, pancreatic cancer, gum disease, heart disease
Cigars (large, little filtered cigars, cigarillos) [17, 19, 20]	Composed of a single type of tobacco that is air-cured and fermented with tobacco leaf wrap	Oral cancer, larynx cancer, esophagus cancer, lung cancer, pancreatic cancer, heart disease, lung disease
Pipe tobacco [17, 21, 22]	Tobacco placed in pipe bowl, not usually inhaled	Lung cancer, oral cancer, larynx cancer, esophageal cancer, throat cancer
Hookah (water pipe) [23-25]	Tobacco smoked is passed through a bowl of water in the hookah device prior to inhalation	Heart disease, stroke, aortic aneurysm, COPD, diabetes, osteoporosis, rheumatoid arthritis, age-related macular degeneration, cataracts, lung infections, cancer: lung, esophagus, larynx oral, and throat
Bidis [17, 26]	Tobacco rolled in a dried tendu tree leaf	Heart attack, oral cancer, throat cancer, larynx cancer, esophageal cancer, and lung cancer
Kreteks [17, 26]	Cigarette made with cloves and tobacco	Lung cancer, lung disease
Cigarettes [7, 27-29]	Tobacco rolled in paper, frequently with a filter	Heart disease, stroke, aortic aneurysm, COPD, diabetes, osteoporosis, rheumatoid arthritis, age-related macular degeneration, cataracts, lung infections, cancer: lung, esophagus, larynx oral, and throat

Smokeless tobacco

The use of smokeless tobacco (SLT) products in the US is far lower than the use of smoked tobacco. SLT refers to products such as chew, snus, dip, and snuff that are used by placing tobacco either between the cheek and gums or into the nasal passages. Users of SLT are at higher risk of various forms of head and neck cancers compared to the non-tobacco using population.[30] SLT still

contains nicotine and leads to nicotine addiction.[7, 30] When youth use SLT products as an entry into nicotine addiction they are more likely to become tobacco smokers.[31] Of the 4.0 million SLT users in the US in 2013-14, 50.6% of them preferred flavored products, and of the flavored product users, a little over 76% of them preferred the menthol flavoring.[32] The prevalence of SLT product use overall in 2016 were 2% higher in high school age youth than in adults with usage at 5.5% and 3.4% of their respective populations. In all tracked categories for race and sex, use of SLT products in 2016 were higher in high school aged youth when compared to adults in the same categories (Figure 1.1), which indicate that SLTs are entry products into nicotine addiction for youth that may lead to the use of other tobacco products in adulthood. Smokeless tobacco use has been increasing since 2005.[7]

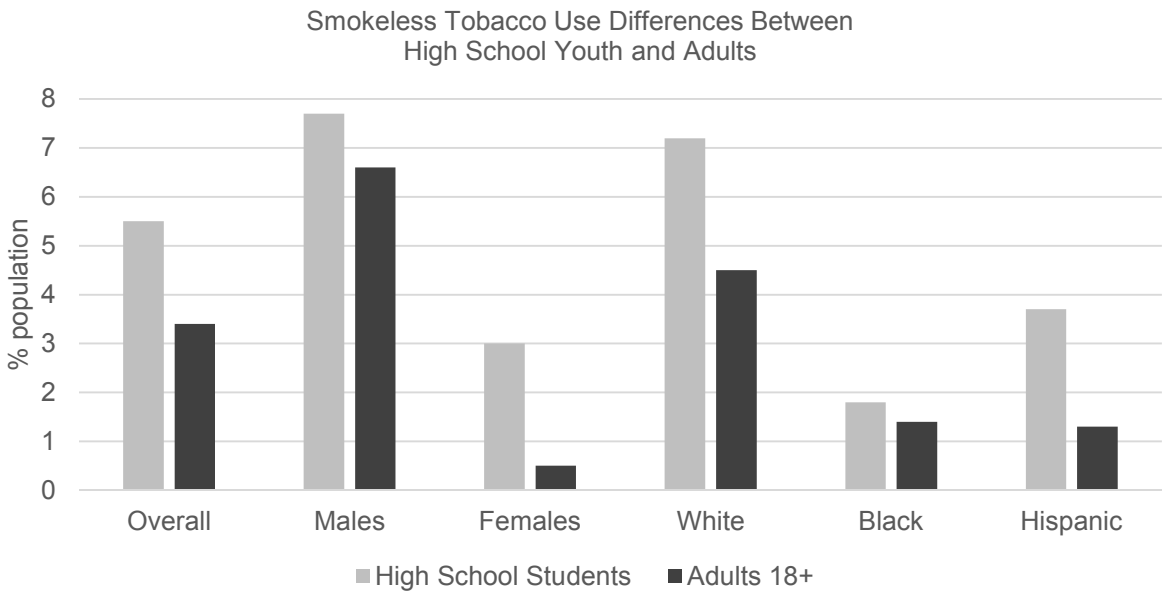

Figure 1.1 Data from the 2014 Surgeon General report titled *Health Consequences of Smoking* reported as % of population surveyed that reported current smokeless tobacco use (defined as use within the last 30 days).

Electronic Nicotine Delivery Systems

Electronic nicotine delivery systems (ENDS) are relatively new to the market, and were newly classified as tobacco products by the US Food and Drug Administration (FDA) in 2016.[33] ENDS describe various types of vaporizers and e-cigarettes which are noncombustible tobacco products. These products heat up a liquid that may or may not contain nicotine to create an aerosol that is inhaled by the user. The use of ENDS have been increasing dramatically since their use started being tracked in 2011; there was a 14.4% increase in 2014-15 alone. The units are sold as disposable or rechargeable vaporizers, during 2014-15 the sale of rechargeable units increased by 5.3% while the sale of the liquid refills increased 307.7%. ENDS have been increasing in popularity among younger users with 3.62 million middle school and high school youth having reported use in 2018, a one year increase of 78% among high school youth and an increase of 48% among middle school youth.[34] In a 2013-14 survey, the most common reason for use of e-cigarettes by youth was reported to be the availability of appealing flavors.[35] A little more than 10 million US adults also use ENDS, with the highest popularity being among young adults 18-24 years old. Adult users also favor the flavored liquids for their ENDS, with 43.9% of users reporting menthol flavoring use and 25.7% reporting either candy, chocolate, or other sweet flavor use.[32]

Cigarettes

The smoking rate has been steadily falling since the CDC began tracking adult tobacco use in the 1970s. The adult smoking rate fell to 14.0% in 2016, the lowest adult smoking rate the US has ever seen.[7] While the smoking rate is relatively low in the US population as a whole, there are disparities in smoking rates between groups of adults based on household income, race, and sex.[10]

For example, men smoke more than women (15.8 and 12.2% respectively), households making less than $35,000 per year have a smoking rate of 21.4% while households that make over $100,000 per year have a smoking rate of 7.6%. In addition, African Americans smoke at a lower rate than Caucasian smokers in the US (14.9 and 15.2% respectively). Smoking rates across the US range from a low of 8.9% in Utah to a high of 26.0% in West Vriginia.[36] While it is well known and documented that these smoking rate disparities exist, little is known about the cause of these disparities. The 2002 National Conference on Tobacco Health Disparities (NCTHD) was held to gather researchers and practitioners to identify key way these disparities can be addressed,[37] but even in this conference the focus was on reducing tobacco use and tobacco-related health disparities rather than identifying the causes of disparities in tobacco use itself.

Menthol is the only flavor of cigarettes currently available on the US tobacco market. Menthol cigarettes make up 35% of the tobacco market[15] with vast racial and age disparities in menthol cigarette use. Around 56% of smokers who were 12-17 years old smoked menthol cigarettes, as well as 45% of 18-25 year olds and up to 34% of adult smokers over the age of 25 smoked menthol cigarettes as well.[38] Racial disparities range from 19.1% of African American to 6.5% of Caucasian Americans who were menthol cigarette smokers in 2010.[39] There were no sex differences reported in 2004-10 National Survey on Drug Use and Health (NSDUH) report for overall menthol cigarette use. The NSDUH report did find that while the use of non-menthol cigarettes fell in each age group reported (12-17, 18-25, and 26+), there were increases in menthol cigarette use among 12-17 year olds (past month menthol use from 7.7 to 8.2%) and 18-25 year olds (from 13.4 to 15.9%). In addition, more than half (51.7%) of those who recently initiated smoking used menthol cigarettes.[39] In 2011 the Tobacco Product Scientific Advisory Committee

(TPSAC) recommended a ban on menthol cigarettes citing that they are an entry product into cigarette use for youth and first time smokers.[40]

Alternative smoked tobacco products

Additional types of smoked tobacco products include cigars, pipe tobacco, hookha, bibis, and kreteks (clove cigarettes). An estimated 4.6% of the population, or 12.3 million people, in the United States reported current cigar use during the 2016 NSDUH.[41] Large cigars typically contain a similar amount of tobacco to a full pack of cigarettes and can take up to 2 hours to smoke, the smoke is not traditionally inhaled. A popular alternative to large cigars are cigarillos which are shorter, ~ 4 inches long, and tend to be a bit narrower. Large cigars and cigarillos combined make up 95% of the cigar market, with little cigars (cigars roughly the size of a cigarette) making up the remaining 5% of the cigar market.[42]

Hookahs are water pipes used to smoke tobacco from the head of the water pipe which contains a bowl with holes in the bottom to draw the tobacco smoke though the water pipe. Hookah smoking is a social activity where the water pipe mouth piece is passed from person to person, or a group smokes from a water pipe with multiple mouth pieces.[24, 43-45] In 2010, the Monitoring the Future survey implemented by the National Institute on Drug Abuse found that 17% and 15% of high school males and females, respectively, had tried a hookah in the last 12 months.[46] A 2012 US Surgeon General report indicated an increase in hookah use among US college students with past year use ranging from 22-40%.[46]

Bidis are tobacco products imported from Southeast Asia. They are tobacco hand rolled in tendu leaves, a tree native to Asia, and can be flavored or unflavored.[47, 48] Kreteks are an imported

clove cigarette from Indonesia that contains a mixture of cloves and tobacco.[49] The 2009 Family Smoking Prevention and Tobacco Control Act passed by the US Congress prohibits the sale of flavored cigarettes in the US, therefore use of flavored bidis and kreteks are no longer tracked by national surveys. Use of unflavored bidis in 2017 was below 1.0% in all age groups surveyed.[50]

Health Impacts of Tobacco

Tobacco-related Diseases

Often, when tobacco is being discussed cancer is the automatic culprit that comes to mind for most people. However, there are many additional disease states that are linked to tobacco use. Tobacco smoking and exposure to tobacco smoke can be linked to around 480,000 premature deaths in the US each year.[7] In addition to the 154,000 deaths from lung cancer, 39% are from heart disease and stroke, 24% are from lung disease, and 1% are from the increased risk for lung infections and aortic aneurysm.[23, 51] Tobacco smoking harms nearly every organ system in the body, diminishes overall health,[7] and leads to a mortality rate in smokers that is 3 times higher than the population that never smoked.[6, 52] Exposure to tobacco of any type has associated disease states. For example, smokeless tobacco have been associated with gum and heart disease,[17, 18] and cigar smoking has been associated with heart and lung disease.[17, 20, 35] A list summarizing some of the major tobacco-related diseases can be found in Table 1.1. In addition to the cancers described below, both cigarette and equally toxic Hookah smoking have been associated with heart disease, stroke, aortic aneurysm, chronic obstructive pulmonary disease (COPD), diabetes, osteoporosis, rheumatoid arthritis, age-related macular degeneration, and cataracts.[7, 23-25, 27, 29, 51] Additionally, smoking may make it harder for a women to get pregnant, and smoking during pregnancy increases

the risk of miscarriage, premature birth, abnormally low birth weight, or having an infant born with a cleft lip or cleft palate.[7]

Tobacco-related Cancers

Tobacco users most frequently get cancer within the tissues with the most frequent and direct exposure to their tobacco product of choice. Combustible tobacco products are more closely associated with lung cancer while smokeless tobacco products placed between the lip and gums are more closely associated with oral cancers.[17] The correlation between tobacco and lung cancer was first published about over a century ago.[4] We now know that 85-90% of all lung cancer cases in the US are directly attributed to tobacco exposure. The relative risk for the development of lung cancer for tobacco smokers is ~20 times higher than the risk for non-smokers.[53] Tobacco-related cancers are caused by the 70 known carcinogens found in tobacco smoke and various tobacco products. Some of the most carcinogenic compounds from tobacco use are: metals such as beryllium, cadmium, and nickel, aromatic amines, arsenic, acetaldehyde, benzene, ethylene oxide, formaldehyde, vinyl chloride, and the 2 classes of compounds with the highest carcinogenic impact and some of the highest concentrations found in tobacco products, PAHs and TSNAs.[7, 51, 54-56]

Health Disparities

The tobacco-related disease health disparities include disparities due to populations with higher tobacco use as well as disparities between groups of smokers who smoke the same numbers of cigarettes per day. During the NCTHD in 2002 health disparities were defined as "differences

in the patterns, prevention, and treatment of tobacco use; the risk, incidence, morbidity, mortality, and burden of tobacco-related illness that exist among specific population groups in the United States; and related differences in capacity and infrastructure, access to resources, and environmental tobacco smoke exposure."[37] At the time this definition was created there were high tobacco-use risk minority groups in the US that were not being tracked in the large national surveys. Questions about sexual minority groups were only added to the CDC National Health Interview Survey (NHIS) in 2013 and, to date, gender minority groups are not being tracked at all.[57] This begs the question: have we defined all existing tobacco-related health disparities yet?

The health disparities between certain racial groups have been well established. Especially when it comes to the higher incidence of lung cancer among African Americans and native Hawaiians when compared to Caucasian and Asian Americans.[58] Similar racial disparities are seen in both oral and throat cancers as well.[59, 60] Interestingly, the groups with the highest rates of tobacco-related cancer are also the racial groups with the highest rates of menthol cigarette smokers.[40] The relationship between menthol and tobacco-related cancers and the possible mechanism of increased risk are discussed in detail in Chapter 3 by addressing the role menthol plays within the detoxification pathway of the TSNAs.

Polycyclic Aromatic Hydrocarbons

PAHs are formed from the incomplete combustion of carbon containing compounds. They are found in any carbon-based material that has been burned, including charbroiled foods and tobacco smoke. There are two mechanisms for the formation of the larger and more toxic PAHs. The first is thermal degradation of organic compounds to form free radicals that recombine to yield

PAHs. The second mechanism involves the cyclization, dehydration, then aromatization of long-chain organic compounds.[61-67] Among tobacco products, PAHs are found in the highest concentrations in tobacco smoke, but low temperature formation of PAHs have been studied and PAHs have been identified in some smokeless tobacco products.[68, 69] While acute, short-term, health effects of PAHs are not well understood, the chronic, long-term, impacts have been well studied.[70] Exposure to PAHs has been linked to an increased risk of epithelial, lung, bladder, and gastrointestinal cancers[71-74] as well as adverse reproductive and developmental effects that have been seen in rodent models.[75] While smoking tobacco during pregnancy has been linked with premature birth as well as low birth weight, these effects have not been directly correlated to PAH exposure in humans thus far.[70] PAHs are classified as pro-carcinogens, meaning that they require metabolic activation to become carcinogenic. Along with activation, PAHs also go through subsequent detoxification and even have some induction effect for specific enzymes. Table 1.2 lists enzymes known to be induced, activate, or detoxify PAHs.

Table 1.2. Enzymes involved in the metabolism of polycyclic aromatic hydrocarbons.

Enzyme	PAH Reaction
CYP1A1	Induced/Activation/Detoxification [76-79]
CYP1A2	Induced/Activation/Detoxification [78-81]
CYP1B1	Induced/Activation [76, 79, 82]
CYP2C9	Activation/Detoxification [79]
CYP2C19	Activation/Detoxification [79]
CYP2E1	Activation/Detoxification [77, 78]
CYP2F1	Activation/Detoxification [77]
CYP3A4	Induced/Activation [79, 83, 84]

Enzyme	PAH Reaction
CYP3A5	Activation [83, 84]
MO	Activation [85-87]
NQO1	Induced/Activation [77, 88-90]
AKR1A1	Activation [80, 91, 92]
AKR1B10	Activation [93]
AKR1C1	Induced/Activation [88, 91, 92, 94]
AKR1C2	Induced/Activation [88, 91, 92, 94]
AKR1C3	Induced [88]
AKR1C4	Activation [91, 92, 95]
HS	Activation [86]
EH	Activation/Detoxification [78]
GSTM	Detoxification [79, 96]
GSTM1	Induced/Detoxification [79, 97, 98]
GSTM3	Induced [79, 96]
GSTP1	Induced [79, 96, 98]
GSTT1	Induced [79, 96]
SULT1A1	Detoxification [99]
SULT1A2	Detoxification [99]
SULT1A3	Detoxification [99]
SULT1B1	Detoxification [99]
AhR	Induced [82]
LXR	Down regulated [96, 100]
PXR	Induced [101]
UGT1A1	Detoxification [102, 103]
UGT1A3	Detoxification [103]
UGT1A7	Detoxification [102, 104, 105]
UGT1A8	Detoxification [102, 106]
UGT1A9	Detoxification [102]

Enzyme	PAH Reaction
UGT1A10	Detoxification [102, 106]
UGT2B7	Detoxification [102, 107]
UGT2B11	Detoxification [107]

Induction

Induction refers to PAHs having been found to be the causal agent for increased production of specific enzymes. This can be beneficial, like how PAHs have been shown to induce certain enzymes within the glutathione-S-transferase (GST) family which are known to detoxify many endogenous compounds.[77, 89] Or induction can be harmful similar to the way PAHs have been shown to increase levels of some cytochrome P450 (CYP) enzymes known to metabolize PAHs into carcinogens in a process referred to as metabolic activation. A complete list of induction activity by PAHs is included in Table 1.2.

Some of the more problematic induction activates of PAHs are the ones that include induction of the CYP enzymes. For example, CYPs 1A1 and 1A2 have been shown to increase in expression with exposure to PAHs;[77, 82, 85] as discussed further below, these enzymes are also known to metabolize PAHs into toxic metabolites. The mechanism of induction was discovered with research into the induction of CYP3A4. It was shown that the Ah receptors (AhR) play a critical role in the induction of CYPs 1A1 and 1B1, and that PHAs have an effect on these receptors[108, 109] as well as the pregnane X receptor (PXR) that regulates CYP3A4 expression.[101] Differential expression of CYP1A1 and 1B1 have been linked to differential susceptibility of adverse actions of PAHs, including colorectal cancer.[78] In addition, CYPs have been shown to

down regulate the liver X receptor (LXR) involved in the GST pathway,[96, 100] as discussed further below, GST enzymes detoxify PAHs.

PAH Activation

The biological activity and levels of genotoxicity of PAHs are related to their structural features. The greatest levels of genotoxicity come from PAHs with condensed aromatic ring structures that form either a "bay" or "fjord" region (Figure 1.2). PAHs with "fjord" regions are less planar and more likely to preferentially bind to adenine nucleotides on DNA, while those with "bay" regions are planar and more likely to bind to guanine nucleotides. PAH genotoxicity decreases as the planar form decreases, thus compounds with both "fjord" and "bay" regions are genotoxic, but "bay" region compounds exhibit stronger genotoxicity.[110-112] While PAHs can bind to DNA through the electron dense "fjord" and "bay" regions, they primarily require metabolic activation to become more potent carcinogens. The most potent of them are the diol epoxide metabolites, which are mutagens that impact cell replication when they interact with DNA.[113-116] One potential mechanism of PAH carcinogenesis is the covalent binding of benzo[*a*]pyrene (B[*a*]P) diol epoxide to guanine (Figure 1.3), when this occurs at sites critical to cell differentiation and growth the cell can become cancerous.[102, 106, 107, 117-119] PAH activation can occur through the CYP,[77-79, 82, 84, 120] monooxygenase (MO),[85-87]

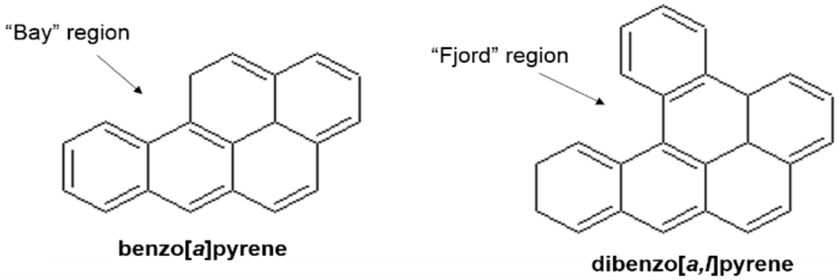

Figure 1.2. PAH confirmations that form the "Bay" and "Fjord" regions.

NADPH quinone oxido-reductase 1 (NQO1),[77, 88-90] hydroxymethyl synthase (HS),[86] and aldo-keto reductase (AKR)[80, 88, 91-95] pathways, with epoxide hydrolase (EH)[78] enzymes mediating a step in both the activation and detoxification pathways.

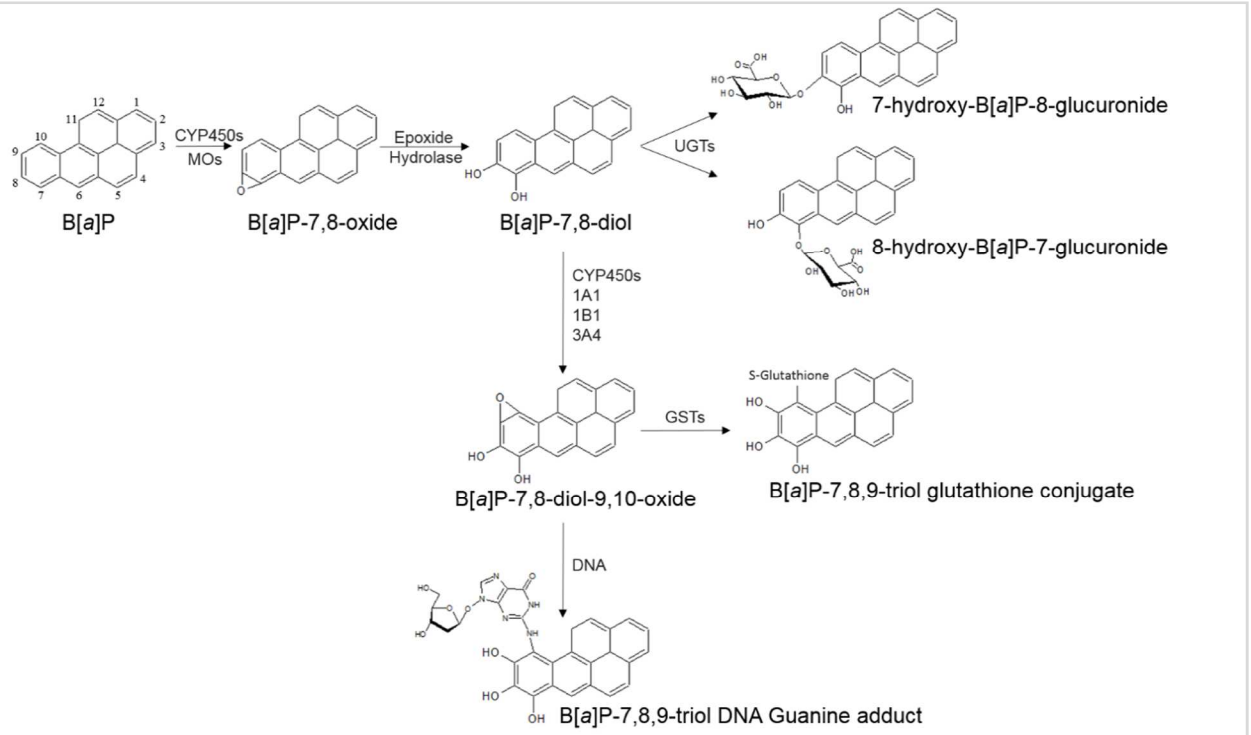

Figure 1.3. Schematic of benzo[a]pyrene (B[*a*]P) metabolism with known enzymes involved with each reaction.

PAH Detoxification

PAHs are most readily cleared from the body after oxidation and conjugation reactions. Some CYPs are necessary for the oxidation step of detoxification, but those same enzymes are also responsible for the subsequent oxidation that leads to the formation of DNA adducts. The final detoxification steps are most commonly conjugation reactions, primarily mediated by UGT,[102-107, 119] GST,[79, 97, 98, 121-123] and sulfotransferase (SULT)[124] enzymes. These enzymes transfer large polar

compounds to the alcohol groups on PAHs to make them more polar for excretion. Examples of UGT and GST detoxification products can be found in Figure 1.3.

PAHs can be oxidized by CYPs to add a single alcohol group or an epoxide group at any outer carbon, represented by numbers on the B[*a*]P compound in Figure 1.3. UGTs transfer glucuronic acid (Gluc) from UDPGA to the oxygen in an alcohol group on an oxidized PAH. GST enzymes add an S-glutathione to these same alcohol groups and genetic variations in these enzymes have been linked to increased risk factors for tobacco-related cancers.[79, 96] SULTs mediate sulfate conjugation to alcohol groups, this activity was identified to occur with PAHs *in vitro* but the corresponding conjugates have not been identified *in vivo*.[99]

Tobacco Specific Nitrosamines

TSNAs are an important class of carcinogens present in both tobacco smoke and smokeless tobacco products.[125-128] This class of carcinogens includes two compounds classified as group 1 carcinogens by the International Agency for Research on Cancer (IARC),[129] 4-(methylnitrosamino)-1-(3-pyridyl)-1-butanone (NNK) and N-nitrosonornicotine (NNN). In addition, the FDA lists both NNK and NNN as carcinogens.[130] The World Health Organization (WHO) has listed both of these compounds in proposed regulations aimed at lowering toxicants in cigarette smoke.[131]

TSNA Formation

Most TSNAs are formed from the nitrosation of alkaloids found in tobacco and they are formed at the highest concentrations during the tobacco curing process.[132] The TSNA class of compounds is comprised of 6 compounds, the group 1 carcinogens NNK, NNN, and the (*R*)- and (*S*)- enantiomers of 4-(methylnitrosamino)-1-(3-pyridyl)-1-butanol (NNAL) as well as N-nitrosoanatabine (NAT) and N-nitrosoanabasine (NAB) which are thought to have weaker carcinogenicity than NNK, NNAL, and NNN.[30] As shown in Figure 1.4 during the curing process NNK is formed from nicotine, NNN is formed from nornicotine, NAT is formed from anatabine, and NAB is formed from anabasine. Formation of these products correlate to the levels of the alkaloids found in tobacco. Tobacco with higher levels of alkaloids tend to have higher levels of TSNAs as well, with TSNA levels in the order of NNN>NNK>NAT>NAB.[30, 128] Different curing methods form TSNAs at different rates with flue-cured tobacco having lower TSNA levels than air-cured tobacco.[132]

Unlike the other TSNAs, both (*R*)- and (*S*)-NNAL are metabolites of NNK which are formed after exposure to NNK by carbonyl reduction.[133-135] Both NNAL enantiomers, like NNK,

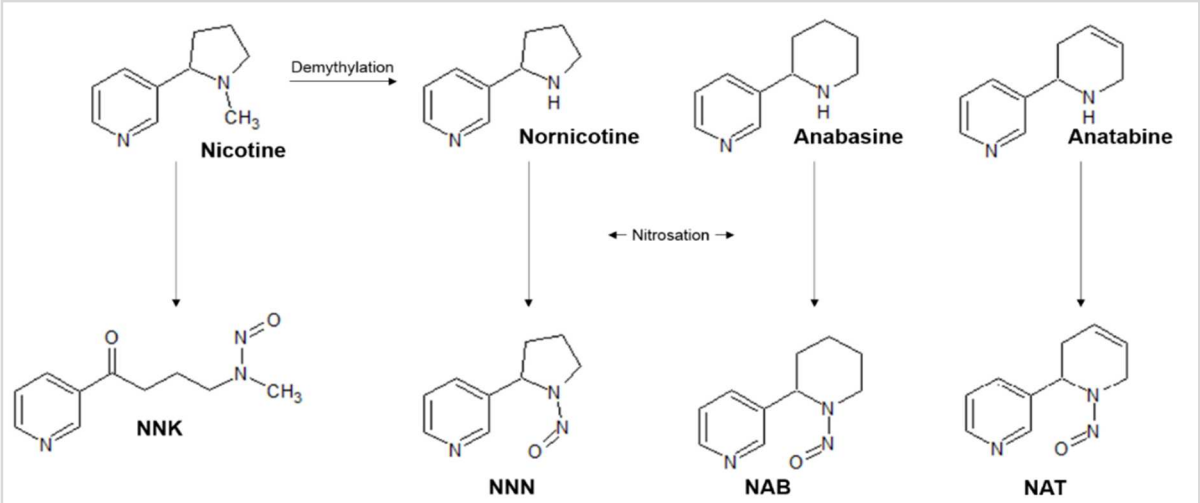

Figure 1.4. Schematic of TSNA formation during the tobacco curing process.

are very potent carcinogens in rodents.[136-139] By measuring NNK in mainstream smoke and urinary NNAL in smokers, it was estimated that 39-100% of NNK was converted to NNAL systemically in smokers.[140] NNK exposure in smokeless tobacco users was measured in saliva and it was estimated that 14-17% of NNK was converted to NNAL within the oral cavity.[141] Additionally, it has been shown that NNAL comprised 82-92% of total NNK metabolites in human lung tissue.[139] The differences in % reduction of NNK to NNAL could be due to differences in reduction enzyme expression between different tissues. There are 7 enzymes known to metabolize NNK to NNAL; hydroxysteroid dehydrogenase (HSD) 11β1 and 17β12, carbonyl reductase type 1 (CBR1), and AKRs 1C1, 1C2, 1C4, and 1B10.[142-145] (*R)*-NNAL is preferentially formed by HSD17β12, while the remaining enzymes primarily form (*S*)-NNAL.[145] Like NNK, both the (*R*)- and (*S*)-enantiomers of NNAL[133-135] are very potent carcinogens in rodents with (*S*)-NNAL exhibiting higher carcinogenic potential than (*R*)-NNAL.[136-139]

A recent publication took a closer look at the reduction of NNK to NNAL directly in human lung tissue.[145] The tissue was homogenized and separated into different fractions, the cytosolic fraction, which contains all soluble enzymes, and the microsomal fraction that contains all enzymes bound to the endoplasmic reticulum. Reduction assays with the different tissue fractions indicated that (*S*)-NNAL is the primary NNAL enantiomer formed in the cytosolic fraction while (*R*)-NNAL is the primary enantiomer formed in human lung microsomes. When the experiment was repeated with human liver tissue, the cytosol had similar activity to lung tissue but the microsomal fraction of liver formed both (*R*)- and (*S*)-NNAL.[145] The differences in tissue specific formation of these enantiomers is important because the major NNAL detoxification enzymes, UGTs, are found in the endoplasmic reticulum, and are not present in cytosol.[146] Tissue-specific detoxification is discussed in depth in Chapter 3.

TSNA metabolism

The full activation and detoxification pathway of NNK is shown in Figure 1.5. TSNAs including NNK are primarily metabolized by CYPs and UGTs. CYPs 2A6 and 2A13 are the enzymes primarily responsible for the α-hydroxylation, also known as activation, pathways of NNK, NNAL, and to a lesser extent NNN.[136, 147, 148] The CYP activation pathway leads to bi-products responsible for the formation of various DNA adducts (Figure 1.5) and are understood to be the causal mechanism for many tobacco-related cancers.[136, 147, 148] The byproducts formed from the α-hydroxylation of NNK to the keto acid (**12**) and from NNAL to the hydroxyl acid (**14**) are known to produce methane diazohydroxide that methylates DNA, a significant contributor to NNK and NNAL carcinogenicity.[136]

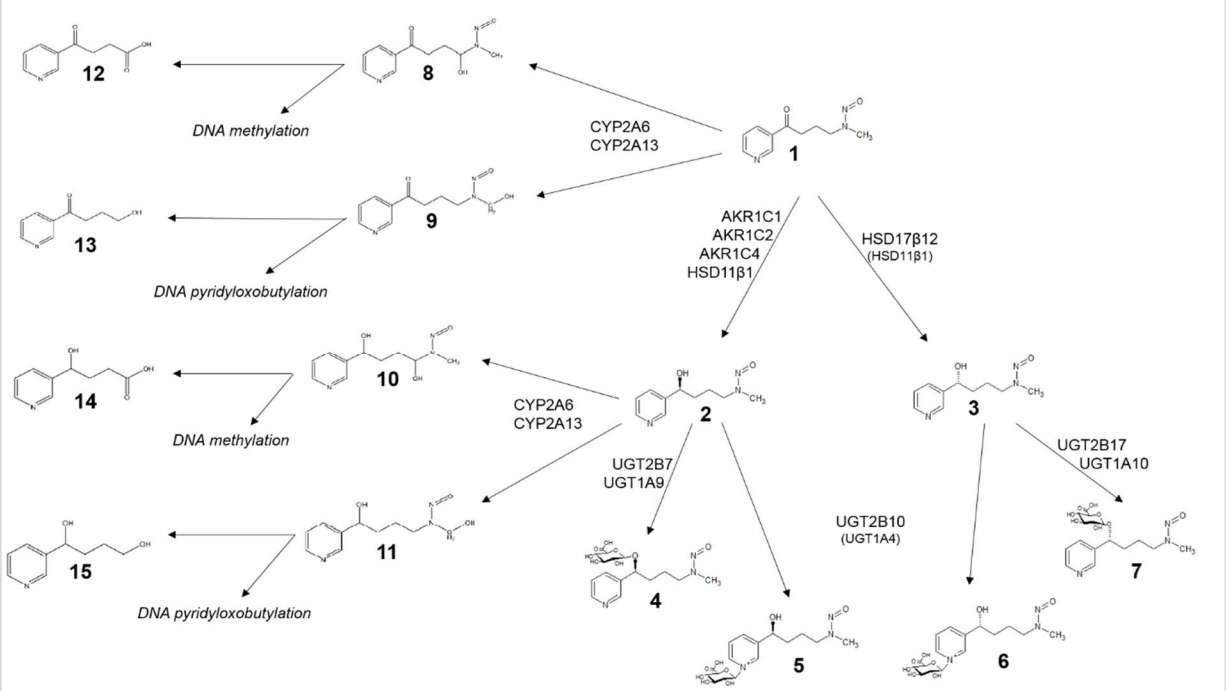

Figure 1.5. Schematic of NNK (1) metabolism. NNK reduction to (S)-NNAL (**2**) and (R)-NNAL (**3**). NNAL glucuronidation to (S)-NNAL-O-Gluc (**4**), (S)-NNAL-N-Gluc (**5**), (R)-NNAL-N-Gluc (**6**), and (R)-NNAL-O-Gluc (**7**). NNK and NNAL α-hydroxylation to α-methylhydroxy-NNK (**8**), α-hydroxymethyl-NNK (**9**), α-methylenehydroxy-NNAL (**10**), α-hydroxymethyl-NNAL (**11**), keto acid (**12**), keto alcohol (**13**), hydroxyl acid (**14**), and diol (**15**). Enzymes in parentheses are minor contributors to the listed pathway.

While low levels of NNK- and NNAL-*N*-oxides were identified in rodents,[149] studies in humans have not been able to identify NNK-*N*-oxide in the urine of smokers or smokeless tobacco users.[150] NNAL-*N*-oxide has been identified in the urine of both smokers and smokeless tobacco users as a minor metabolite[150] and is considered to be a detoxification product due to its carcinogenicity being 1/10th that observed for NNK in rodents.[149] It has been proposed that the NNAL-*N*-oxide is mediated by CYPs, but to date, the exact enzymes involved in NNAL-*N*-oxide formation have not been identified.[136]

While NNK glucuronides have not been identified in biological assays, the glucuronidation of NNAL is considered to be an important mechanism for NNK detoxification.[126, 136, 140, 151-158] This is assumed to be due to the rapid metabolism of NNK either by reduction to NNAL or by α-hydroxylation as described previously. NNN, on the other hand, is glucuronidated directly to NNN glucuronide (NNN-Gluc). NNAL can be glucuronidated at the chiral alcohol (*O*-Gluc) or at the nitrogen within the pyridine ring (*N*-Gluc). NNAL has a chiral center; therefore, there are 4 glucuronide products that can be formed for NNAL; (*R*)-NNAL-*O*-Gluc, (*S*)-NNAL-*O*-Gluc, (*R*)-NNAL-*N*-Gluc, (*S*)-NNAL-*N*-Gluc. Each of the NNK metabolites have been identified in smoker's urine directly, with NNAL-*N*-Gluc [(*R*)-NNAL-*N*-Gluc + (*S*)-NNAL-*N*-Gluc], NNAL-*O*-Gluc [(*R*)-NNAL-*O*-Gluc + (*S*)-NNAL-*O*-Gluc], and free NNAL accounting for 22-23%, 48-50%, and 27-31% of urinary NNK metabolites, respectively.[3, 159]

In contrast, NNN has a single glucuronidation site on the nitrogen within the pyridine ring to form NNN-*N*-Gluc. Urinary NNN-*N*-Gluc concentrations are often too low for direct detection but can be quantified after incubation with sodium hydroxide. This reaction cleaves the glucuronide from NNN with a hydrolysis reaction, where levels of NNN are measured before and

after the reaction; NNN-*N*-Gluc comprises ~50% of the total NNN measured in smokers. The levels of total urinary NNAL (free NNAL + all NNAL-Glucs) have been shown to be ~10 fold higher than total NNN levels in the urine of smokers.[160] Decreases in NNAL-*O*-Gluc formation have been linked to lung cancer risk,[161] while decreases in NNN-*N*-Gluc formation have been linked to esophageal incidents.[160] Tissue-specific differences in cancer risk between TSNAs could be linked to difference in enzyme expression between tissues. As both NNAL and NNN are activated and detoxified by some of the same enzymes, it is likely that the driver of tissue-specific cancer susceptibility is driven by differences in the expression and/or activity of these enzymes. This topic is further explored in Chapters 2 and 3.

In contrast to the relatively high tumorigenicity exhibited by both (*R*)- and (*S*)-NNAL, NNAL-Gluc is non-tumorigenic after subcutaneous injection into A/J mice.[162] It has been shown that NNAL glucuronides are formed extensively in human liver microsomes (HLM) Studies indicate that (*S*)-NNAL may be stereo-selectively retained in smokeless tobacco users[163] yet it exhibits a higher rate of glucuronidation in the patas monkey.[151]

Uridine Diphosphate Glucuronosyltransferase

UGTs catalyze the glucuronidation of many endogenous and xenobiotic compounds and are found to be expressed in both the plant and animal kingdoms.[164] These enzymes are considered to be an important mechanism in removing many hazardous compounds from the body including endogenous compounds like bilirubin and catecholamines as well as environmental toxins like PAHs and TSNAs.

UGT genes

The human UGT superfamily of enzymes is split into four branches, UGT1, UGT2, UGT3, and UGT8. Of the 22 enzymes within the 4 UGT branches of the family tree, the UGT1A and UGT2 have been the most extensively studied (Figure 1.6). The *UGT1A* gene complex is located on chromosome 2q37 and they share an identical C-terminal coding sequence comprised of common exons 2-5.[165] The N-terminus, which translates to ~246 amino acids, share 24-49%

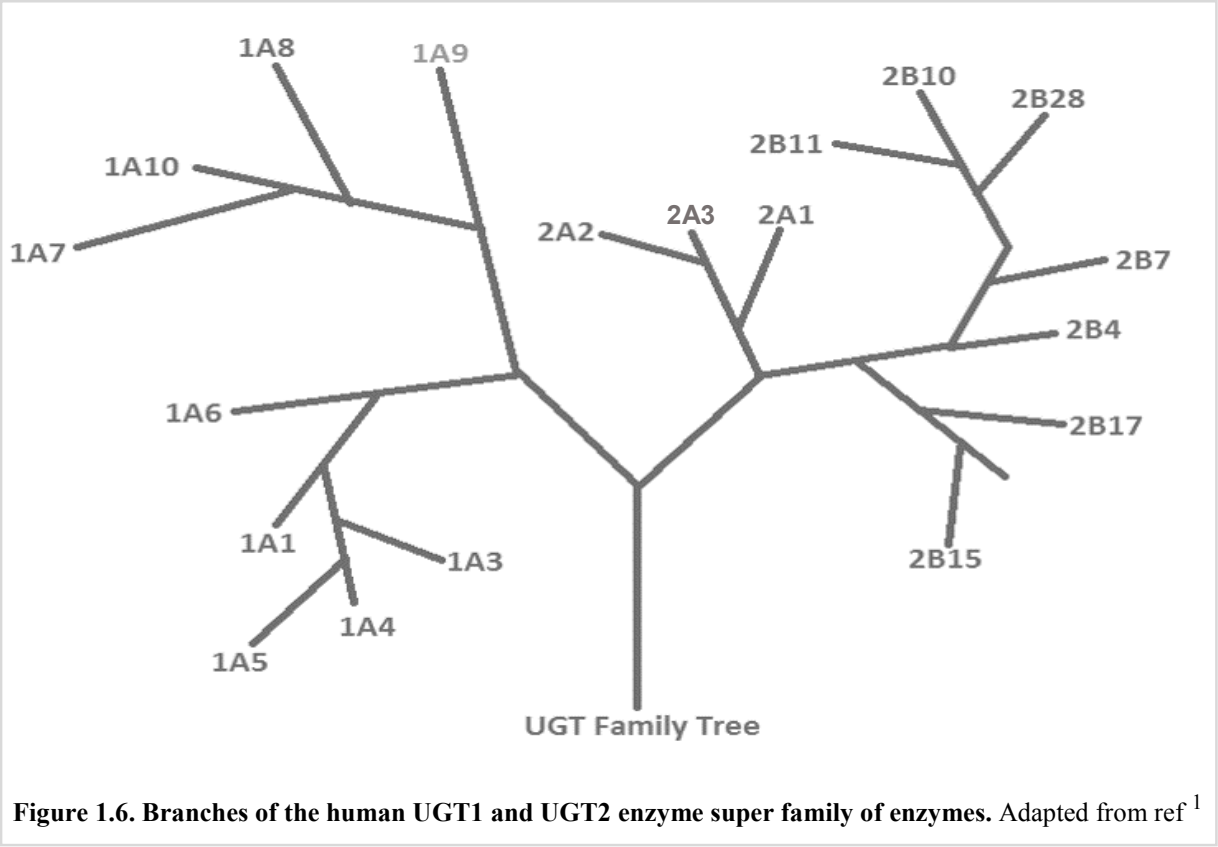

Figure 1.6. Branches of the human UGT1 and UGT2 enzyme super family of enzymes. Adapted from ref [1]

sequence homology and are made up of a unique first exon for each enzyme.[164, 166] The UGT2 branch of the UGT family tree is split into UGT2A and UGT2B enzymes based on both evolutionary divergence and sequence homology.[1] The *UGT2* genes are located on chromosome 4q13. While the UGT2B enzymes are coded by 6 unshared exons, the UGT2A enzymes arose from differential splicing of an individual first exon to 5 shared exons similar to the UGT1A enzymes.[1]

UGT enzyme structure and function

UGTs are membrane bound proteins that are anchored to the endoplasmic reticulum (ER) with the active site on the luminal side of the ER membrane. These phase II enzymes are frequently the rate limiting step in the clearance of endogenous and xenobiotic compounds from the body. Difficulty in crystalizing membrane proteins has led to a lack of a full crystal structure for mammalian UGT enzymes.[167] The UGTs in the UGT1 and UGT2 human UGT family are comprised of approximately 530 amino acids that includes a conserved region for the binding of the UDPGA common cofactor.[168] Additionally, a dimerization motif has been identified in many UGT isoforms. UGTs have been known to form both homo- and hetero-dimers.[169-171] While it has not yet been determined if dimerization is required for UGT activity,[172] dimerization has been shown to have the ability to regulate UGT activity, discussed in further detail below.

Most of the UGT isoforms are fairly promiscuous enzymes, this family of enzymes has few examples of isoform specific substrates and each isoform has activity against a range of substrates. The best example of substrate specificity is UGT1A1[173]: while bilirubin glucuronidation is specific to this UGT, UGT1A1 is able to interact with many other bulky molecules and some small planar molecules as well (e.g. the simple PAH 1-naphthol)[174, 175] Additional isoform-specific substrates have been identified: sipoglitazar is considered specific for UGT2B15,[176] propofol is considered to be a specific substrate for UGT1A9 in liver,[177] and serotonin has been used as a specific substrate for UGT1A6.[178] Unlike bilirubin, all of these additional "specific" substrates have other UGT isoforms known to have activity against them, but at a much lower rate. UGT1A4 and UGT2B10 have a tendency for higher rates of formation for substrates with tertiary amines or pyridine rings indicating a preference of activity towards these

functional groups.[179-182] The UGT2B enzymes are known to be important in the metabolism of many hormones and other endogenous compounds.[183] Overall, most UGT isoforms exhibit activity for a broad range of substrates with some functional group specificity.

The UGT3A and UGT8 all use alternative co-substrates in their conjugation reactions. Instead of using UDPGA as the UGT1 and UGT2 families do, UGT3A1 uses N-acetylglucosamine,[184] UGT3A2 uses uridine diphosphate glucose and xylose,[185, 186] and UGT8 uses uridine diphosphate galactose.[187, 188] Sugar selectivity of the UGT3A family has been attributed to a single amino acid difference in the usually conserved co-substrate binding region.[185] The UGT3A and UGT8 enzymes are each coded by unique genes and share ~40% overall homology with UGT1As.[184] UGT8 in particular, is unlike other UGTs in that, rather than playing a role in metabolism, UGT8 mediates a key synthesis step within the nervous systems. This UGT isoform mediates the transfer of galactose to ceramide which is a key step in the biosynthesis of galactoceredrosides.[187, 188] These compounds are abundant in the sphingolipids of the myelin sheathes of the central and peripheral nervous systems. Changes in levels of galactoceredrosides have been associated with several neurodegenerative and autoimmune disorders.[189, 190]

UGT Stereospecificity

Many endogenous and xenobiotic UGT substrates contain chiral centers. Differential and stereospecific metabolism has been identified in a few UGT isoforms. While specifics on stereo-selective glucuronidation of tobacco carcinogens is extensively covered in Chapter 2, stereo-selectivity is not isolated to tobacco carcinogens. UGT2B7 has a stereo-preference for the formation of α estrogen metabolites while UGT1A10 activity is decreased and UGT2B17 activity

is not detectable when comparing α to β estrogen metabolites.[191-193] Interestingly, UGT1A3 stereoselective activity for the α vs. β estrogen metabolites and was additionally region-specific to the location of the α or β alcohol functional group within the molecule.[193] One of the first publications to identify stereospecific glucuronidation of a pharmaceutical drug was a study on the clearance of an anxiolytic drug, (*R*,*S*)-oxazepam. Kinetic analysis of glucuronidation activity with individual UGTs indicated stereospecific clearance of S- and R-oxazepam by UGT2B15 and UGT1A9 respectively.[194] Prominent stereospecific clearance of ornidazole, an anti-microbial agent, was observed with UGT1A9 forming the (*R*)-isoform glucuronide and UGT2B7 forming the (*S*)-isoform glucuronide.[195] Analysis of stereoselective clearance of drugs by specific UGTs aides in the development of therapies designed to remain in the body longer, by identifying the stereo confirmation of the drug that will avoid clearance by specific UGTs. Additionally, stereospecific inhibition has been accessed for specific UGT isoforms to determine possible drug-drug or drug-herb interactions. One study examined the differential inhibition by (*R*)- and (*S*)-isomers of ginsenoside, found in ginseng, and observed that the strongest stereoselective inhibition for many of the ginsenoside compounds was observed for UGT1A8, indicating a strong possibility for interactions with drugs metabolized by UGT1A8.[196]

Tissue Expression of UGTs

In humans, UGTs have been found to be expressed in all human tissue types. Yet, each tissue type exhibits tissue-specific expression of each UGT isoform and each tissue type has varying levels of UGT expression. These enzymes have been identified in metabolic tissues such as the liver and kidneys, but have also been identified in the areodigestive tract, sex organs, brain, and skin. Liver, the main metabolic organ, expresses 12 of the human UGTs (UGTs 1A1,

1A3, 1A4, 1A6, 1A9, 2A3, 2B4, 2B7, 2B10, 2B11, 2B15, 2B17, and 2B28) at higher expression levels than other tissues.[197-199] UGT2A1 and UGT3A1, while expressed in the liver, are higher expressed in the lung and kidney respectively.[184, 200, 201]

Table 1.3. UGT expression in metabolic and tobacco-related cancer tissues.

Tissue Types	UGTs
Metabolism and Excretion Tissues	
Liver [197, 199, 202-213]	1A1, 1A3, 1A4, 1A5, 1A6, 1A7, 1A9, 1A10, 2A1, 2A3, 2B4, 2B7, 2B10, 2B11, 2B15, 2B17, 2B28, 3A1
Stomach [184, 197, 199, 203-205, 212, 214]	1A1, 1A3, 1A4, 1A5, 1A6, 1A7, 1A9, 1A10, 2B7, 2B11, 2B15, 2B17, 2B28, 3A1
Intestine [197, 199, 203-206, 209, 212, 213, 215-218]	1A1, 1A3, 1A4, 1A5, 1A6, 1A7, 1A8, 1A9, 1A10, 2A3, 2B7, 2B15, 2B17
Colon [184, 197, 199, 203-205, 212, 215, 216, 219, 220]	1A1, 1A3, 1A4, 1A5, 1A6, 1A7, 1A8, 1A9; 1A10, 2A1, 2A3, 2B4, 2B7, 2B11, 2B15, 2B17, 3A1
Kidney [184, 197, 199, 203-207, 209, 212, 213]	1A1, 1A3, 1A4, 1A5, 1A6, 1A7, 1A8, 1A9, 1A10, 2A2, 2A3, 2B4, 2B7, 2B11, 2B15, 2B17, 3A1, 3A2
Bladder [197, 212, 221]	1A1, 1A3, 1A4, 1A5, 1A6, 1A7, 1A8, 1A9, 1A10, 2B4, 2B7, 2B10, 2B11, 2B15, 2B28
Tobacco-related Cancer Tissues	
Lung [197, 199-203, 205, 207, 208, 212, 219, 222, 223]	1A3, 1A5, 1A6; 1A10, 2A1; 2A3, 2B4, 2B7, 2B10, 2B11, 2B15, 2B17
Larynx [202, 208, 212, 215, 219]	1A6, 1A7, 1A8, 1A10, 2A1, 2A2, 2A3, 2B4, 2B10, 2B11, 2B15, 2B17
Esophagus [102, 199, 202, 208, 215]	1A6, 1A7, 1A8, 1A9, 1A10, 2B4, 2B7, 2B10, 2B11, 2B15, 2B17
Oral cavity [202, 203, 205, 208, 215]	1A1, 1A3, 1A4, 1A5, 1A6, 1A7, 1A10, 2B4, 2B10, 2B11, 2B15, 2B17, 2B28
Tonsil [202, 208, 212, 219]	1A6, 1A7, 1A10, 2A1, 2A3, 2B4, 2B10, 2B11, 2B15, 2B17
Tongue [202, 208]	1A6, 1A7, 1A10, 2B4, 2B10, 2B11, 2B17

Extra-hepatic tissues tend to express fewer UGT isoforms and those that are expressed tend to be expressed at lower levels relative to their expression in liver.[208] UGT1A7, once thought to be a stomach specific UGT isoform,[214, 224] had been detected in the intestine, colon, and bladder along with UGTs 1A6, 1A8, and 1A10.[197, 206, 215, 216, 218, 220, 225] The UGT2As had expression of 2A1 and 2A2 in nasal tissue and 2A1 and 2A3 have been detected in lung tissue.[205, 226] UGT1A1

has been shown to exhibit expression in a wide range of tissues including tissues of the aerodigestive tract, sex organs, muscle, and bone marrow. [197, 200, 205, 209, 227] UGT2B28 has only been shown to be expressed in liver, salivary glands, breast, and bladder. [197, 205, 227] The expression of extra-hepatic UGTs has tended to be analyzed in small sample batches, and it is often the case that there are different UGTs detected from one publication to another. UGTs that have been detected in metabolic tissues, excretion tissues, and tobacco-related cancer target tissues are listed in Table 1.3.[197, 202, 205, 208]

Of particular interest to the studies in this dissertation were the extra hepatic UGT1 and UGT2 enzymes expressed in tobacco-related cancer target tissues. Variations in expression of UGTs within each of these tissues as well as variations in expression between tissues directly exposed to tobacco products could be the driving indication of tissue susceptibility to tobacco-related cancers. Tissue expression and activity of UGTs within upper areodigestive tract are discussed in depth Chapter 3.

UGT Regulation

Poor correlations have been observed for some UGTs between mRNA levels and protein levels, particularly for UGTs 1A4, 1A6, and 2B7.[198] Additionally, as outlined in the previous section, difference in tissue specific UGT expression can vary widely between studies as well as between individuals within the same study. These differences may be attributed to various UGT regulatory mechanisms including alternative splicing, dimerization, pseudogenes, and microRNA (miRNA). Each of these regulatory mechanisms have been shown to alter UGT protein levels and/or function.

UGT splice variants are alternatively spliced exons that can form functional enzymes as with the UGT1A enzymes, or it can create a variety of non-functional variants. This occurs when exons are deleted or replaced and can even occur when intron regions are spliced into enzyme transcripts. It has been estimated that roughly 95% of multi exon genes have well expressed splice variants.[228] Several studies have found that UGT splice variants contain the UGT dimerization motif or a similar enough amino acid sequence to dimerize with functional UGTs and alter the protein activity.[229, 230]

In addition to UGT dimerization with non-functional splice variants, dimerization between functional UGTs has also been shown to impact UGT activity. The proposed dimerization motif region (figure 1.7) has both conserved and non-conserved regions that would allow for differential binding potentials between different UGT isoforms where some isoforms may be more likely to dimerize.[2, 166] Interestingly, even in the conserved region of the dimerization motif there are a couple of UGTs (1A3-6) that all have the same amino acid modification. [2] UGT dimerization can occur as a homodimer, where the same UGT isoforms dimerize, or as heterodimers, where 2 different UGT isoforms dimerize. Dimerization can cause an increase of activity, as indicated by the 33% increase in UGT2B7 glucuronidation activity for estriol when UGT2B7 is dimerized with UGT1A6 when compared to UGT2B7 alone.[231] This effect was shown to be even stronger for serotonin, where the glucuronidation activity was 4

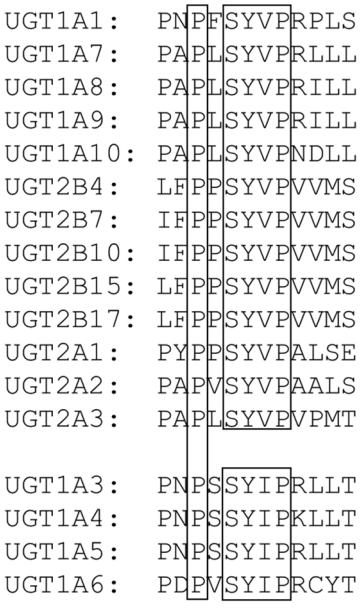

Figure 1.7. Proposed dimerization motif of UGTs 1A, 2B and 2A. The amino acid sequence is contained within exon 1 for each UGT enzyme. The amino acids common to each UGT are contained within the boxes. Figure from ref [2]

times greater with the UGT1A6 and UGT2B7 dimers when compared to the activity of UGT1A6 alone.[231] As shown in figure 1.7, UGT1A6 and UGT2B7 have relatively few amino acids in common within the dimerization motif region,[2] yet still exhibit dimerization activity indicating that UGT dimerization is not well understood The variation in UGT activity differences upon dimerization with functional or non-functional enzymes indicates that the characterization of the activity and/or function of a single UGT may not provide an accurate portrait of its contribution of glucuronidation activity *in vivo*.

Psuedogenes are genes that usually code for non-functional proteins. It is thought that these genes have lost their catalytic function over time due to an accumulation of DNA mutations,[232] but may persist due to their function as post-translational gene regulators through dimerization.[233] While these genes have lost their function over time, they retain some homology to functional UGTs and could include the dimerization motif and may exhibit UGT regulation similar to UGT splice variants. Psuedogenes have been identified in both the UGT1A and UGT2B families.[166, 234, 235] These genes can have exons that are identical and/or similar to the genes for UGT1A enzymes and may cause overestimation of mRNA levels due to inadvertent and primer dependent amplification.

An additional regulatory mechanism is through miRNA, which are small non-coding RNA that can regulate protein expression through interaction with mRNA.[236] This generally occurs when miRNA interact with the 3' untranslated region of mRNA. This interaction can inhibit the translation of RNA into protein or can tag the mRNA for degradation.[237] Some studies have found that miRNA additionally have the ability to bind to the 5' untranslated region[238] or even the coding region of mRNA[239] to similarly delay translation or degrade the mRNA.[240] Several studies have

been published on the miRNA regulation of both UGT1A[241-244] and UGT2B enzymes.[245-248] Each of these studies screened anywhere from a handful to thousands of miRNA at a time and were able to identify specific miRNA with the ability to regulate UGT1A and/or UGT2B activity. As the UGT1A enzymes all share the same 3' untranslated region of mRNA, the miRNA that regulate one of the UGT1A enzymes should regulate all of them. Each of the UGT2B enzymes, because they are each their own gene, have an individual 3' untranslated region of their mRNA and therefore must be tested individually susceptibility to miRNA regulation. Of the UGT2Bs, 2B4, [247, 249] 2B7, [247-249] 2B10, [249] and 2B15[245, 246, 248] have all been shown to be regulated by specific miRNAs.

Any of these regulatory mechanisms could explain the lack of correlation in mRNA and protein levels seen for UGT2B7 [198] and could even play a role in inter-individual protein expression and protein activity. There is a lack of understanding of the potential combined impacts of these regulatory mechanisms, and future work is needed to determine any cumulative effects of UGT regulation on the expression and function of UGTs.

UGTs and TSNA metabolism

There are 6 UGTs know to metabolize NNAL; UGTs 1A4, 1A9, 1A10, 2B7, 2B10, and 2B17. Three enzymes, UGT1A9,[250, 251] UGT2B7,[153, 251, 252] and UGT2B17[161, 251, 253, 254] were previously found to mediate hepatic NNAL-*O*-Gluc formation in humans, with UGT2B17 exhibiting the lowest K_M *in vitro*. While both UGTs 1A4[250, 251, 255] and 2B10[251, 256, 257] mediate NNAL-*N*-Gluc formation in humans,[250, 255, 258-261] UGT2B10 is responsible for >90% of NNAL-*N*-Gluc formation in HLM and in the urine of smokers.[3, 256, 257, 262] The variability in the urinary

ratios of NNAL-Gluc:NNAL[263, 264] and NNAL-*O*-Gluc:NNAL-*N*-Gluc[259] from smokers is substantial, suggesting large inter-individual variability within the detoxification pathway of NNK and in the ability to form different NNAL glucuronides.[263, 264] Variation in the levels of NNAL-*O*-Gluc and NNAL-*N*-Gluc formation was also observed HLM assays both between purchased small pool specimens as well as individual liver specimens.[250, 253] This variation has been suggested to be partially mediated by genetic polymorphisms in UGT2B17 and UGT2B10. Previous studies have shown that the prevalent *UGT2B17* whole-gene deletion polymorphism [31-33% allelic prevalence in Caucasians][254, 265-267] and the UGT2B10 codon 67 Asp>Tyr SNP [9.1% allelic prevalence in Caucasians][251, 268] are associated with large variability in hepatic NNAL-*O*-Gluc and NNAL-*N*-Gluc formation activities, respectively.[251, 253, 254, 256, 257] In addition, the UGT2B17 gene deletion polymorphism was significantly associated with lung cancer risk in women.[161] These data suggest an important role for glucuronidation-mediated detoxification of NNAL in tobacco-related cancer risk.

The TSNAs NNN, NAT, and NAB are only able to form a single glucuronide at the nitrogen within the pyridine ring (Figure 1.8). NNN-, NAT-, and NAB-*N*-Gluc were only formed by UGT1A4 and UGT2B10 of all the UGTs screened.[256] The *N*-Glucs of NNN, NAT, and NAB comprised 59-90% of total urinary NNN, NAT, and NAB in both tobacco smokers and smokeless tobacco users.[269] Lower levels of NNN-*N*-Gluc formation, rather than NNAL-Gluc formation, have been associated with esophageal cancer incidents.[160]

Determination of the stereo-selectivity of individual UGT enzymes towards individual NNAL enantiomers and the determination of whether the *UGT2B17* deletion polymorphism is correlated with altered levels of (*R*)- versus (*S*)-NNAL-*O*-Gluc formation activity in HLM is

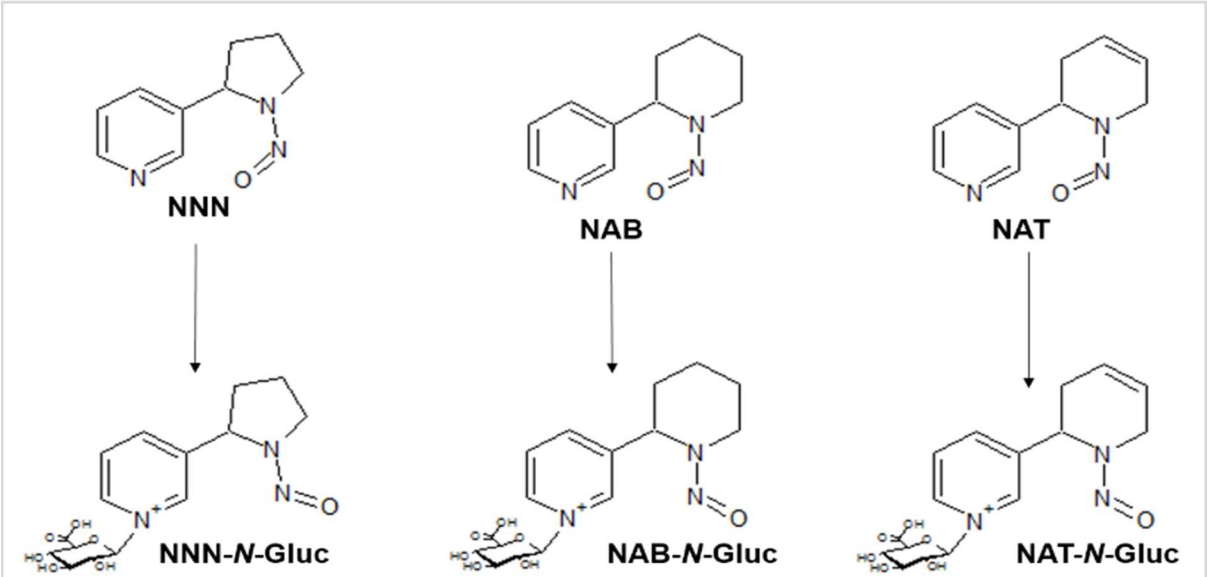

Figure 1.8. Formation of NNN, NAB, and NAT glucuronides.

discussed in more detail in Chapter 2. It is demonstrated that UGTs 1A10, 2B17, and 2B7 exhibit high stereo-selectivity for (*R*)- and (*S*)-NNAL, respectively, and that there is a significant change in the (*R*)- to (*S*)-NNAL-*O*-Gluc ratio associated with the *UGT2B17* null genotype in HLM. In a genotype/phenotype correlation study, the *UGT2B17* null genotype was associated with a 30% reduction in the formation of (*R*)-NNAL-*O*-Gluc.[3]

Menthol

Menthol is a chiral aliphatic alcohol, with each enantiomer either called D- or L-menthol and the racemic mixture referred to as DL-menthol. The only naturally occurring enantiomer, the one found in and isolated from a variety of mint plant species, is L-menthol. The other enantiomer, D-menthol, is a product of the Haarmann & Reimer industrial synthesis process which yields a DL-menthol mixture.[270] It has been long known that D-menthol doesn't produce the same smell

and taste profile normally associated with naturally occurring menthol and that its analgesic properties are greatly reduced when compared to L-menthol. [271-273] When menthol is the active ingredient in over-the-counter pharmaceuticals, such as lozenges, only the active L-menthol enantiomer is present; however, the same may not be true for tobacco products. Studies have examined the total menthol content in both menthol and non-menthol cigarettes, which can range from 1.0-0.3% wt/wt [274] in menthol cigarettes and up to 0.03% wt/wt menthol in non-menthol cigarettes.[275] DL-menthol has been identified as an inhibitor of both NNAL-*O*- and NNAL-*N*-Gluc production in HLM.[276] As it is known that menthol is rapidly cleared from the body as a menthol glucuronide (MG; see Figure 1.9),[277, 278] the same clearance pathway as the TSNAs. Analysis of the UGTs know to form MG are discussed further in Chapter 4 which outlines a study to identify the enzymes responsible for the metabolism of both L- and D-menthol to their respective

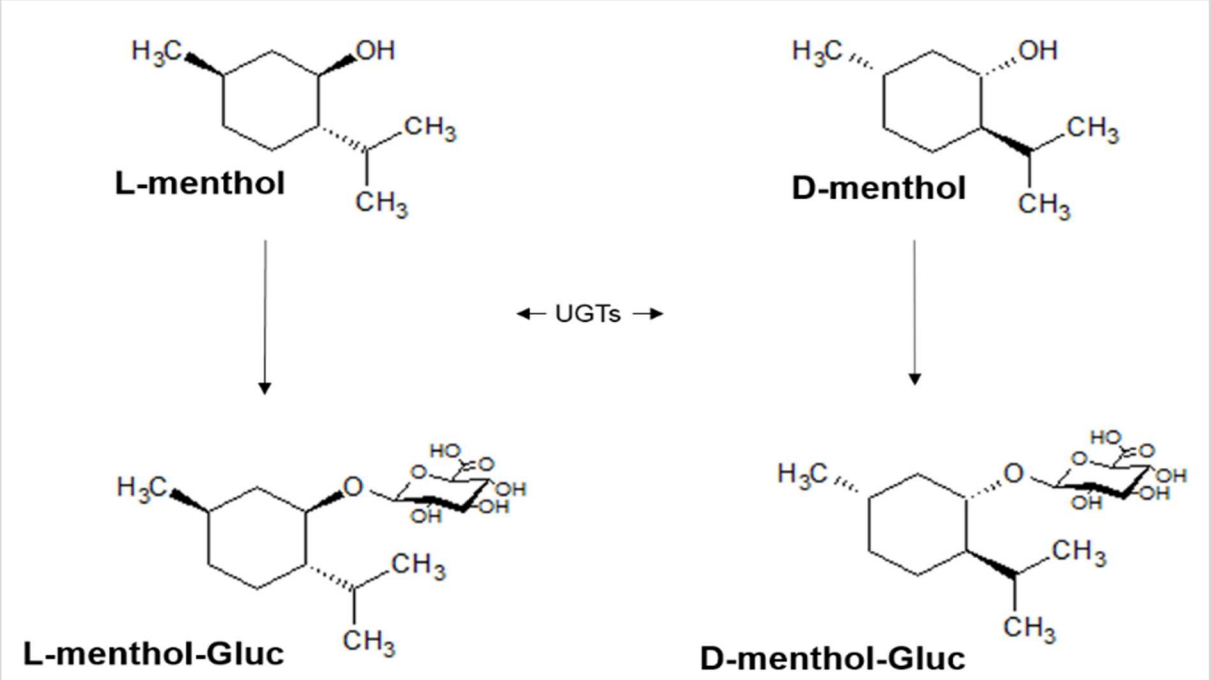

Figure 1.9. Schematic of the formation of L- and D-menthol glucuronides.

glucuronides, as both could possibly be found in tobacco products [40] and to investigate the inhibition of each menthol enantiomer on NNAL-glucuronide formation *in vivo*.

Hypothesis and Aims

The central hypothesis investigated in this dissertation was that stereospecific detoxification of the potent tobacco carcinogen, NNAL is mediated by specific UGTs and that there are genotypes and tobacco additives that slow down this detoxification pathway. This hypothesis was interrogated by the following aims:

1) Identify the stereospecificity of each UGT isoform as well as each tobacco-related cancer tissue type for the formation of NNAL glucuronides.
2) Investigate UGT genotypes and tissue-specific UGT expression that may lead to differential stereo-specific detoxification of NNAL.

   and
3) Characterize the inhibition of the NNAL detoxification pathway by the common tobacco additive, menthol.

CHAPTER TWO

STEREOSPECIFIC METABOLISM OF THE TOBACCO SPECIFIC NITROSAMINE, NNAL

[Reprinted with permission from Kozlovich S, Chen G, Lazarus P. Stereospecific Metabolism of the Tobacco-Specific Nitrosamine, NNAL. *Chem Res Toxicol*. Copyright 2015 American Chemical Society https://pubs.acs.org/doi/10.1021/acs.chemrestox.5b00278]

Shannon Kozlovich[§], Gang Chen[§] and Philip Lazarus[*§]

[§]Department of Pharmaceutical Sciences, College of Pharmacy, Washington State University, Spokane WA 99210

[*]Corresponding author: Philip Lazarus, Ph.D., Department of Pharmaceutical Sciences, College of Pharmacy, Washington State University, Spokane WA 99210; Email: phil.lazarus@wsu.edu

Running Title: Stereospecific Glucuronidation of NNAL

Abstract

Among the most potent carcinogens in tobacco are the tobacco-specific nitrosamines (TSNAs), with 4-(methylnitrosamino)-1-(3-pyridyl)-1-butanone (NNK) the most potent as well as one of the most abundant. NNK is extensively metabolized to the equally carcinogenic 4-(methylnitrosamino)-1-(3-pyridyl)-1-butanol (NNAL). Of the two NNAL enantiomers, (*S*)-NNAL appears to be preferentially glucuronidated and excreted in humans, but also exhibits higher stereoselective tissue retention in mice and humans and has been shown to be more carcinogenic in mice than its (*R*)- counterpart. Due to the differential carcinogenic potential of the NNAL enantiomers, it is increasingly important to know which UGT enzyme targets the specific NNAL

enantiomers for glucuronidation. To examine this, a chiral separation method was developed to isolate entiomerically pure (*S*)- and (*R*)-NNAL. Comparison of NNAL glucuronides (NNAL-Glucs) formed in reactions of UGT2B7-, UGT2B17-, UGT1A9-, and UGT2B10-over-expressing cell microsomes with pure NNAL enantiomers showed large differences in kinetics for (*S*)- versus (*R*)-NNAL, indicating varying levels of enantiomeric preference for each enzyme. UGT2B17 preferentially formed (*R*)-NNAL-*O*-Gluc and UGT2B7 preferentially formed (*S*)-NNAL-*O*-Gluc. When human liver microsomes (HLM) were independently incubated with each NNAL enantiomer, the ratio of (*R*)-NNAL-O-Gluc to (*S*)-NNAL-O-Gluc formation in HLM from subjects exhibiting the homozygous deletion UGT2B17 (*2/*2) genotype was significantly lower (p=0.012) than HLM from wild-type (*1/*1) subjects. There was a significant trend (p=0.015) towards decreased (*R*)-NNAL-O-Gluc:(*S*)-NNAL-O-Gluc ratio with increasing numbers of the UGT2B17*2 deletion allele. These data demonstrate that variations in the expression or activity of specific UGTs may affect the clearance of specific NNAL enantiomers known to induce tobacco-related cancers.

Introduction

Tobacco-specific nitrosamines (TSNAs) are an important class of carcinogens present in both tobacco smoke and smokeless tobacco products.[125-128] The most potent and one of the most abundant TSNAs is 4-(methylnitrosamino)-1-(3-pyridyl)-1-butanone (NNK).[136, 140, 263, 279, 280] The major metabolic pathway for NNK (Figure 2.1) is carbonyl reduction to both the (*R*)- and (*S*)-enantiomers of 4-(methylnitrosamino)-1-(3-pyridyl)-1-butanol (NNAL),[133-135] which, like NNK, are very potent carcinogens in rodents.[136-139] It was originally estimated, by measuring NNK in mainstream smoke and urinary NNAL in smokers, that 39-100% of NNK was converted to NNAL in smokers.[140] In more recent studies where NNK exposure was measured using the in saliva of smokeless tobacco users, it was estimated that 14-17% of NNK was converted to NNAL.[141] It was also shown that NNAL comprised 82-92% of total NNK metabolites in human lung tissue.[139]

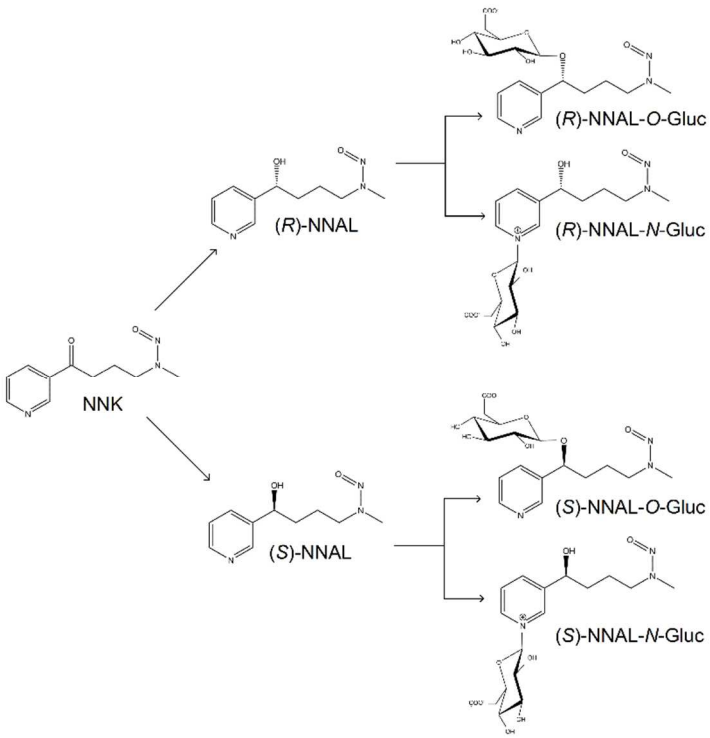

Figure 2.1. Simplified schematic of NNK metabolism to each NNAL-Gluc regioisomer and diastereomer.

The glucuronidation of NNAL is considered to be an important mechanism for NNK detoxification.[126, 136, 140, 151-158] In contrast to the relatively high tumorigenicity exhibited by both (*R*)- and (*S*)-NNAL, glucuronidated NNAL (NNAL-Gluc) is non-tumorigenic after subcutaneous injection into A/J mice.[162] It has been shown that NNAL glucuronides are formed extensively in

human liver microsomes (HLM)[153, 255] and can be measured in the urine of past and current smokers.[156, 157, 260, 264] It has been found that while (*S*)-NNAL is stereoselectively retained in rat lung and has a higher tumorigenicity than (*R*)-NNAL, (*R*)-NNAL exhibits a higher rate of glucuronidation in rats[135, 281-283] and the A/J mouse.[135, 162] However, studies indicate that (*S*)-NNAL may be stereo-selectively retained in smokeless tobacco users[163] yet it exhibits a higher rate of glucuronidation in the patas monkey.[151]

NNAL glucuronidation can occur at both the carbinol group (NNAL-*O*-Gluc)[136, 140, 151-153, 159, 250, 253, 259, 261, 276] and the nitrogen on the pyridine ring (NNAL-*N*-Gluc).[159, 255, 257, 259, 261] Three enzymes, UGT1A9,[250, 251] UGT2B7[153, 251, 252] and UGT2B17,[161, 251, 253, 254] were previously found to mediate hepatic NNAL-*O*-Gluc formation in humans, with UGT2B17 exhibiting the lowest K_M *in vitro*. While both UGTs 1A4[250, 251, 255] and 2B10[251, 256, 257] mediate NNAL-*N*-Gluc formation in humans,[250, 255, 258-261] UGT2B10 was shown to account for ~95% of total hepatic NNAL-*N*-Gluc activity in HLM.[256]

The variability in the urinary ratios of NNAL-Gluc:NNAL[263, 264] and NNAL-*O*-Gluc:NNAL-*N*-Gluc[259] from smokers is substantial, suggesting that individuals may differ greatly in their ability to detoxify NNK and form different NNAL glucuronides. In addition, variation in the levels of NNAL-*O*-Gluc and NNAL-*N*-Gluc formation was also observed in assays performed using HLM specimens.[250, 253] This variation was suggested to be, in part, mediated by genetic polymorphisms in UGT2B17 and UGT2B10. Previous studies have shown that the prevalent *UGT2B17* whole-gene deletion polymorphism [31-33% allelic prevalence in Caucasians][254, 265-267] and the UGT2B10 codon 67 Asp>Tyr SNP [9.1% allelic prevalence in Caucasians][251, 268] are associated with large variability in hepatic NNAL-*O*-Gluc and NNAL-*N*-Gluc formation activities, respectively.[251, 253, 254, 256, 257] In addition, the UGT2B17 gene deletion polymorphism was

significantly associated with lung cancer risk in women.[161] These data suggest an important role for glucuronidation-mediated detoxification of NNAL in tobacco-related cancer risk.

The goal of the present study was to characterize the stereo-selectivity of individual UGT enzymes towards individual NNAL enantiomers and determine whether the *UGT2B17* deletion polymorphism is correlated with altered levels of (*R*)- versus (*S*)-NNAL-*O*-Gluc formation activity in human liver microsomes (HLM). The results demonstrate that UGT2B17 and UGT2B7 exhibit high stereo-selectivity for (*R*)- and (*S*)-NNAL, respectively, and that there is a significant change in the (*R*)- to (*S*)-NNAL-*O*-Gluc ratio associated with the *UGT2B17* null genotype in HLM.

Materials and Methods

Chemicals and materials. *rac*-NNAL (#M325740) and NNK (#KIT0565) were purchased from Toronto Research Chemicals (Toronto, ON, Canada); UDP glucuronic acid (UDPGA), alamethicin, kanamycin, chloramphenicol, imidazole, methanol (MeOH) and isopropanol were purchased from Sigma (St Louis, MO); Dulbecco's modified Eagle's medium, fetal bovine serum (FBS), geneticin and penicillin-streptomycin were purchased from Life Technologies (Carlsbad, CA); silver stain, isopropyl β-D-1-thiogalactopyranoside (IPTG), bicinchoninic acid (BCA), ammonium acetate and formic acid were purchased from Fisher Scientific (Fair Lawn, NJ); Luria broth base and Tris-glycine gels (1.0 mm) were purchased from Invitrogen (Carlsbad, CA).

Tissues. A description of the normal human liver tissue microsomes used for the current studies were previously described.[250] Tissue samples were quick-frozen at -70°C within 2 h post-surgery. Liver microsomes were prepared through differential centrifugation as previously described[284] and stored (2.5-5 mg protein/mL) at -80°C. Microsomal protein concentrations were

measured using the BCA assay. The *UGT2B17* gene deletion analysis was performed previously [253] utilizing *UGT2B17* deletion locations as determined by Wilson *et al*.[266]

Cell lines and microsomal preparation. HEK293 cells overexpressing wild-type UGT1A9, UGT2B7, UGT2B10 and UGT2B17 have been described previously.[153, 285, 286] All HEK293 cell lines were grown to 80% confluence in Dulbecco's modified Eagle's medium supplemented with 10% fetal bovine serum, 100 U/mL penicillin and 100 μg/mL streptomycin, and maintained in 700 μg/mL of geneticin for selection of UGT overexpression, in a humidified incubator atmosphere of 5% CO_2. For the preparation of cell microsomal fractions, cells were suspended in Tris-buffered saline (25 mM Tris base, 138 mM NaCl, 2.7 mM KCl; pH 7.4) and subjected to five rounds of freeze/thaw before gentle homogenization. The cell homogenate was centrifuged at 9,000 *g* for 30 min at 4°C. The supernatant was then centrifuged at 105,000 *g* for 60 min at 4°C. The microsomal pellet was suspended in Tris-buffered saline and stored in 100 μL aliquots at -80°C. Total microsomal protein concentrations were determined using the BCA protein assay.

AKR1C1 induction and purification. Transformation-ready expression plasmids (6X N-term His tag, pQE-T7 vector; Qiagen, Venlo, Limburg) with the *AKR1C1* gene were introduced to BL21 *E. coli*. The transformed *E. coli* were grown on kanamycin selection plates for 12 h and screened for plasmid uptake by DNA sequencing. AKR1C1-expressing *E. coli* were incubated on a shaker for 1.75 h at 37°C in Luria broth (25 μg/μL) containing kanamycin (17 μg/μL) and chloramphenicol (8 μg/μL). Protein expression was induced with the addition of IPTG (25 mM) and incubated while shaking at 37°C for 3 h. The recombinant histidine-tagged protein was

purified from cell lysate on a Ni-NTA column (Fisher Scientific, #PI-88225). Lysate was loaded onto the column in a 1:1 mixture with 10 mM imidazole and washed four times with increasing concentrations of imidazole (2 mL; 20 mM, 60 mM, 100 mM, 250 mM), then eluted with 2 mL of 500 mM imidazole. Eluted protein was then dialyzed in a Slide-A-Lyzer G2 dialysis cassette (Fisher Scientific) against PBS for a total of 8 h at 4°C. Purity (>80%) was assessed via SDS-PAGE using a 4-20% Tris-Glycine gradient gel and silver staining; protein quantity was determined using the BCA assay.

NNK reduction assay. The NNK reduction assay was adapted from a previously determined method[143] using the following conditions: AKR1C1 (1 μg) was incubated (50 μL final volume) with 1 mM NNK in buffer (0.1 M monopotassium phosphate, 0.4 mM potassium chloride, 0.2 mM magnesium chloride; pH 7.4) and NADPH regeneration system (2.5 μL solution A plus 0.5 μL solution B; Corning, Corning, NY) at 37°C for 1 h. Reactions were terminated by the addition of an equal volume of methanol on ice. The precipitate was removed by centrifugation and the supernatant was saved for LC-MS analysis.

***rac*-NNAL chiral separation and collection.** NNAL enantiomer separation was achieved by liquid chromatography (LC) using the following system: an Acquity (model BSM) ultra-performance LC (Waters) equipped with an automatic injector (model SM) and a UV detector operated at 254 nm (model TUV). LC was performed using a Lux 3u Amylose-2 column (150x4.6 mm; Phenomex, #00F-4471-E0) at 23ºC with an isocratic elution of 30% ultra-pure water and 70% 3:1 methanol/isopropanol at 0.3 mL/min. Peaks 1 and 2 (see Figure 1) were collected from 6.95 to 7.45 min and 7.50 to 8.20 min, respectively. This method was developed to optimize for (*R*)- and

(*S*)-NNAL enantiomer separation, with the *E/Z* NNAL rotamers contained within the (*R*)- and (*S*)-NNAL peaks.

NNAL glucuronidation assay. The rate of (*R*)- and (*S*)-NNAL-*O*-Gluc formation by HLM and UGT over-expressing cell microsomes was determined after pre-incubation with alamethicin (50 μg/mg protein) for 10 min on ice using the following conditions: UGT over-expressing cell microsomes (15-20 μg protein) or HLM (10 μg protein) were incubated (10 μL, final volume) in 50 mM Tris-HCl (initial pH 7.4), 10 mM $MgCl_2$, 4 mM UDPGA, and each NNAL enantiomer (UGT over-expressing cell microsomes: 0.5-16 mM; HLM: 4 mM) at 37°C for 1 h; as described previously, glucuronidation reactions were rate linear for up to 2 h incubation times.[257] Reactions were terminated by the addition of an equal volume of methanol on ice and spiked with 2 μL of the appropriate deuterated internal standard (see below). The precipitate was removed by centrifugation and the supernatant was saved for LC-MS analysis as described below. Three individual HLM specimens from each genotype were assayed with each individual NNAL enantiomer. Each reaction was run in triplicate.

Synthesis and purification of D_4-NNAL-*O*- and *N*-Gluc standards. To obtain D_4-NNAL-*N*-Gluc and D_4-NNAL-*O*-Gluc, bovine liver microsomes (5 mg protein/mL reaction) were used to catalyze D_4-NNAL (a kind gift from Shantu Amin; Penn State University, Hershey, PA)[287] conjugation with glucuronic acid. Bovine liver microsomes were initially incubated with alamethicin (50 μg/mg protein) on ice for 15 min, then were incubated with D_4-NNAL (20 mM) at 37°C in Tris buffer (50 mM, pH 7.5), $MgCl_2$ (10 mM), UDPGA (8 mM) for 2 h. The reaction was quenched with the addition of equal volume of ice cold acetonitrile. Protein was removed by

centrifugation at 16,000 *g* for 10 min at 4°C and the acetonitrile was removed by evaporation. D_4-NNAL-*N*-Gluc and D_4-NNAL-*O*-Gluc were purified by HPLC using previously described methods.[256] The collection of D_4-NNAL-*N*-Gluc and D_4-NNAL-*O*-Gluc were confirmed by LC-MS as described below and aliquots were stored at concentrations of 1 ppm.

LC-MS analysis. LC separation was achieved using an Acquity H class UPLC (Waters) equipped with an auto sampler (model FTN). NNAL peaks were analyzed with the same column and isocratic method as described above; glucuronide peaks were analyzed with a HSS T3 1.8 μm column (2.1x100 mm; Acquity, Waters, Milford, MA) at 30°C with gradient elution at 0.4 mL/min using the following conditions: 0.5 min with 99% buffer A (5 mM ammonium acetate with 0.01% formic acid) and 1% buffer B (100% MeOH), followed by a linear gradient for 3.0 min to 20% buffer B, and a subsequent linear gradient for 1.0 min to 95% buffer B. The column was washed with a 1.0 min linear gradient to 1% buffer B and regenerated for 1.0 min in 1% buffer B.

The Waters Xevo TQD tandem mass spectrometer was equipped with a Zspray electrospray ionization interface operated in the positive ion mode, with capillary voltage at 0.6 kV. Nitrogen was used as both the cone gas and desolvation gas at 50 and 800 L/hr, respectively. Ultra-pure argon was used for collision-induced dissociation. The desolvation temperature and the ion source temperature were 500°C. For the detection of NNAL enantiomers and NNAL-Glucs, the mass spectrometer was operated in the multiple reaction monitoring mode (MRM). The ion related parameters for each transition were monitored as follows: NNAL, MS transition of 210.1>180.1 with cone voltage and collision energy at 30 and 10 V, respectively; NNAL-*N*-Gluc, MS transition of 386.2>180.1 with cone voltage and collision energy at 15 and 20 V, respectively; NNAL-*O*-Gluc, MS transition of 386.2>162.1 with the cone voltage and collision energy each at

15 V. The MS transitions and LC retention times for each molecule were compared to purchased NNAL, NNAL-*O*-Gluc and NNAL-*N*-Gluc standards (Toronto Research Chemicals) for each metabolite. NNAL-*O*-Gluc and NNAL-*N*-Gluc formation was quantified by dividing their peak areas by the peak areas for deuterated NNAL-*O*-Gluc and NNAL-*N*-Gluc internal standards, respectively, and quantified against a standard curve made from purchased NNAL-*O*-Gluc (Toronto Research Chemicals) of known quantity.

Statistical analysis. The Student's t-test was used to compare the ratio of (R)- to (S)-NNAL-*O*-Gluc in subjects with *UGT2B17* null (*2/*2) genotype versus subjects with the *UGT2B17* (*1/*1) genotype. The linear trend test was used to examine the ratio of (R)- to (S)-NNAL-*O*-Gluc in HLM with decreasing copies of the *UGT2B17* alleles. Kinetic constants were determined, and statistical analysis were performed using Prism version 6.01 (GraphPad Softwear, San Diego, CA).

Results

To separate the individual NNAL enantiomers, a LC chiral separation method was developed using purchased (Toronto Research Chemicals) *rac*-NNAL (Figure 2.2, panel A). This method produced two distinct peaks, peak 1 (retention time of approximately 7.25 min) and peak 2 (retention time of approximately 7.85 min). Both peaks were collected and examined for purity using the same UV-monitored LC method (Figure 2.2, panels B and C); NNAL enantiomers corresponding to the respective peaks were collected with an enantiomeric purity of >99%. AKR1C1 was previously shown to be selective for the formation of (*S*)-NNAL.[142, 143, 288] To

examine which of the peaks observed by LC separation corresponded to the (*S*)- versus (*R*)-NNAL enantiomers, peaks 1 and 2 were compared to the product of an AKR1C1-mediated NNK reduction assay as described in the Materials and Methods. The identity of the peaks were verified by the MRM transitions and confirmed by comparison to the purchased *rac*-NNAL standard (Toronto Research Chemicals). The AKR1C1 (*S*)-NNAL peak was observed at 6.50-7.30 min (Figure 2.2, panel D), and was identical to that observed for peak 1 (Figure 2.2, panel E), indicating that peak 1 is (*S*)-NNAL. Since peak 2 was observed at a different retention time (7.10-7.95 min), this suggests that peak 2 corresponds to (*R*)-NNAL (Figure 2.2, panel F).

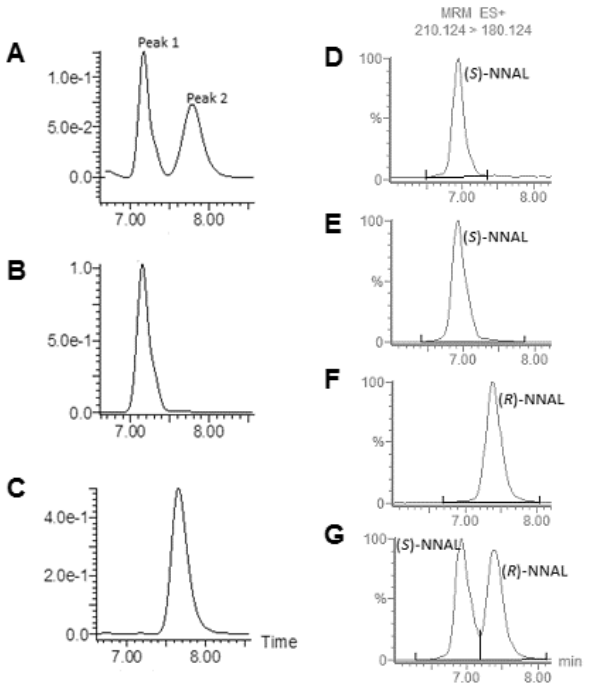

Figure 2.2. *rac*-NNAL separation and NNAL enantiomer analysis. Panels A-C, *rac*-NNAL was separated by an isocratic method as described in the Materials and Methods and monitored by UV at 254 nm using LC (right panels). (A), *rac*-NNAL; (B), enantiomerically pure peak 1 collected from panel A; and (C), enantiomerically pure peak 2 collected from panel A. Panels D-G, LC-MS analysis of NNAL enantiomers. (D), AKR1C1-generated (S)-NNAL; (E), LC-collected peak 1 from panel A; (F) LC-collected peak 2 from panel A; and, (G) *rac*-NNAL. For panel D, AKR1C1 (1 µg total protein; >80% purity) was incubated at 37°C for 1 h with 1 mM NNK and NADPH regeneration system, and LC-MS was performed as described in the Materials and Methods. The *E* and *Z* rotomers of (*R*)- and (*S*)-NNAL were not separated using this LC procedure.

Previous studies have shown that the UGTs 2B7,[153, 250-253] 2B17,[161, 251, 253, 254] 1A9[250, 251] and 2B10,[251, 256, 257] are the major enzymes responsible for the hepatic glucuronidation of NNAL. To determine whether any or all of these enzymes exhibit stereo-selectivity against the individual NNAL enantiomers, the activity of each UGT was examined using microsomes from UGT over-

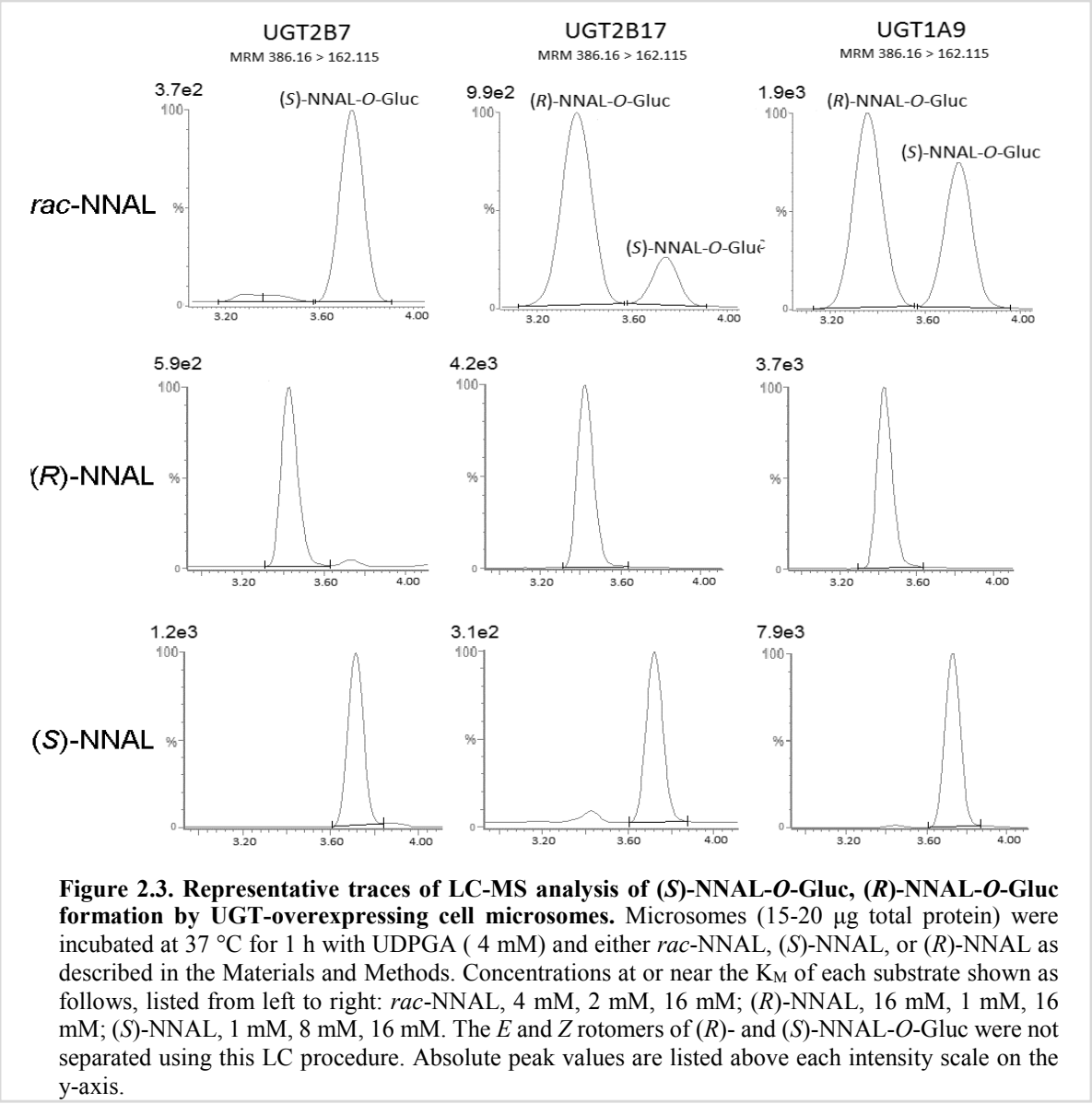

Figure 2.3. Representative traces of LC-MS analysis of (*S*)-NNAL-*O*-Gluc, (*R*)-NNAL-*O*-Gluc formation by UGT-overexpressing cell microsomes. Microsomes (15-20 µg total protein) were incubated at 37 °C for 1 h with UDPGA (4 mM) and either *rac*-NNAL, (*S*)-NNAL, or (*R*)-NNAL as described in the Materials and Methods. Concentrations at or near the K_M of each substrate shown as follows, listed from left to right: *rac*-NNAL, 4 mM, 2 mM, 16 mM; (*R*)-NNAL, 16 mM, 1 mM, 16 mM; (*S*)-NNAL, 1 mM, 8 mM, 16 mM. The *E* and *Z* rotomers of (*R*)- and (*S*)-NNAL-*O*-Gluc were not separated using this LC procedure. Absolute peak values are listed above each intensity scale on the y-axis.

expressing cells against (*R*)- and (*S*)-NNAL collected as described above. Using a LC-MS method developed to separate the *O*-Glucs of the (*S*)- versus (*R*)-NNAL enantiomers, UGT2B7 was shown to preferentially form the *O*-Gluc of (*S*)-NNAL while UGT2B17 preferentially forms the *O*-Gluc of (*R*)-NNAL (Figure 2.3). Representative plots of glucuronidation rate versus substrate concentration for individual UGT enzymes against (*R*)- versus (*S*)-NNAL are shown in Figure 2.4.

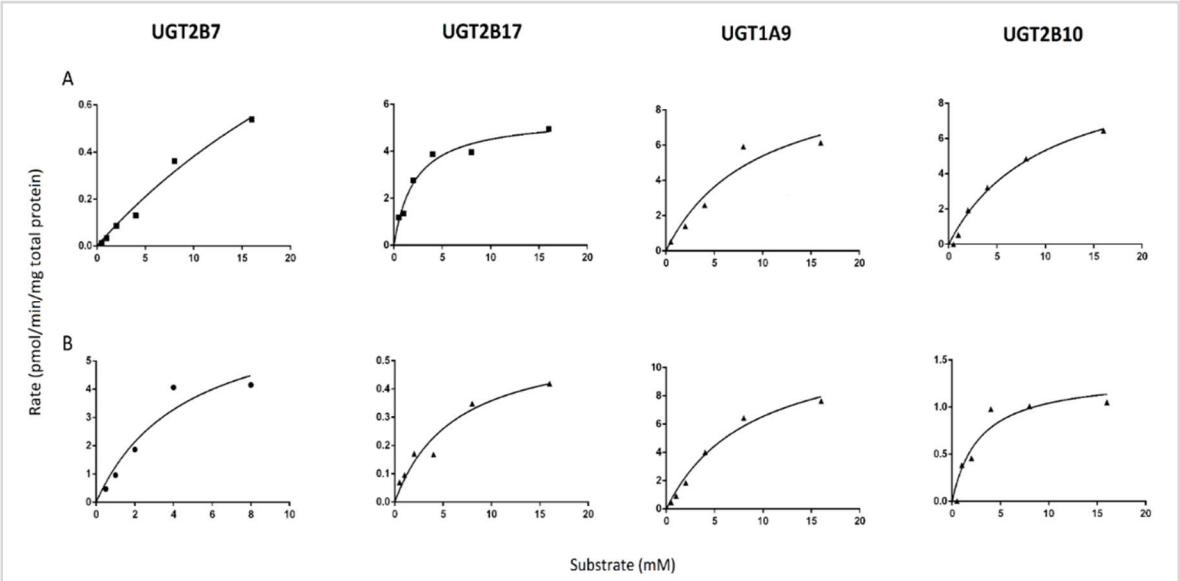

Figure 2.4. Representative concentration curves and kinetic analysis for (*R*)-NNAL- and (*S*)-NNAL-Gluc formation with microsomes from UGT2B7, UGT2B17, UGT1A9 and UGT2B10 overexpressing cells. Glucuronide formation assays were performed at 37 °C for 1 h using 15-20 µg total UGT-overexpressing cell microsomal protein and increasing concentrations of (*R*)-NNAL (panel A) and (*S*)-NNAL (panel B) as described in the Materials and Methods. Rate, V_{max} values are expressed per mg of total protein. Representative curves are shown; complete kinetic analysis was performed in three independent experiments.

The V_{max}/K_M for UGT2B7 was 30-fold higher for (*S*)-NNAL as compared to (*R*)-NNAL (Table 1) and exhibited a K_M that was $\geq$1.5-fold lower than the other UGTs for (*S*)-NNAL. In contrast, the V_{max}/K_M for UGT2B17 for (*S*)-NNAL was 12-fold lower as compared to (*R*)-NNAL while exhibiting a K_M > 5.6-fold lower than any other UGT for (*R*)-NNAL. By comparison, while UGT1A9 exhibited a relatively high K_M (>8 mM) against both (*S*)- and (*R*)-NNAL, UGT1A9 does not appear to exhibit the same level of stereo-specificity as the other *O*-glucuronidating enzymes (Figure 2), with a V_{max}/K_M for (*S*)-NNAL that was 1.8-fold higher than that observed for (*R*)-NNAL (Table 2.1).

Table 2.1. Kinetics of UGT metabolism of (*R*)- versus (*S*)-NNAL.[a]

TSNA	enzyme	V_{max}[b] (pmol/mg protein/min)	K_M (mM)	V_{max}/K_M[b] (nL/min/mg protein)
(R)–NNAL	UGT2B7	3.1 ± 1.5	51 ± 9.6[c]	0.06
	UGT2B17	3.0 ± 2.3	1.8 ± 0.47	1.7
	UGT1A9	13 ± 9.8	13 ± 4.5	1.0
	UGT2B10	8.0 ± 3.1	9.8 ± 4.1	0.81
(S)–NNAL	UGT2B7	4.8 ± 2.3	2.7 ± 1.7	1.8
	UGT2B17	0.54 ± 0.26	4.0 ± 1.9	0.14
	UGT1A9	16 ± 14	8.7 ± 2.0	1.8
	UGT2B10	1.6 ± 0.27	4.1 ± 1.2	0.40

[a] Data are expressed as the mean ± SD of three independent experiments.
[b] Units are expressed per mg total microsomal protein.
[c] Estimated K_m calculated by GraphPad; the actual value determined experimentally was >16 mM.

Table 2.2. Rate of NNAL-*O*-Gluc formation stratified by UGT2B17 deletion genotype.[a]

Genotype	Subject	(*R*)-NNAL-*O*-Gluc	(*S*)-NNAL-*O*-Gluc
*1/*1	1	360	1106
	2	422	747
	3	360	593
	Mean ± SD	380 ± 36	815 ± 263
*1/*2	4	316	855
	5	496	928
	6	140	1007
	Mean ± SD	317 ± 178	930 ± 76
*2/*2	7	333	2784
	8	4.8	174
	9	144	1181
	Mean ± SD	161 ± 165	1380 ± 1317

[a] Rate units are expressed as pmol/min/mg total HLM protein. Values shown for each HLM specimen are the mean of three independent assays.

While the individual (*R*)- and (*S*)-NNAL-*N*-Glucs could not be separated using this LC-MS method, NNAL-*N*-Gluc (retention time = 2.30-2.90 min; data not shown) was separated from the NNAL-*O*-Gluc peaks (retention times = 3.20 – 4.00 min; Figure 2). Similar to that observed for UGT1A9 (which forms NNAL-*O*-Gluc), the NNAL-*N*-Gluc forming UGT2B10 does not appear to exhibit the same level of stereo-specificity as the *O*-Gluc forming UGTs 2B7 and 2B17 against the (*R*)- and (*S*)-NNAL enantiomers, with a V_{max}/K_M ratio for (*S*)-NNAL:(*R*)-NNAL of 0.49 (Table 2.1).The UGT2B17 deletion polymorphism has previously been shown to be significantly associated with decreased NNAL-*O*-Gluc formation in HLM.[161, 253, 254] To determine whether UGT2B17 genotype affects the stereo-selectivity of HLM glucuronidation activities against (*R*) versus (*S*)-NNAL enantiomers, HLMs from subjects exhibiting either the (*1/*1), (*1/*2) and (*2/*2) genotypes were examined. While there was some individual differences in the total levels of NNAL-*O*-Gluc formation in the individual HLMs within genotype groups (Table 2.2), the ratio of (*R*)-NNAL-*O*-Gluc to (*S*)-NNAL-*O*-Gluc formation in HLM from (*2/*2) subjects was significantly lower (p=0.012) than HLM from (*1/*1) subjects (Figure 2.5). There was a significant trend (p=0.015) towards decreased (*R*)-NNAL-O-Gluc:(*S*)-NNAL-O-Gluc ratio with increasing numbers of the UGT2B17*2 allele.

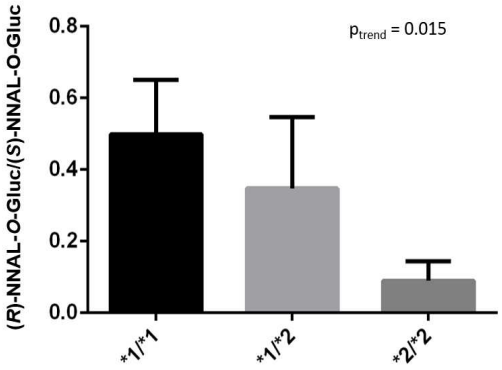

Figure 2.5. The (*R*)-NNAL-*O*-Gluc to (*S*)-NNAL-O-Gluc ratio in HLM stratified by UGT2B17 genotype. HLM (10 µg total protein) were incubated at 37 °C for 1 h with UDPGA and 4 mM (*R*)- or (*S*)-NNAL as described in the Materials and Methods. Columns represent the mean ± SD of three randomly chosen HLM specimens from different subjects for each of the three UGT2B17 genotype groups (indicated within the bars within the figure). *1 refers to the wild-type UGT2B17 allele, *2 refers to the UGT2B17 gene deletion allele. ‡ p=0.012.

Discussion

In the present study, UGT2B7 exhibited the highest stereo-specificity of all of the NNAL glucuronidating UGTs, with a V_{max}/K_M that was 30-fold higher for (*S*)-NNAL as compared to (*R*)-NNAL, suggesting that UGT2B7 is relatively selective for the *O*-Gluc formation of (*S*)-NNAL. No detectable (*R*)-NNAL-*O*-Gluc formation was observed in assays with *rac*-NNAL for UGT2B7 until the substrate concentration approached the K_M towards *rac*-NNAL,[153] and the K_M of UGT2B7 against enantiomerically pure (*R*)-NNAL was >50 mM, suggesting that UGT2B7 is unlikely to contribute to (*R*)-NNAL-*O* -Gluc formation *in vivo*. The K_M for UGT2B7 against (*S*)-NNAL was similar to that observed for UGT2B17 and 3.2-fold lower than that observed for UGT1A9, suggesting that multiple UGTs may be involved in (*S*)-NNAL-Gluc formation in different human tissues. However, the hepatic expression of UGT2B7 is higher than other NNAL-glucuronidating UGTs,[208, 289] this suggests that hepatic (*S*)-NNAL-Gluc formation is largely mediated by UGT2B7.

UGT2B17 exhibited high *O*-glucuronidation activity against (*R*)-NNAL and exhibited a K_M that was >5.6-fold lower than any other UGT. In addition, the ratio of (*R*)- to (*S*)-NNAL-*O*-Gluc formation significantly decreased in HLM from subjects with increasing numbers of the UGT2B17 gene deletion allele. The ratio of (*R*)- to (*S*)-NNAL-*O*-Gluc formation decreased in HLM from subjects with the UGT2B17 (*2/*2) genotype by 5.5-fold as compared to HLM from subjects with the wild-type UGT2B17 (*1/*1) genotype, suggesting that UGT2B17 is the major enzyme involved in hepatic (*R*)-NNAL-*O*-Gluc formation.

The data in the current study are consistent with previous studies indicating that hepatic NNAL-*N*-Gluc formation is generally less prominent than hepatic NNAL-*O*-Gluc formation:[250, 255, 257] i) (*S*)-NNAL-*O*-Gluc was the major NNAL-*O*-Gluc form in HLM irrespective of UGT2B17

genotype in the present study; ii) while the K_M observed for UGT2B10 against (*S*)-NNAL in the present study was comparable to that observed for UGT2B7 (1.5-fold higher), previous studies indicate that its expression in human liver appears to be 4- to 15-fold lower than UGT2B7;[208, 289] and iii) previous studies have consistently demonstrated that the mean levels of urinary NNAL-*O*-Gluc is higher than urinary NNAL-*N*-Gluc in smokers.[259, 263, 264] Given the low K_M's observed for UGT1A9 forming the *O*-Gluc of either the (*S*) or (*R*)-NNAL enantiomers, the present studies are also consistent with previous studies[153] demonstrating that UGT1A9 plays only a minor role in NNAL glucuronidation.

(*S*)-NNAL-*O*-Gluc comprised at least 60% of the total NNAL-*O*-Gluc in HLM in the present study. These data are consistent with previous studies demonstrating that (*S*)-NNAL-Gluc is the major excreted form of NNAL-Gluc in humans, accounting for 68% of the NNAL-Gluc formed in current smokers[259] and was nearly 3 times the amount of the (*R*)-NNAL-Gluc metabolite in smokeless tobacco product users.[163]

Previous studies indicate that the expression of UGT2B17 is roughly 10-fold higher in lung and significantly higher in tissues of the aerodigestive tract including larynx, tonsil, tongue and esophagus [208] as compared to the expression of UGTs 2B7 and 2B10. Therefore, the glucuronidation of (*R*)-NNAL may play a relatively more important role in NNAL detoxification in tobacco target tissues than what might be observed hepatically. This possibility is consistent with the fact that (*R*)-NNAL is the major enantiomer of NNAL formed in both lung microsomes and homogenates *in vitro* (unpublished results), a pattern not observed for hepatic fractions. Direct assessment of (*R*)-NNAL vs (*S*)-NNAL glucuronidation rates in lung tissue and aerodigestive tract tissues will be required to better assess this important possibility.

In summary, this study is the first to identify the UGTs responsible for the glucuronidation for individual NNAL enantiomers, with both UGTs 2B7 and 2B17 exhibiting high stereo-specificity. More comprehensive studies examining how changes in the expression or activity of these enzymes affect the production of NNAL glucuronide enantiomers will be required to better determine the potential impact of such changes on cancer susceptibility.

Funding Support

This work was supported in part by the National Institutes of Health, National Institutes of Environmental Health Sciences [Grant R01-ES025460, to P Lazarus] and the Health Sciences and Services Authority of Spokane, WA.

Acknowledgements

We thank Amity Platt for her outstanding work and for providing purified AKR1C1 protein. We also thank the MS Core Facility at Washington State University Spokane for their help with LC-MS.

Abbreviations

Tobacco-specific nitrosamines (TSNAs), 4-(methylnitrosamino)-1-(3-pyridyl)-1-butanone (NNK), 4-(methylnitrosamino)-1-(3-pyridyl)-1-butanol (NNAL), racemic NNAL (*rac*-NNAL), glucuronidated NNAL (NNAL-Gluc), human liver microsomes (HLM).

CHAPTER THREE

PROMINENT STEREOSELECTIVITY OF NNAL GLUCURONIDATION IN UPPER AERODIGESTIVE TRACT TISSUES

Shannon Kozlovich[§], Gang Chen[§], Christy JW Watson[§] and Philip Lazarus[*§]

[§]Department of Pharmaceutical Sciences, College of Pharmacy, Washington State University, Spokane WA 99210

[*]Corresponding author: Philip Lazarus, Ph.D., Department of Pharmaceutical Sciences, College of Pharmacy, Washington State University, Spokane WA 99202; Email: phil.lazarus@wsu.edu

Abstract

Tobacco specific nitrosamines (TSNAs) are among the most potent carcinogens found in cigarettes and smokeless tobacco products. Decreases in TSNA detoxification, particularly 4-(methylnitrosamino)-1-(3-pyridyl)-1-butanone (NNK), have been associated with tobacco-related cancer incidence. NNK is metabolized by carbonyl reduction to its major carcinogenic metabolite, 4-(methylnitrosamino)-1-(3-pyridyl)-1-butanol (NNAL), which is detoxified by glucuronidation at the nitrogen within the pyridine ring or at the chiral alcohol to form four glucuronide products: (*R*)-NNAL-*O*-Gluc, (*S*)-NNAL-*O*-Gluc, (*R*)-NNAL-*N*-Gluc, (*S*)-NNAL-*N*-Gluc. Stereo-selective NNAL-Gluc formation and the relative expression of NNAL-glucuronidating UGTs (1A4, 1A9, 1A10, 2B7, 2B10, 2B17) were analyzed in 39 tissue specimens from the upper aerodigestive tract [esophagus (n=13), floor of mouth (n=4), larynx (n=9), tongue (n=7), and tonsil (n=6)]. All tissue types preferentially formed (*R*)-NNAL-*O*-Gluc in the presence of racemic-NNAL; only esophagus

exhibited any detectable formation of (*S*)-NNAL-*O*-Gluc. For every tissue type examined, UGT1A10 exhibited the highest level of expression for the NNAL-*O*-glucuronidating UGTs, ranging from 36% (tonsil) to 49% (esophagus), followed by UGT1A9>UGT2B7>UGT2B17. UGT1A10 also exhibited similar or higher levels of expression as compared to both NNAL-*N*-glucuronidating UGTs, 1A4 and 2B10. In a screening of cells expressing individual UGT enzymes, all NNAL glucuronidating UGTs exhibited some level of stereo-specific preference for individual NNAL enantiomers, with UGTs 1A10 and 2B17 forming primarily (*R*)-NNAL-*O*-Gluc. Kinetic analysis indicated that 2B17 exhibited at least a 9-fold lower K_M than UGT1A10. These data suggest that UGTs 1A10 and 2B17 may be important enzymes in the detoxification of TSNAs like NNK in tissues of the upper aerodigestive tract.

Introduction

Tobacco use has been linked to lung cancer for over a century,[4] and remains the leading cause of preventable premature death in adults world-wide.[5] In the United States, tobacco smokers have a mortality rate three times higher than individuals who have never smoked.[6] Cigarette smoking is highly associated with cancers in the airway such as lung and laryngeal cancers, [7, 27-29] while smokeless tobacco use has been associated with cancers of the mouth and throat such as oral and esophageal cancers.[17, 18]. While cigarette smoking is highly associated with cancers in the airway such as lung and laryngeal cancers,[7, 27-29] smokeless tobacco use has been associated with cancers of the mouth and throat such as oral and esophageal cancers.[17, 18] A major class of carcinogens in both tobacco smoke and smokeless tobacco products are the tobacco-specific nitrosamines (TSNAs).[125-128] This class of carcinogens includes 4-(methylnitrosamino)-1-(3-pyridyl)-1-butanone (NNK), a compound classified as a group 1 carcinogen by the International Agency for Research on Cancer (IARC).[129] NNK is rapidly metabolized in the body to the (*R*)- and (*S*)- enantiomers of 4-(methylnitrosamino)-1-(3-pyridyl)-1-butanol (NNAL) by carbonyl reduction.[133-135] NNAL can undergo the same CYP-mediated α-hydroxylation pathways as NNK to form reactive intermediates which form DNA adducts.[290-295] It is thought that NNK carcinogenicity is largely manifested via the NNAL formation pathway, with 14%-100% of the NNK dose metabolized to NNAL.[133, 139-141, 296, 297] By measuring NNK in mainstream smoke vs. urinary NNAL in smokers, it was estimated that 39-100% of NNK was converted to NNAL systemically in smokers.[140] NNK exposure in smokeless tobacco users was measured in saliva and it was estimated that 14-17% of NNK was converted to NNAL within the oral cavity.[141] Additionally, it has been shown that NNAL comprised 82-92% of total NNK metabolites in human lung tissue.[139] NNK and NNAL have been extensively studied for carginogenicity in animal

models and have been shown to methylate and pryidyloxobutylate DNA after metabolic activation by cytochrome P450 enzymes in oral and lung tissues [162, 281-283, 298], suggesting that NNK and NNAL are strong oral and lung carcinogens

There are seven enzymes known to metabolize NNK to NNAL: hydroxysteroid dehydrogenases (HSD) 11β1 and 17β12, carbonyl reductase type 1 (CBR1), and aldo-keto reductases (AKR) 1C1, 1C2, 1C3, 1C4, and 1B10.[142-145] These studies further demonstrated that NNK and NNAL are oral and lung carcinogens, indicating that they are likely to be important carcinogens in the tobacco-related cancer incidence observed in tobacco users. (*R)*-NNAL is preferentially formed by HSD17β12, while the remaining enzymes primarily form (S)-NNAL.[145] Like NNK, both (*R*)- and (*S*)-NNAL[133-135] are very potent carcinogens in rodents, with (S)-NNAL exhibiting higher carcinogenic potential than (R)-NNAL.[136-139] These studies further demonstrated that NNK and NNAL are oral and lung carcinogens indicating that they are likely to be important carcinogens in the tobacco-related cancer incidence observed in tobacco users.

Glucuronidation is a conjugation reaction that is mediated by UDP-glucuronosyltransferase (UGT) enzymes. UGT enzymes catalyze the transferring of a glucuronic acid from a UDP-glucuronic acid (UDPGA) cofactor to a nucleophilic functional group. Acceptor functional groups for glucuronidation reactions can be hydroxyl (aliphatic or phenolic), carboxylic acid, amines, thiol groups, and acidic carbon atoms.[8] The UGT superfamily of enzymes consists of 21 functional human enzymes which are responsible for the glucuronidation of drugs, non-drug xenobiotics, and various endogenous compounds.[1, 9] The UGTs are expressed in many of the target tissues exposed to tobacco and/or tobacco smoke and play a primary role in the detoxification of many tobacco carcinogens including TSNAs.[197, 202]

It has been found that (*S*)-NNAL is stereoselectively retained in rat lung and has a higher tumorigenicity than (*R*)-NNAL, and that (*R*)-NNAL exhibits a higher rate of glucuronidation in rats [135, 281-283] and the A/J mouse.[135, 162] However, studies indicate that (*S*)-NNAL may be stereo-selectively retained in smokeless tobacco users [163] yet it exhibits a higher rate of glucuronidation in the patas monkey.[151] It is not clear if either NNAL enantiomer has higher carcinogenic potential in humans.

In contrast to the relatively high tumorigenicity exhibited by both (*R*)- and (*S*)-NNAL, NNAL-Gluc was found to be non-tumorigenic.[162] NNAL can be glucuronidated at the hydroxy group (NNAL-*O*-Gluc) or at the nitrogen within the pyridine ring (NNAL-*N*-Gluc). Since NNAL has a chiral center there are four glucuronide products that can be formed; (*R*)-NNAL-*O*-Gluc, (*S*)-NNAL-*O*-Gluc, (*R*)-NNAL-*N*-Gluc, (*S*)-NNAL-*N*-Gluc. Each of these NNK metabolites have been identified in smoker's urine directly, with NNAL-*N*-Gluc [(*R*)-NNAL-*N*-Gluc + (*S*)-NNAL-*N*-Gluc], NNAL-*O*-Gluc [(*R*)-NNAL-*O*-Gluc + (*S*)-NNAL-*O*-Gluc], and free NNAL accounting for 22-23%, 48-50%, and 27-31% of urinary NNK metabolites, respectively.[3, 159] Few studies have yet explored the tissue specific glucuronidation of NNAL and, to the best of our knowledge, no studies have directly compared the tissue-specific expression of all six NNAL glucuronidating enzymes in the upper aerodigestive tract. The goal of the present study was to characterize the (*R*)- and (*S*)-NNAL clearance capacity of upper aerodigestive tract tissues as well as to determine which UGTs may be driving NNAL clearance in these tobacco-target tissues.

Materials and Methods

Chemicals and materials. Racemic (*rac*)-NNAL (#M325740), NNAL-*N*-Gluc (M325745), NNAL-*O*-Gluc (M325720), and the internal standards (IS) NNAL-*N*-Gluc-d_3

(M325747), and NNAL-*O*-Gluc-d_5 (M325722) were purchased from Toronto Research Chemicals (Toronto, ON, Canada). UDP glucuronic acid (UDPGA), alamethicin, methanol (MeOH) and isopropanol were purchased from Sigma (St Louis, MO), and Dulbecco's modified Eagle's medium, fetal bovine serum (FBS), TaqMan Fast Advanced Master Mix, TaqMan Gene Expression Assays, Pure Link RNA extraction kit, TriZol reagent, SuperScript VILO cDNA synthesis kit, geneticin, and penicillin-streptomycin were all purchased from Life Technologies (Carlsbad, CA). Pooled human liver microsomes (HLM) and pooled human intestinal microsomes (HIM) were purchased from XenoTech (Kansas City, KS) while the Pierce BCA protein assay kit, ammonium acetate and formic acid were purchased from Fisher Scientific (Fair Lawn, NJ).

Tissue Specimens. Human tissue specimens (n=39) were procured from the Cooperative Human Tissue Network (CHTN) or the National Disease Research Institute (NDRI; esophagus, n=13; floor of mouth, n=4; larynx, n=9; tonsil, n=6; tongue n=7). All tissues were normal tissue harvested during surgery or postmortem and were flash frozen in liquid nitrogen upon procurement. Tissue specimens were received via dry ice shipment and were stored at -80°C. Tissues were concurrently prepared for both protein and RNA extractions while specimens were still frozen on dry ice.

Cell lines and tissue protein fractions. HEK293 cells expressing UGT1A4, UGT1A9, UGT1A10, UGT2B7, UGT2B10 and UGT2B17 have been described previously.[153, 285, 286] HEK293 cell lines were grown to 80% confluence in Dulbecco's modified Eagle's medium supplemented with 10% FBS, 100 U/mL penicillin and 100 μg/mL streptomycin, and maintained in 400 μg/mL of geneticin in a humidified incubator atmosphere of 5% CO_2 at 37°C. For the

preparation of cell microsomal fractions, cells were suspended in phosphate-buffered saline (PBS) and subjected to five rounds of rapid freeze/thaw before gentle homogenization. The cell homogenate was centrifuged at 9,000 *g* for 30 min at 4°C. The supernatant was then centrifuged at 105,000 *g* for 60 min at 4°C. The microsomal pellet was suspended in PBS and at -80°C. Total microsomal protein concentrations were determined using the Pierce BCA protein assay.

Each tissue specimen was homogenized in a TissueLyser (Qiagen) for 45 sec at 30 Hz with 500 μL of PBS per 100 μg of tissue. Lysed tissue was then centrifuged for 30 min at 9,000 *g* and the supernatant (S9) was stored at -80°C. Total S9 protein concentrations were determined using the Pierce BCA protein assay. Activity assays were performed for pooled tissue specimens using equivalent protein amounts for each of the pooled specimens.

NNAL glucuronidation assay. The activity of (*R*)- and (*S*)-NNAL-*N*-Gluc, as well as (*R*)- and (*S*)-NNAL-*O*-Gluc formation for tissue S9 fractions and UGT-expressing cell microsomes were determined using the following conditions: after pre-incubation with alamethicin (50 μg/mg total protein) for 10 min on ice, UGT-expressing cell microsomes (15-20 μg total protein), head and neck pooled tissue S9 (8-12 μg total protein), or purchased HLM and HIM (20 ug) were incubated (20 μL, final volume) in 50 mM Tris-HCl (pH 7.4), 10 mM $MgCl_2$, 4 mM UDPGA, and each NNAL enantiomer (UGT over-expressing cell microsomes only, 0.5-16 mM) or *rac*-NNAL (1 mM or 4 mM) at 37°C for 1 h. As described previously, glucuronidation reactions were rate linear for up to 2 h.[257] Reactions were terminated by the addition of an equal volume of cold methanol and spiked with 2 μL of deuterated NNAL-*N*-Gluc and NNAL-*O*-Gluc internal standard mix. The precipitate was removed by centrifugation at 16,000 *g* for 10 min at 4°C and the organic solvent in supernatant was removed by centrifugation under vacuum at room temperature for 20

min prior to transfer to glass vials for liquid chromatography mass spectrometry (LC-MS) analysis. All reactions were performed in triplicate.

LC-MS analysis. LC separation of NNAL-*N*-Glucs and *O*-Glucs was achieved using an Acquity H class ultra-pressure liquid chromatograph (UPLC; Waters) equipped with an auto sampler (model FTN). NNAL-*N*-Gluc, (*R*)-, and (*S*)-NNAL-*O*-Gluc were separated using a method optimized from a previous publication.[299] Briefly, NNAL glucuronide were analyzed with a HSS T3 1.8 μm column (2.1x100 mm; Acquity, Waters, Milford, MA) at 30°C with gradient elution at 0.35 mL/min using the following conditions: 0.5 min with 99% buffer A (5 mM ammonium formate with 0.01% formic acid) and 1% buffer B (100% MeOH), followed by a linear gradient for 3.0 min to 20% buffer B, and a subsequent linear gradient for 1.0 min to 95% buffer B. The column was washed with a 1.0 min linear gradient to 1% buffer B and re-equilibrated for 1.0 min in 1% buffer B.

For analysis of kinetics and S9 activity the Waters Xevo TQD tandem MS was equipped with a Zspray electrospray ionization interface operated in the positive ion mode, with capillary voltage at 0.6 kV. Nitrogen was used as both the cone gas and desolvation gas at 50 and 800 L/hr, respectively. Ultra-pure argon was used for collision-induced dissociation. The desolvation temperature and the ion source temperature were 500 and 150°C respectively. The cone voltage was 20V each and the collision energies were 15 and 20V for NNAL-*N*-Gluc and NNAL-*O*-Gluc diastereomers respectively.

(*R*)- and (*S*)-NNAL-*N*-Glucs were separated using the same UPLC system with gradient elution at a 0.2 mL/min flow rate using the following conditions: a 1 min linear gradient of 100% buffer A (5 mM ammonium formate with 0.01% formic acid) to 99% buffer A and 1% buffer B

(100% acetonitrile), a subsequent isocratic gradient of 99% buffer A for 9 min, followed by a linear gradient for 8 min to 97% buffer A. After an additional 8 min at 97% buffer A, columns were then cleaned with 95% buffer B and re-equilibrated to initial conditions before the next sample injection.

For the analysis of separated (*R*)- and (*S*)-NNAL-*N*-Glucs, the Waters Xevo G2-S Qtof MS was used for the increased resolution. The MS operated in positive electrospray ionization MS/MS sensitive mode, with capillary voltage at 0.6 kV. Nitrogen was used for both cone and desolvation gases at 50 L/h and 800 L/h, respectively. Ultra-pure argon was used as the collision gas with a flow rate of 0.1 L/h for collision-induced dissociation. The source temperature was 120ºC, desolvation gas temperature was 500ºC. The dwell time for each ion was 0.1 sec. The cone voltage 25V and the collision energy was 20V.

For the detection of all NNAL-Glucs, each MS was operated in the multiple reaction monitoring mode (MRM). The ion related parameters for each transition were monitored as follows: NNAL-*N*-Gluc, MS transition of 386.2 *m/z* > 180.1 *m/z* (IS: 389.2 *m/z* > 183.1 *m/z*) and NNAL-*O*-Gluc, MS transition of 386.2 *m/z* > 162.1 *m/z* (IS: 391.2 *m/z* > 167.1 *m/z*). MS transitions and LC retention times for each molecule were compared to purchased NNAL-*O*-Gluc and NNAL-*N*-Gluc standards (Toronto Research Chemicals) for each metabolite. NNAL-*O*-Gluc and NNAL-*N*-Gluc formation was quantified by dividing their peak areas by the peak areas for deuterated NNAL-*O*-Gluc and NNAL-*N*-Gluc internal standards, respectively, and quantified against a standard curve made from purchased NNAL-*O*-Gluc and NNAL-*N*-Gluc (Toronto Research Chemicals) of known quantity.

Determination of UGT Relative Expression Levels. All tissues were treated to by an initial homogenization for 45 sec at 30 Hz with 500 µL of TriZol per 25 µg of tissue. RNA was then extracted from tissue homogenates using a Pure Link RNA kit. RNA concentrations were determined on a Thermo Scientific Nano Drop 2000 spectrophotometer. Reverse transcription was performed using the SuperScript VILO cDNA synthesis kit with 280 ng of starting RNA per reaction.

qPCR was carried out using 10 ng RNA equivalent of cDNA as template. Expression levels of each UGT mRNA was normalized to the expression of ribosomal protein lateral stock P0 (RPLP0). Quadruplicate qPCR was performed for each tissue sample using a 10 µL final reaction volume containing 5 µL of TaqMan Master Mix, 4.5 µL diluted cDNA, and 0.5 µL of UGT specific TaqMan Gene Expression Assay for UGTs 1A4 (Hs01655285_s1), 1A9 (Hs02516855_sh), 1A10 (Hs02516990_s1), 2B7 (Hs00426592_m1), 2B10 (Hs04195423_s1), or 2B17 (Hs00854486_sh) alongside the TaqMan RPLP0 endogenous control assay (Hs99999902_m1). Assays were performed using the Bio-Rad CFX384 Real-Time System under the following conditions: 1 cycle at 95 °C for 10 min, and 40 cycles of 95 °C for 15 sec and 60 °C for 1 min. Relative expression was calculated using the ΔCt method. ΔCt was calculated as the target gene Ct minus the Ct of the control gene (RPLP0). Relative expression within each tissue type was determined with the equation $2^{-\Delta Ct}$. As previously described, UGT genes that amplified with a mean Ct > 35 cycles were determined to be below the limit of quantification (BLQ).[208]

Data Analysis. Kinetic parameters were determined using Prism version 7.0 (GraphPad Software, San Diego, CA). When calculating the mean relative expression values, BLQ transcripts were included in the analysis as zero expression.

Results

Stereospecificity of NNAL-Gluc formation in human upper aerodigestive tract tissues was examined in pooled S9 fractions, assayed as described above and containing 1 mM *rac*-NNAL, consisting equal amount of S and R-NNAL. All upper aerodigestive tract tissues, as well as commercial intestinal microsomes, preferentially formed (*R*)-NNAL-*O*-Gluc over (*S*)-NNAL-*O*-Gluc; only commercial liver microsomes preferentially formed (*S*)-NNAL-*O*-Gluc (Figure 3.1). Intestinal microsomes and esophageal S9 fractions favored the formation of (*R*)-NNAL-*O*-Gluc but also exhibited detectable levels of (*S*)-NNAL-*O*-Gluc formation. S9 fractions from floor of mouth, larynx, tongue, and tonsil exhibited no detectable levels of (*S*)-NNAL-*O*-Gluc formation. None of

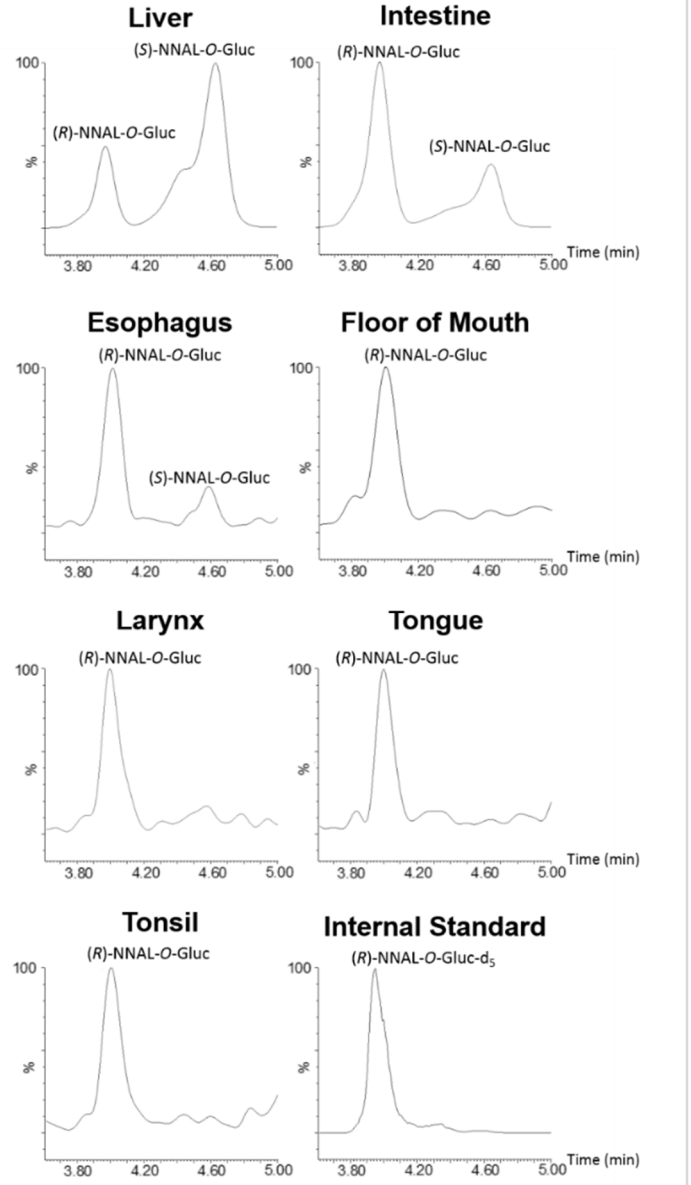

Figure 3.1. Representative traces of LC-MS analysis of NNAL-*O*-Gluc formation by pooled human tissue specimens. Pooled human tissue S9 fractions (8-12 ug total protein) were incubated with 1 mM of *rac*-NNAL and 4 mM UPGA co-substrate as described in the Materials and Methods. Representative traces for (*R*)- and (*S*)-NNAL-*O*-Gluc (**top**) assay products and the (R)-NNAL-O-Gluc-d_5 (**bottom**) are shown. The y-axis is an intensity scale for each panel while the x-axis is time (min).

the tissues examined exhibited detectable levels of NNAL-*N*-Gluc formation except for HLM (data not shown).

Stereo-selective NNAL-*O*-Gluc formation by all 4 UGT enzymes known to form NNAL-O-Gluc was examined by incubating microsomes from HEK293 cells that express UGTs previously examined (UGTs 1A9, 1A10 2B7, 2B17)[299, 300] were incubated with up to 4 mM *rac*-NNAL, by the LCMS method described in method section. Representative chromatograms of each cell line are shown in Figure 3.2A. UGT1A9 exhibited the lowest level of stereo-specificity, with ~55% of total NNAL-*O*-Gluc formation being (*R*)-NNAL-*O*-Gluc. UGTs 2B7 and 1A10 exhibited the highest levels of stereo-specificity, each forming $\leq$5% (*S*)- or (*R*)-NNAL-*O*-Gluc, respectively. UGT2B17 exhibited stereo-selectivity for the formation of (*R*)-NNAL-*O*-Gluc with ~10% of the total NNAL-*O*-Gluc formation being (*S*)-NNAL-*O*-Gluc.

A method was developed to separate and identify (*R*)- and (*S*)-NNAL-*N*-Glucs formed by UGT2B10 and UGT1A4. Microsomes from HEK293 cell lines expressing each UGT were incubated with 4 mM *rac*-NNAL or 2 mM of each NNAL enantiomer, as described above. Separation of the NNAL-*N*-Gluc diastereomers was achieved but with overlap between the minor rotamer (*R*)-NNAL-*N*-Gluc peak and the main rotamer peak of (*S*)-NNAL-*N*-Gluc (Figure 3.2B). Because these rotamers are created by the rotation of the nitroso group that can be sterically hindered by proximity to the chiral alcohol group and the free movement of the nitroso bond, these compounds that cannot be isolated from each other. The retention time of the main (*R*)-NNAL-*N*-Gluc peak was 5.6 min and was identified by the retention time of the peak formed when (*R*)-NNAL was incubated with each UGT. The retention time of the main (*S*)-NNAL-*N*-Gluc peak was 5.9 min and was identified by matching with the retention time of the peak formed when (*S*)-NNAL was incubated with each UGT. UGT1A4 appears to exhibit a slight preference for the

formation of (*S*)-NNAL-*N*-Gluc when incubated with *rac*-NNAL while UGT2B10 appears to have a slight preference for the formation of (*R*)-NNAL-*N*-Gluc with the same assay.

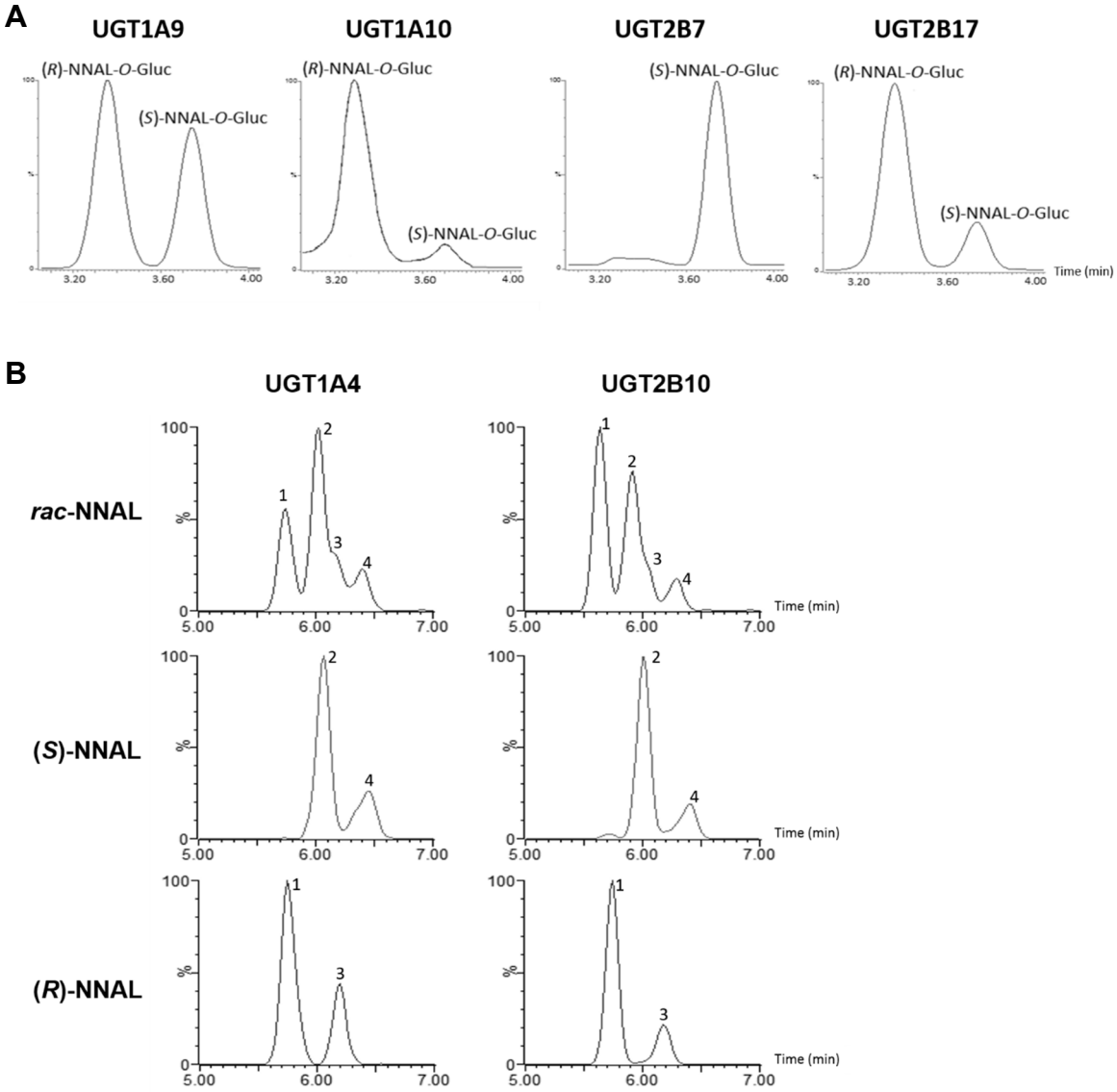

Figure 3.2. Representative traces of LC-MS analysis of NNAL-*O*-Gluc and NNAL-*N*-Gluc formation from *rac*-NNAL. UGTOver-expressing cell microsomes (15-20 ug total protein) were incubated for 1 h at 37ºC with 4 mM of the co-substrate UDPGA and substrate *rac*-NNAL, (*S*)-NNAL, or (*R*)-NNAL as described in the Materials and Methods. Concentrations of *rac*-NNAL were at 4 mM or at the K_M for each enzyme, whichever was smaller. The y-axis isare scaled arbitrary units where 100% is the highest peak in each assay. (*S*)- and (*R*)-NNAL-*O*-Gluc peaks (panel A) are single peaks that contain the NNAL-*O*-Gluc rotamers. (*S*)- and (*R*)-NNAL-*N*-Gluc peaks (panel B; peaks 2 and 4, and 1 and 3, respectively) are the separate NNAL-*N*-Gluc rotamers. From the *rac*-NNAL assay, the shoulder (peak 3) on the (*S*)-NNAL-*N*-Gluc peak (peak 2) was attributed to one of the (*R*)-NNAL-*N*-Gluc rotamers by retention times matched to assays with (*R*)- and (*S*)-NNAL. The y-axis is an intensity scale for each panel while the x-axis is time (min).

The UGT stereo-specificity against NNAL was further characterized enzyme kinetic analysis. Microsomes from cells overexpressing each of the previously characterized NNAL glucuronidating enzymes (UGTs 1A9, 2B7, 2B10, and 2B17)[299] in addition to UGTs 1A4 and 1A10 were incubated with the (*R*)- and (*S*)-NNAL enantiomers separately, over a concentration range from 0.5-16 mM NNAL (Figure 3.3). Comparing kinetic curves for (*R*)- and (*S*)-NNAL UGTs 1A10 and 2B17 exhibited a clear difference in the rates of (*R*)-NNAL-*O*-Gluc vs (*S*)-NNAL-*O*-Gluc formation, clearly favoring the (*R*)-NNAL enantiomer as substrate (Figure 3.3A). While accurate kinetic values could not be determined for UGT1A10, there was a 1.9-fold lower K_M and a 11-fold higher V_{max}/K_M observed for UGT2B17 for NNAL(*R*)-Gluc vs. NNAL(*S*)-Gluc formation (Table 3.1). UGT2B7 also exhibited a clear difference in the rate of formation for each NNAL-*O*-Gluc diastereomer, clearly favoring (*S*)-NNAL as substrate (Figure 3A). This is consistent with the >3.3-fold lower K_M observed for UGT2B7 for NNAL-(*S*)-Gluc vs. NNAL-(*R*)-

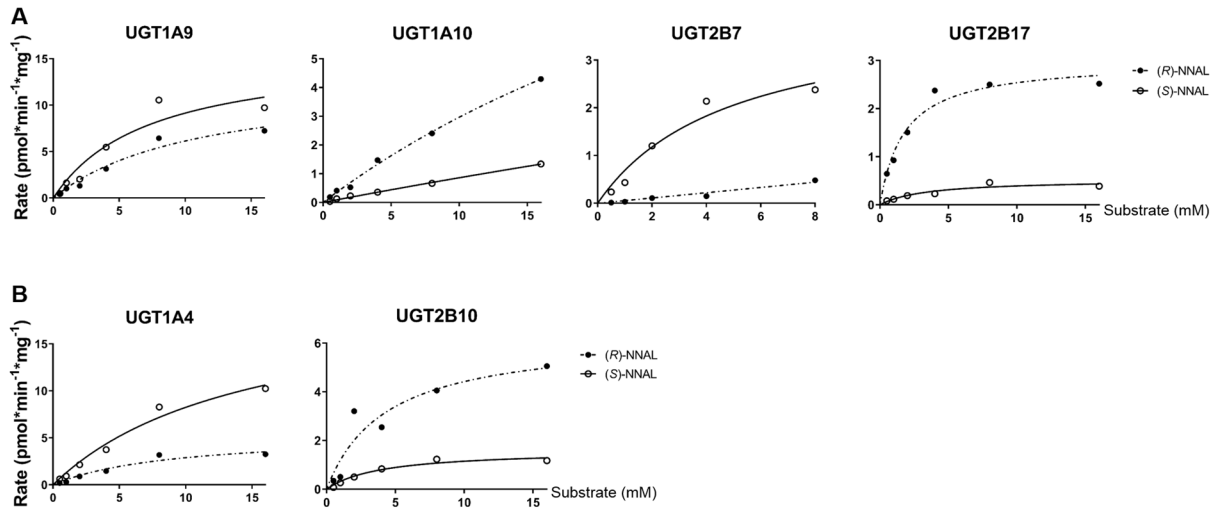

Figure 3.3. Representative concentration curves for the formation of NNAL-O-Gluc and NNAL-N-Gluc by individual UGT enzymes. A, NNAL-O-Gluc formation by UGTs 1A9, 1A10, 2B7 and 2B17. **B**, NNAL-N-Gluc formation by UGTs 1A4 and 2B10. Glucuronide formation assays were performed with 15-20 µg of UGT-T overexpressing microsomal protein and 0.5-16 mM of either (R)-NNAL (●) or (S)-NNAL (○) incubated at 37°C for 1 h.

Gluc formation (Table 3.1). While UGT1A9 exhibited marginal specificity for (*R*)-NNAL-O-Gluc formation when incubated with rac-NNAL (Figure 2A), UGT1A9 indicated a marginally faster rate of NNAL-*O*-Gluc formation with pure (*S*)-NNAL as substrate (Figure 3.3A), a pattern consistent with its marginal 1.5-fold lower K_M and 1.6-fold higher V_{max}/K_M for (*S*)-NNAL-*O*-Gluc vs. (*R*)-NNAL-*O*-Gluc formation (Table 3.1).

Cell microsomes expressing the two enzymes that form NNAL-*N*-Gluc (UGTs 1A4 and 2B10) were also incubated with (*R*)- and (*S*)-NNAL in separate reactions. UGTs 1A4 and 2B10 exhibited stereoselectivity, with UGT1A4 exhibiting a faster rate of (*S*)-NNAL-*N*-Gluc formation and UGT2B10 exhibiting a faster rate of (*R*)-NNAL-*N*-Gluc formation (Figure 3B). These data are consistent with the 2.3- and 2.4-fold higher V_{max}/K_M observed for (*S*)-NNAL-*N*-Gluc and (*R*)-NNAL-*N*-Gluc formation for UGTs 1A4 and 2B10, respectively (Table 3.1).

Table 3.1. Michaelis-Menton kinetic values of UGT-expressing microsomes with each NNAL enantiomer.[a,b]

		NNAL-*O*-Gluc				NNAL-*N*-Gluc	
		UGT1A9	UGT1A10	UGT2B7	UGT2B17	UGT1A4	UGT2B10
(R)-NNAL	K_M[c]	11 ± 5.0	>16	>16	1.8 ± 0.40	9.0 ± 4.7	4.3 ± 2.5
	V_{max}[d]	13 ± 3.2	ND	ND	3.0 ± 0.20	5.5 ± 1.4	6.3 ± 1.5
	V_{max}/K_M[e]	0.58 ± 0.49	ND	ND	1.7 ± 1.0	0.61 ± 0.30	0.99 ± 0.62
(S)-NNAL	K_M[c]	7.3 ± 4.5	>16	4.9 ± 2.6	3.4 ± 1.7	15 ± 6.0	4.0 ± 1.4
	V_{max}[d]	16 ± 4.6	ND	4.0 ± 1.1	0.50 ± 0.10	21 ± 5.0	1.6 ± 0.20
	V_{max}/K_M[e]	0.94 ± 0.88	ND	1.9 ± 0.54	0.16 ± 0.11	1.4 ± 0.81	0.41 ± 0.057

[a] Substrate concentration ranges tested were 0.5-16 mM.
[b] All values are expressed as mean ± SD for 3 independent experiments.
[c] K_M values are in mM concentrations.
[d] V_{max} are in pmol· min^{-1}· mg total protein.
[e] V_{max}/K_M are in min^{-1}·mg total $protein^{-1}$·nL.
ND, indicates unsaturated curves where values could not be determined.

The inter-individual level of expression of each UGT with known NNAL activity was measured by qPCR in several aerodigestive tract tissues including esophagus, floor of mouth, larynx, tongue, and tonsil (Figure 3.4). Previous studies using the same UGT expression kits as used in the present study demonstrated minimal differences in expression efficiencies.[208] The house keeping gene RPLP0 was selected as the experimental endogenous control due to known gene stability and high expression levels across tissue types as determined by the manufacturer (Applied Biosystems). No expression of any gene, including the housekeeping RPLP0 gene, was observed for three specimens (one each of esophagus, larynx, and tongue), and these specimens were excluded from the data set. Any UGT gene that amplified with a mean Ct > 35 cycles was determined to be below the limit of quantification (BLQ) and were included in the calculations of mean relative expression as exhibiting zero gene expression. Each UGT was stratified by relative non-zero expression in each tissue tested for both NNAL-*O*-Gluc (Figure 3.4A) and NNAL-*N*-Gluc forming enzymes (Figure 3.4B). UGTs 1A9 and 1A10 exhibited the highest inter-individual differences in expression in esophagus and tongue with a 100-fold difference in expression between the lowest and highest expressing samples, while floor of mouth and tonsil exhibited the least variation in expression between specimens with up to a 10-fold difference in relative expression between samples for both sites. UGTs 2B7 and 2B17 exhibited the largest inter-individual expression differences in larynx and tongue with a 100-fold difference in expression between the highest and lowest expressing samples. Similar to UGTs 1A9 and 1A10, UGTs 2B7 and 2B17 exhibited the lowest inter-individual expression differences in floor of mouth and tonsil.

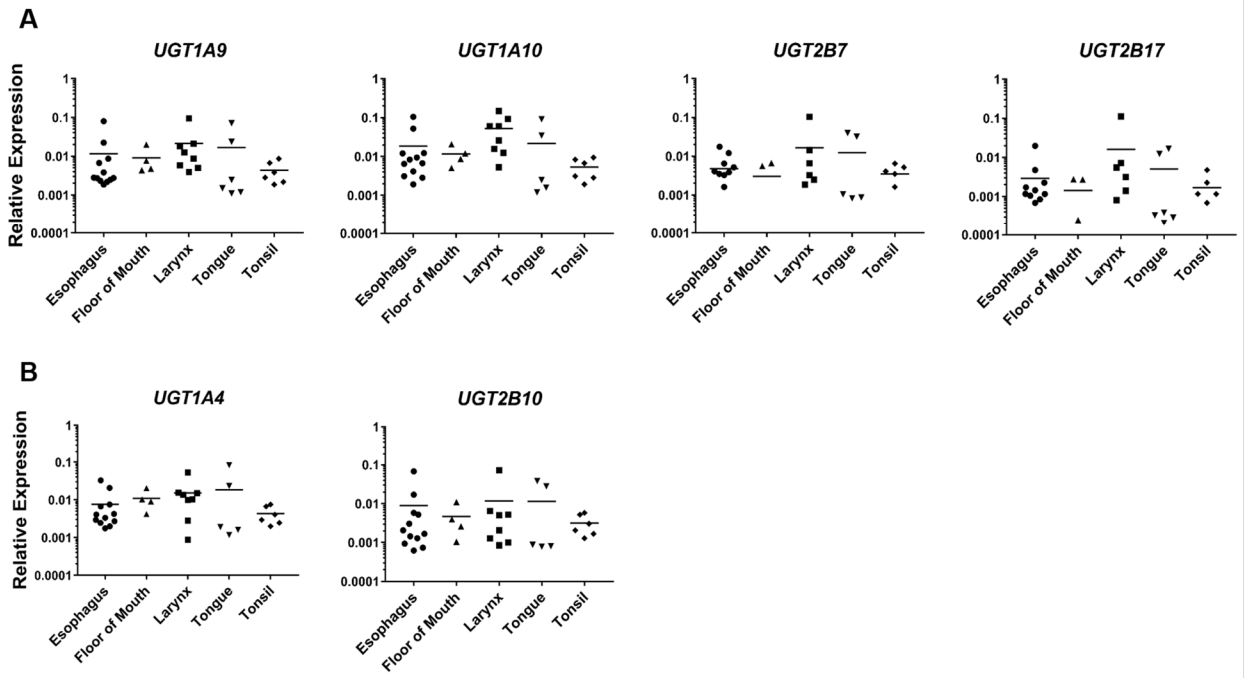

Figure 3.4. Relative expression levels of UGT genes in upper aerodigestive tract tissues. UGT mRNA expression levels were calculated in 36 normal tissue specimens: esophagus (n=12), floor of mouth (n=4), larynx (n=8), tongue (n=6), and tonsil (n=6). Expression was calculated as arbitrary units relative to the housekeeping gene RPLP0 via the ΔCt method, with each point representing the $2^{-\Delta Ct}$ for each UGT in each specimen and separated by NNAL-*O*-Gluc forming UGTs (Panel A) and NNAL-*N*-Gluc forming UGTs (Panel B). Specimens with UGT expression below the limit of quantification (mean Ct > 35 cycles) are not shown (UGT1A10, n=1; UGT2B17, n=9; UGT2B17, n=7). The y-axis is relative expression (arbitrary units).

The most highly expressed NNAL-*O*-glucuronidating UGT in upper aerodigestive tract tissues was UGT1A10 (Table 3.2). UGT1A10 exhibited mean values between 1.6- and 6.6-fold higher than mean values of expression in esophagus, 1.3 and 8.6-fold higher than floor of mouth, 2.5- and 4.4-fold higher than larynx, 1.2- and 4-fold higher than tongue, and 1.3- and 3-fold higher than tonsil, as compared to the other *O*-glucuronidating UGTs. UGT1A9 was the second most highly expressed *O*-glucuronidating UGT, followed by UGT2B7 and UGT2B17, in all tissues examined. For the NNAL-*N*-glucuronidating UGTs, 1A4 and 2B10 exhibited similar levels of expression in all aerodigestive tract tissues examined except floor of mouth, where UGT1A4

Table 3.2. Mean[a] relative UGT expression in human tissue specimens.[b]

		NNAL-*O*-Gluc				NNAL-*N*-Gluc	
		UGT1A9	UGT1A10	UGT2B7	UGT2B17	UGT1A4	UGT2B10
Esophagus	Mean	1.16E-02	1.87E-02	4.81E-03	2.91E-03	7.64E-03	9.00E-03
	SE	6.45E-03	8.75E-03	1.52E-03	1.58E-03	2.75E-03	5.53E-03
	% Total	30.5%	49.2%	12.7%	7.7%	45.9%	54.1%
	# BLQ	0 of 12	0 of 12	3 of 12	2 of 12	0 of 12	0 of 12
Floor of Mouth	Mean	9.18E-03	1.16E-02	3.06E-03	1.43E-03	1.10E-02	4.67E-03
	SE	3.63E-03	3.35E-03	1.78E-03	7.57E-04	3.41E-03	2.20E-03
	% Total	36.3%	46.0%	12.1%	5.7%	70.3%	29.7%
	# BLQ	0 of 4	0 of 4	2 of 4	1 of 4	0 of 4	0 of 4
Larynx	Mean	2.12E-02	5.26E-02	1.65E-02	1.62E-02	1.51E-02	1.18E-02
	SE	1.07E-02	1.74E-02	1.25E-02	1.36E-02	5.72E-03	8.66E-03
	% Total	19.9%	49.4%	15.5%	15.2%	56.3%	43.7%
	# BLQ	0 of 8	0 of 8	2 of 8	2 of 8	0 of 8	0 of 8
Tongue	Mean	1.68E-02	2.18E-02	1.24E-02	5.02E-03	1.86E-02	1.15E-02
	SE	1.14E-02	1.48E-02	7.46E-03	3.04E-03	1.35E-02	7.01E-03
	% Total	30.0%	38.9%	22.1%	9.0%	61.7%	38.3%
	# BLQ	0 of 6	1 of 6	1 of 6	0 of 6	1 of 6	1 of 6
Tonsil	Mean	4.35E-03	5.40E-03	3.47E-03	1.68E-03	4.30E-03	3.19E-03
	SE	1.12E-03	1.29E-03	9.61E-04	6.90E-04	9.48E-04	7.83E-04
	% Total	29.2%	36.2%	23.3%	11.3%	57.4%	42.6%
	# BLQ	0 of 6	0 of 6	1 of 6	1 of 6	0 of 6	0 of 6

[a] Mean relative expression (arbitrary units) was calculated to include UGTs with no expression.
[b] The % total for the expression of each UGT was calculated separately for NNAL-*O*-Gluc and NNAL-*N*-Gluc enzymes.
BLQ, below limit of quantification (mean Ct > 35 cycles).

exhibited 2.3-fold higher levels of expression as compared to UGT2B10 (Table 3.2). In addition, the expression of UGTs 1A4 and 2B10 was either similar to or less than UGT1A10 in all tissues examined.

Discussion

Glucuronidation is the primary detoxification pathway for TSNAs. Previous studies into the stereo-specificity of NNAL glucuronidation focused primarily on hepatic UGTs and systemic NNAL clearance.[3, 299] The present study focuses on understanding the stereo-specific glucuronidation of NNAL in aerodigestive tract tissues, which are targets for tobacco-induced cancer.[17] One of the major findings from the present study is that all of the aerodigestive tract tissues tested exhibited a strong preference for (*R*)-NNAL-*O*-Gluc formation. S9 fractions from tissues within the oral cavity (floor of mouth, tongue, tonsil) and airways (larynx) exhibited low levels of (*S*)-NNAL-*O*-Gluc formation capacity (<5%). This pattern is similar to that observed previously in human lung microsomes.[145] While HIM and the S9 fraction from esophagus exhibited higher ratios of (*S*)-NNAL-*O*-Gluc:(*R*)-NNAL-*O*-Gluc formation capacity than other aerodigestive tract tissues, the levels of (*S*)-NNAL-*O*-Gluc formation were still less than 10% of the total NNAL-*O*-Gluc in both cases. This preference for (*R*)-NNAL-*O*-Gluc formation contrasts with that observed in HLM where (*S*)-NNAL-*O*-Gluc formation is preferentially formed.

Data from the present study suggest that the differences in stereo-selectivity for (*R*)-NNAL-*O*-Gluc formation [over (*S*)-NNAL-*O*-Gluc formation] in aerodigestive tract tissues vs liver may be due to differences in the expression of the UGTs expressed within these tissues. Each of the four enzymes that mediate the formation of NNAL-*O*-Gluc exhibit a distinctive stereo-

selective glucuronide formation profile when incubated with *rac*-NNAL. The pattern of stereo-selectivity observed for each enzyme upon incubation with *rac*-NNAL was also observed at each concentration tested for the separate NNAL enantiomers. As observed in previous studies, UGT1A9 exhibited the least stereo-specificity for NNAL enantiomers.[299] UGTs 1A10 and 2B17 each exhibited a strong preference for (*R*)-NNAL, with UGT2B7 being the only UGT to exhibit a preference for (*S*)-NNAL.[3, 299] The kinetic parameters for each UGT isoform were similar to previously published values for (*R*)- and (*S*)-NNAL,[299] except for UGTs 1A10 and 1A4, which did not have previously reported values. UGT1A10 exhibited a much higher rate of formation for (*R*)-NNAL-*O*-Gluc at every concentration tested, but did not yield kinetic values within the Michaelis-Menten kinetic equation at the substrate levels tested.

Limitations of the present study include the use of mRNA quantification, rather than direct measurement of protein levels. To the best of our knowledge, protein detection methods for each UGT sensitive enough for the tissue specimens within this study have not yet been developed. Additional limitations include small sample sizes for each tissue type that doesn't allow for age, sex, or race comparisons. However, future studies could include larger samples sizes to further explore the impact of *UGT1A10* and *UGT2B17* gene polymorphisms on the rate of detoxification in aerodigestive tract tissues. This study is the first to develop a direct separation method for the detection of (*R*)- and (*S*)-NNAL-*N*-Gluc. UGT2B10 and UGT1A4 exhibit activity with *rac*-NNAL similar to the stereo-preferences exhibited by the enantio-specific kinetic assays with preferences for (*R*)- and (*S*)-NNAL respectively. The separation method resulted in some overlap between the minor peak of (*R*)-NNAL-*N*-Gluc and the major peak of (*S*)-NNAL-*N*-Gluc, which limits the ability of this method to quantify the levels of each *N*-Gluc diastereomer. A qualitative assessment indicated that the pattern of (*R*)- and (*S*)-NNAL-N-Gluc formation from assays with *rac*-NNAL

match the differences observed in the kinetic analysis performed for UGT2B10 and UGT1A4 with each NNAL enantiomer separately, where UGT2B10 exhibits a preference for (*R*)-NNAL and UGT1A4 exhibits a preference for (*S*)-NNAL. Previous *in vivo* studies have indicated that UGT2B10 is responsible for >90% of NNAL-N-Gluc formation.[3] These data indicate that the NNAL-*N*-Gluc identified *in vivo* may primarily be the (*R*)-NNAL-*N*-Gluc form. Interestingly, none of the aerodigestive tract tissues tested in the present study exhibited detectable levels of NNAL-*N*-Gluc when incubated with *rac*-NNAL. Since UGT2B10 and UGT1A4 expression was observed in each of these tissue types, the lack of NNAL-*N*-Gluc formation in upper aerodigestive tract tissues may be due to limitations in assay sensitivity. Alternatively, the V_{max} values described for the UGT-expressing microsomes in this study are per mg of total protein, not per UGT protein. Therefore, they are not a reflection of actual V_{max} differences between individual enzymes and are useful only when comparing kinetic values of the same UGT for different substrates. It is possible, therefore, that UGTs 2B10 and 1A4 exhibit significantly lower actual V_{max} values as compared to the NNAL-*O*-glucuronidating UGTs (including UGT1A0 and UGT2B17), resulting in limited upper areodigestive tract tissue NNAL-*N*-Gluc formation capacity even though both UGTs 2B10 and 1A4 are expressed in these tissues.

UGT1A10 has often been overlooked for contribution to NNAL metabolism because it is the only extra-hepatic enzyme with NNAL glucuronidation activity.[197] The data from the present study show that UGT1A10 was the most highly expressed NNAL-glucuronidating UGT in tissues of the upper aerodigestive tract. UGT1A10 comprised nearly half of the total NNAL-*O*-Gluc forming UGT genes in esophagus, floor of mouth, and larynx, and nearly 40% of the total in tongue and tonsil. The high stereo-specificity exhibited by UGT1A10 for (R)-NNAL-O-Gluc formation is consistent with the similar stereo-specificity exhibited for (R)-NNAL-O-Gluc formation in

aerodigestive tract tissues. The other UGT with high stereo-specificity for (R)-NNAL-O-Gluc formation, UGT2B17, is expressed at 3.2- to 8.6-fold lower levels than UGT1A10 in the aerodigestive tract tissues examined. While the K_M was higher for UGT1A10 than UGT2B17 for (R)-NNAL, an assessment of differences in V_{max} between enzymes could not be examined due to reaction rates being calculated per mg of total microsomal protein for each UGT-expressing cell line.

The low levels of (*S*)-NNAL-*O*-Gluc formation [relative to (*R*)-NNAL-*O*-Gluc formation] in upper aerodigestive tract tissues is consistent with the low levels of UGT2B7 expression in these tissues. UGT2B7 is the only enzyme that exhibits high stereo-specific activity for (*S*)-NNAL, and although NNAL glucuronidation has not been observed in assays with lung tissue, (*R*)-NNAL glucuronidation may also form at a higher rate [relative to (*S*)-NNAL-*O*-Gluc] in lung as UGT2B17 has been shown to be higher expressed that UGT2B7 in lung tissue.[208] It is interesting that UGT1A9 exhibits relatively high levels of expression in upper aerodigestive tract tissues. However, it exhibits a relatively high K_M against both NNAL enantiomers, and its V_{max} against both NNAL enantiomers could not be compared with the other UGT enzymes. The fact that relatively low levels of (*S*)-NNAL-*O*-Gluc formation was observed in upper aerodigestive tract tissues suggests a limited role for both UGTs 1A9 and 2B7 in the glucuronidation of NNAL in these tissues.

The data presented in this study suggests that UGT1A10 may be an important enzyme in the detoxification of NNAL, and therefore NNK, in upper aerodigestive tract tissues. In addition to detoxifying NNAL, UGT1A10 exhibits glucuronidating activity against the carcinogenic polycyclic aromatic hydrocarbons found in tobacco smoke.[285, 301] Additionally, UGT1A10 polymorphisms have been identified as independent risk factors for upper areodigestive tract

cancer in smokers.[302] Therefore, UGT1A10 may be an important enzyme in the detoxification of tobacco carcinogens in upper aerodigestive tract tissues.

CHAPTER FOUR

THE ROLE OF L- AND D-MENTHOL IN THE GLUCURONIDATION AND DETOXIFICATION OF THE MAJOR LUNG CARCINOGEN, NNAL

Shannon Kozlovich[§], Gang Chen[§], Christy JW Watson[§], William J Blot[+] and Philip Lazarus[*§]

[§]Department of Pharmaceutical Sciences, College of Pharmacy and Pharmaceutical Sciences, Washington State University, Spokane WA

[+]Division of Epidemiology, Vanderbilt University Medical Center, Nashville TN

[*]Corresponding author: Philip Lazarus, Ph.D., Department of Pharmaceutical Sciences, College of Pharmacy and Pharmaceutical Sciences, Washington State University, Spokane WA 99210; Email: phil.lazarus@wsu.edu

Abstract

Menthol, which creates mint flavor and scent, is often added to tobacco in both menthol and non-menthol cigarettes. 4-(methylnitrosamino)-1-(3-pyridyl)-1-butanone (NNK), a potent tobacco carcinogen, is extensively metabolized to equally carcinogenic chiral 4-(methylnitrosamino)-1-(3-pyridyl)-1-butanol [(*R*)- or (*S*)-NNAL]. NNAL is detoxified by several UDP-glucuronosyltransferase (UGT) enzymes with glucuronidation occurring on either NNAL's pyridine ring nitrogen (NNAL-*N*-Gluc) or the chiral alcohol [(*R*)- or (*S*)-NNAL-*O*-Gluc]. Evidence suggests that menthol may decrease NNAL detoxification, yet the underlying mechanism of menthol interaction within this pathway remains unclear. To identify the UGTs involved in menthol metabolism and inhibition of NNAL glucuronidation *in vitro* menthol

glucuronidation assays and menthol inhibition of NNAL-Gluc formation assays were performed. Additionally, NNAL and menthol glucuronides (MG) were measured in the urine of smokers (n=100) from the Southern Community Cohort Study. UGTs 1A9, 1A10, 2A1, 2A2, 2A3, 2B4, 2B7 and 2B17 exhibited glucuronidating activity against both L- and D-menthol. In human liver microsomes, both L- and D-menthol inhibited the formation of each NNAL-Gluc, with a stereospecific difference observed between the formation of (*R*)-NNAL-*O*-Gluc and (*S*)-NNAL-*O*-Gluc in the presence of D-menthol but not L-menthol. Urinary MG was detected in menthol and non-menthol smokers with D-MG only contributing 1.3% to total MG levels. Levels of urinary NNAL-*N*-Gluc significantly ($p<0.05$) decreased among subjects with high levels of total urinary MG, indicating that the presence of menthol could lead to NNAL being retained in the body longer, which could increase the opportunity for NNAL to damage DNA and lead to the development of tobacco-related cancers.

Introduction

Tobacco use is considered by the World Health Organization to be the leading cause of preventable premature death in adults worldwide.[303] Tobacco specific nitrosamines (TSNAs) including (methylnitrosamino)-1-(3-pyridyl)-1-butanone (NNK) are among the most potent carcinogens found in both tobacco smoke and smokeless tobacco. NNK is rapidly metabolized in smokers by carbonyl reduction to both the (*R*)- and (*S*)- enantiomers of the equally potent carcinogen, 4-(methylnitrosamino-1-(3-pyridyl)-1-butanol (NNAL).[297] NNK metabolism occurs rapidly enough that NNK levels have not been detected in the urine of smokers, and is therefore measured by levels of NNAL and NNAL metabolites.[304] The glucuronidation of NNAL by the UDP glucuronosyltransferase (UGT) family of enzymes is considered to be an important mechanism for NNK detoxification,[162] forming an *O*-glucuronide (*O*-Gluc) on the alcohol within the NNAL side chain or an *N*-glucuronide (*N*-Gluc) on the nitrogen of the NNAL pyridine ring. UGTs 1A9, 1A10, 2B7, and 2B17 have been shown to form NNAL-*O*-Gluc.[153, 250-252, 254, 300] UGTs 2B7 and 2B17 exhibiting high levels of stereospecific formation of (*S*)-NNAL-*O*-Gluc and (*R*)-NNAL-*O*-Gluc, respectively.[299] While both UGTs 2B10 and 1A4 were shown to form NNAL-*N*-Gluc *in vitro*,[250, 255, 256, 299] UGT2B10 was responsible for >90% of NNAL-*N*-Gluc formation in human liver microsomes (HLM) and in the urine of smokers. [3, 257, 262]

Menthol is a flavor additive in many brands and types of tobacco products. It is listed by the FDA as 'generally regarded as safe' (GRAS) but is regulated as a drug when it is the active ingredient in a medication and subsequently has required dosage labeling in these situations. However, when used as a flavor additive in tobacco products, there are no labeling requirements for the amount of menthol added.[40] While a cohort study reported an increased risk of developing

lung cancer for male menthol smokers when compared to non-menthol smokers,[305] other epidemiologic investigation have not found similar trends.[306-313] Indeed, epidemiology data from the entire Southern Community Cohort Study, from which the urine samples in the present analysis were drawn, show a significantly lower lung cancer risk, by about 30%, among menthol than non-menthol smokers for both black and white racial groups,[311, 313] and two meta analyses likewise show lower rather than higher risks of lung cancer among menthol compared to non-menthol smokers.[314, 315] However, with the presence of menthol in many edible and topical products in the U.S., the presence of either L- or D-menthol metabolites in the urine of smokers could be from menthol sources other than tobacco. Previously, urinary menthol was not found to be associated directly with levels of dietary menthol,[316] and potentially could arise from a complex mix of exposures from edible, topical, and tobacco products in both menthol and non-menthol smokers. Since the underlying mechanism to determine menthol's impact for health risk in smokers is currently unknown, an understanding of the molecular basis of menthol clearance and the mechanism of inhibition within the clearance pathway of tobacco carcinogens may aid in understanding the health disparities for the racial groups with the highest rate of menthol cigarette use.

Menthol is a chiral aliphatic alcohol, existing as either the D- or L-menthol and the racemic mixture referred to as DL-menthol. The only naturally occurring enantiomer, the one found in and isolated from a variety of mint plant species, is L-menthol. The other enantiomer, D-menthol, is a product of the Haarmann & Reimer industrial synthesis process which yields a DL-menthol mixture.[270] It has been long known that D-menthol doesn't produce the same smell and taste profile normally associated with naturally occurring menthol and that its analgesic properties are greatly reduced when compared to L-menthol.[271-273] When menthol is the active ingredient in over-the-

counter pharmaceuticals, such as lozenges, only the L-menthol enantiomer tends to be present,[317] however, the same may not be true for tobacco products. Studies have examined the total menthol content in both menthol and non-menthol cigarettes, which can range from 1.0-0.3% wt/wt [274] in menthol cigarettes and up to 0.03% wt/wt menthol in non-menthol cigarettes.[275] While DL-menthol has previously been identified as an inhibitor of both NNAL-*O*-Gluc and NNAL-*N*-Gluc production in HLM,[276] no studies have been performed to determine which UGT enzymes are being inhibited or which menthol enantiomer is driving the inhibition.

The racial groups in the U.S. with the highest rate of menthol smokers, African Americans [305] and Native Hawaiians,[40] also have the highest rate of tobacco-related cancers among smokers.[58-60, 318, 319] It has been shown that while African Americans smoke fewer cigarettes per day than smokers in other racial groups,[320-322] they may be exposed to more toxins per cigarette,[323, 324] Native Hawaiians have a higher rate of tobacco-related DNA damage when compared to Caucasian and Japanese Americans.[325] Genetic differences in the tobacco addiction pathway do not seem to account for the differences in cancer risk observed between these populations.[58]

The underlying mechanism or interaction of menthol within the tobacco carcinogen pathway has yet to be fully elucidated. L-menthol exhibits inhibition of CYP2A6 and CYP2A13 carcinogen activation and nicotine metabolism,[326] but CYPs do not directly metabolize menthol. It is known that menthol is rapidly cleared from the body as a menthol glucuronide (MG),[277, 278] the same clearance pathway as the TSNAs. Yet, no previous research has described the complete clearance pathway of menthol enantiomers. The goal of the present study was to identify the enzymes responsible for the metabolism of both L- and D-menthol to their respective glucuronides,

as both could possibly be found in tobacco products,[40] and to investigate the potential impact of each menthol enantiomer on NNAL glucuronide formation *in vivo*.

Methods

Chemicals and materials. *rac*-NNAL (M325740), NNAL-*N*-Gluc (M325745), NNAL-*O*-Gluc (M325720), NNAL-$13C_6$ (M325741), L-MG (M218880), L-MG-d_4 (M218882) NNAL-*N*-Gluc-d_3 (M325747), and NNAL-*O*-Gluc-d_5 (M325722) were purchased from Toronto Research Chemicals (Toronto, ON, Canada). L- and D-menthol (W266523, 224464), UDP glucuronic acid (UDPGA), alamethicin, methanol (MeOH) and acetonitrile (ACN) were purchased from Sigma (St Louis, MO). Dulbecco's modified Eagle's medium, fetal bovine serum (FBS), geneticin and penicillin-streptomycin were purchased from Life Technologies (Carlsbad, CA). The Pierce BCA protein assay kit, ammonium acetate and formic acid were purchased from Fisher Scientific (Fair Lawn, NJ).

Subjects and biospecimens. Urine and subject demographics were obtained from 100 self-identified current smokers upon recruitment into the Southern Community Cohort Study (SCCS), a prospective cohort of over 84,000 participants recruited between 2002 and 2009.[327] One-time spot urine samples (~60 mL) were collected from SCCS participants at community health centers beginning in 2004. Samples were refrigerated on-site and shipped overnight to Vanderbilt Medical Center where urine was mixed with a small amount of ascorbic acid and stored at -80°C.

Urine specimens (150 μL each) were randomly chosen from 50 menthol smokers and 50 non-menthol smokers, were received at Washington State University College of Pharmacy and

Pharmaceutical Sciences for analysis by overnight shipment, and subsequently stored at -80°C. Smoking preference for menthol cigarettes was self-identified at the time of urine sample collection. Subjects were 34% white, 60% black, 1% Hispanic, and 5% mixed race, and comprised 56% women.

Pooled (n=200) HLM and pooled (n=10) human intestinal microsomes (HIM) were purchased from Xenotech (Lenexa, KS).

Cell lines and microsomal preparation. HEK293 cells expressing each of the 18 human UGTs 1A1, 1A3, 1A4, 1A5, 1A6, 1A7, 1A8, 1A9, 1A10, 2A1, 2A2, 2A3, 2B4, 2B7, 2B10, 2B11, 2B15, and 2B17 have been described previously [153, 285, 286]. All HEK293 cell lines were grown to 80% confluence in 30 mL of Dulbecco's modified Eagle's medium supplemented with 10% fetal bovine serum, and maintained in 400 μg/mL of geneticin in a humidified incubator atmosphere of 5% CO_2. For the preparation of cell microsomal fractions, cells were suspended in phosphate buffered saline (PBS) and subjected to five rounds of freeze/thaw before gentle homogenization. The cell homogenate was centrifuged at 9,000 *g* for 30 min at 4°C and the supernatant was further centrifuged at 105,000 *g* for 60 min at 4°C. The microsomal pellet was re-suspended in PBS and stored at -80°C. Total microsomal protein concentrations were determined using the BCA protein assay.

L- and D-menthol glucuronidation assay. L- and D-MG formation was determined in HLM (10 μg protein), HIM (20 μg protein), and UGT-expressing cell microsomes (15-20 μg protein) after pre-incubation with alamethicin (50 μg/mg protein) for 10 min on ice. Incubations (20 μL, final volume) included 50 mM Tris-HCl (initial pH 7.4), 10 mM $MgCl_2$, 4 mM UDPGA,

2% BSA, and either D- or L-menthol. Screening assays used 1.0 mM D- or L-menthol as substrate while kinetic analysis used a range of 0.02-2.5 mM D- or L-menthol. Reactions were carried out at 37°C for 30 min and terminated by the addition of an equal volume of methanol on ice and spiked with 2 μL of L-MG-d_4 (1 ppm). The precipitate was removed by centrifugation at 16,000 *g* for 10 min at 4°C and the supernatant was analyzed by liquid chromatography mass spectroscopy (LC-MS) as described below. Each analysis was performed in triplicate.

NNAL-Gluc inhibition assay. L- and D-menthol inhibition of NNAL-Gluc formation in HLM and UGT-expressing cell microsomes was performed as described above using *rac*-NNAL (1 mM) as substrate and each menthol enantiomer (1.0-2,500 μM) as inhibitor. Reactions were performed at 37°C for 60 min, terminated by the addition of an equal volume of methanol on ice, and spiked with 2 μL of NNAL-Gluc internal standard mix (NNAL-*N*-Gluc-d_3 and *rac*-NNAL-*O*-Gluc-d_5, 2 ppm). Precipitate was removed by centrifugation at 16,000 *g* for 10 min at 4°C and the supernatant was analyzed by LC-MS as described below. Each analysis was performed in triplicate.

LC-MS analysis. For *in vitro* activity assays with HLM, HIM or HEK293 UGT-expressing cell microsomes, LC separation of NNAL metabolites was achieved using an Acquity H class ultra-performance liquid chromatography [UPLC; Waters, Milford, MA]. NNAL-Gluc peaks were analyzed with a HSS T3 1.8 μm column (2.1x100 mm; Acquity, Waters) at 30ºC by gradient elution at a flow rate of 0.35 mL/min using the following conditions: 0.5 min with 99% buffer A (5 mM ammonium acetate with 0.01% formic acid) and 1% buffer B (100% MeOH), followed by a linear gradient for 3.0 min to 20% buffer B, and a subsequent linear gradient for

1.0 min to 95% buffer B. The column was subsequently washed with a linear gradient to 1% buffer B for 1.0 min and re-equilibrated for 1.0 min in 1% buffer B.

MG peaks were analyzed using the same LC-MS system with the column at 30ºC with gradient elution at 0.3 mL/min using the following conditions: 0.5 min with 95% buffer A (5 mM ammonium acetate): 5% buffer B (100% acetonitrile), followed by a linear gradient for 9.5 min to 25% buffer A, and a subsequent linear gradient for 3 min to 5% buffer A. Equilibrium was reestablished in a 1 min linear gradient to 95% buffer A.

The Waters Xevo TQD tandem mass spectrometer (MS) was equipped with a Zspray electrospray ionization interface operated in the positive ion mode for NNAL-Gluc detection, with capillary voltage at 0.6 kV. Nitrogen was used as both the cone gas and desolvation gas at 50 and 800 L/hr, respectively. Ultra-pure argon was used for collision-induced dissociation. The desolvation temperature and the ion source temperature were 500°C and 150°C, respectively. For the detection of NNAL-Glucs, the mass spectrometer was operated in the multiple reaction monitoring mode (MRM) with the following transitions: NNAL-*N*-Gluc, MS transition of 386.2 *m/z* >180.1 *m/z* with cone voltage and collision energy at 15 and 20 V, respectively; NNAL-*O*-Gluc, MS transition of 386.2 *m/z* >162.1 *m/z* with the cone voltage and collision energy each at 15 V.

MG detection was performed on the same Xevo TQD instrument with the electrospray interface operated in the negative ion mode with capillary voltage at 2.0 kV. Nitrogen was used as both the cone gas and desolvation gas at 50 and 800 L/h, respectively. Ultra-pure argon was used for collision-induced dissociation and the desolvation temperature and the ion source temperature were 500 and 150°C, respectively. For the detection of MGs, the mass spectrometer

was operated in the MRM mode with a transition of 331.0 *m/z* >84.9 *m/z* with cone voltage and collision energy at 46 and 24 V, respectively.

For analysis of urine specimens, 2x 10 µl aliquots of each specimen were spiked with either 5 µl of an internal standard mixture that included NNAL-$^{13}C_6$, NNAL-*N*-Gluc-$^{13}C_6$ and NNAL-*O*-Gluc-$^{13}C_6$ (NNAL-Gluc-$^{13}C_6$ was biosynthesized from NNAL-$^{13}C_6$ using a previously published method;[3] 0.1 ppm each) or 5 µL of L-MG-d_4 (3 ppm). After the addition of 10 µl of 0.5 M ammonium formate, the mixture was vortexed thoroughly. All precipitate was removed by centrifugation at 16,000 *g* for 10 min at 4°C. The supernatant was transferred into 350 µl conical glass sample vials for LC-MS analysis. MGs were detected and quantified using the same LC-MS methods described above for *in vitro* assays. NNAL and its metabolites were detected and quantified with minor changes from a previously described method [3] using an Acquity UPLC, with an HSS T3 (100 X 2.1 mm, 1.8 µm) UPLC column and a Xevo G2-S Qtof MS. The LC method was performed using a 5 µl sample injection volume, a 25°C column temperature and a flow rate of 0.2 mL/min using the following conditions: a 1 min linear gradient of 100% buffer A (5 mM ammonium formate: 0.01% formic acid) to 99% buffer A: 1% buffer B (100% acetonitrile), a subsequent isocratic gradient of 1% buffer B for 9 min, followed by a linear gradient for 8 min to 97% buffer A: 3% buffer B. After an 8 additional minutes at 97% buffer A: 3% buffer B, columns were then cleaned with 95% buffer B and re-equilibrated to initial conditions before the next sample injection.

The Waters Xevo G2-S Qtof MS was operated in positive electrospray ionization MS/MS sensitive mode, with capillary voltage at 0.6 kV. Nitrogen was used for both cone and desolvation gases at 50 L/h and 800 L/h, respectively. Ultra-pure argon was used as the collision gas with a flow rate of 0.1 L/h for collision-induced dissociation. The source temperature was

120ºC, desolvation gas temperature was 500ºC. The dwell time for each ion was 0.1 sec. The cone voltage was 15, 25 and 15 V and the collision energies were 10, 20 and 15 volts for NNAL, NNAL-*N*-Gluc and NNAL-*O*-Gluc, respectively. The MS transition traces for quantification for NNAL-*N*-Gluc, NNAL-*O*-Gluc, NNAL and respective internal standards (IS) are 386.2>180.124 (IS: 392.2>186.144), 386.2>162.115 (IS: 392.2>168.135) and 210.1>180.124 (IS: 216.2 >186.144), respectively.

The MS transitions and LC retention times for each molecule were compared to purchased NNAL-*O*-Gluc, NNAL-*N*-Gluc, and MG standards. NNAL-*O*-Gluc, NNAL-*N*-Gluc, and MG formation were quantified by dividing their peak areas by the peak areas for each respective heavy isotope internal standard, and then quantified against a standard curve made from purchased NNAL-*O*-Gluc, NNAL-*N*-gluc or MG of known quantity. NNAL and NNAL-glucs were measured simultaneously, L- and D-MG were measured simultaneously *in vivo* with the methods listed above.

Statistical analysis. Kinetic and inhibition constants, non-parametric ANOVA (Kruskal-Wallis) with Dunn's post-test, Student's t-test, and Spearman correlations were determined using Prism version 7.0 (GraphPad Software, San Diego, CA).

Results

In order to develop a separation and detection method for L- and D-MG peaks, racemic DL-menthol was incubated with HLM. As shown in Figure 4.1, efficient separation of D- and L-MG peaks was observed using the LC-MS method described in this study. This method produced

two distinct peaks: L-MG with a retention time of approximately 5.76 min and D-MG with a retention time of approximately 5.85 min (panel A). The L-MG peak was confirmed by comparison to commercial L-MG-d_4 internal standard (retention time = 5.75 min; panel B). While pure deuterated D-MG was not available as an internal standard, the second peak exhibited a different retention time with the same mass transition, suggesting that this peak corresponds to D-MG. The coefficient of variation for the detection of L-MG and/or D-MG from assays with DL-menthol, L-menthol, and D-menthol were 12%, 9%, and 15% respectively.

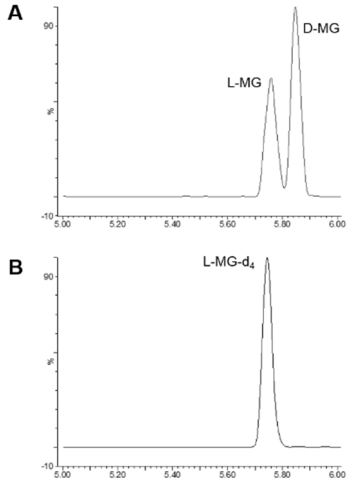

Figure 4.1. Separation and detection of L- and D-MG. Racemic DL-menthol was incubated with human liver microsomes to form both L- and D-menthol glucuronide (**A**), with D_4-L-menthol glucuronide (**B**) spiked into the assay after incubation, prior to quenching the reaction. Peaks were detected by LCMS with baseline separation between the product peaks.

To determine which UGTs form the glucuronide for either L- or D-menthol, 18 human UGTs were screened for glucuronidation activity using UGT-expressing cell microsomes. UGTs 1A9, 1A10, 2A1, 2A2, 2A3, 2B4, 2B7 and 2B17 exhibited detectable levels of glucuronidation activity for both menthol enantiomers. While UGT1A7 exhibited detectable glucuronidating activity for L-menthol, no detectable activity was observed for D-menthol for this enzyme. UGTs 1A1, 1A3, 1A4, 1A5, 1A6, 1A8, 2B10, 2B11 and 2B15 all exhibited no detectable activity for either menthol enantiomer. UGT2B7 exhibited the lowest apparent K_M (0.35 μM) for L-menthol, followed by UGT2B17 < UGT2A1 $\simeq$ UGT1A9 < UGT1A0 (Table 4.1). A similar pattern was observed for D-menthol, with UGTs 2B7 and 2A1 exhibiting the lowest apparent K_M's (0.33 and 0.37 μM, respectively), followed by UGT2B17 $\simeq$ UGT1A9 < UGT1A10. The apparent K_M's observed by kinetic analysis for active UGT-expressing cell microsomes ranged from 0.35 – 4.1

mM for L-menthol and 0.22 – 1.9 mM for D-menthol, and were comparable to that observed for HLM (0.89 and 0.54 mM for L- and D-menthol, respectively) and HIM (1.7 and 0.99 mM for L- and D-menthol, respectively; Table 4.1). Kinetic parameters could not be obtained for UGTs 1A7, 2A2, 2A3, and 2B4 due to relatively low overall activity. With the exception of UGT2B7, all of the UGTs as well as HLM, and HIM exhibited higher turnover rates (V_{max}/K_M) for D-menthol than L-menthol (Table 4.1) suggesting that active UGTs have a higher clearance for D-menthol as a substrate. There was a 1,220- and 2,315-fold higher V_{max}/K_M observed for HLM than HIM for D- and L-menthol, respectively.

Table 4.1. Kinetics for L- and D-menthol with UGT-expressing HEK293 cell lines.[a,b]

	L-menthol			D-menthol		
Enzyme	K_M[c]	V_{max}[d]	V_{max}/K_M[e]	K_M[c]	V_{max}[d]	V_{max}/K_M[e]
UGT1A9	2.1 ± 2.0	3.1 ± 2.2	1.7	0.80 ± 0.43	8.6 ± 2.3	12
UGT1A10	4.1 ± 0.9	16 ± 3.3	3.9	1.9 ± 1.2	16 ± 7.0	8.9
UGT2A1	1.8 ± 0.9	28 ± 7.2	16	0.37 ± 0.12	42 ± 3.6	120
UGT2B7	0.35 ± 0.03	54 ± 6.2	155	0.33 ± 0.12	48 ± 7.5	154
UGT2B17	0.70 ± 0.24	4.0 ± 1.3	5.9	0.76 ± 0.09	10 ± 1.7	14
HLM	0.89 ± 0.13	4167 ± 326	4802	0.54 ± 0.22	2805 ± 293	5721
HIM	1.7 ± 1.1	1.8 ± 0.90	1.1	0.99 ± 0.18	2.3 ± 0.25	2.3

[a] Data are expressed as the mean ± SD of three independent experiments.
[b] Seventeen human UGTs were screened for L- and D-menthol activity. UGTs 1A1, 1A3, 1A4, 1A5, 1A6, 1A8, 2B10 and 2B11 exhibited no activity when incubated with either L- or D-menthol. While UGTs 2A2, 2A3, and 2B4 exhibited glucuronidation activity against menthol enantiomers, it was too low to determine enzyme kinetics for both L- and D-menthol; UGT1A7 exhibited no detectible activity for D-menthol and its L-menthol glucuronidation activity was too low to determine enzyme kinetics.
[c] Units are expressed as mM
[d] Units are expressed as pmol·mg total microsomal protein^{-1}·min^{-1}
[e] Units are expressed as nL· mg total microsomal protein^{-1}·min^{-1}

To determine the potential impact of menthol on NNAL glucuronidation, assays were performed with HLM as well as each UGT overexpressing cell line, 1 mM *rac*-NNAL, and each menthol enantiomer ranging in concentration from 1.0-2,500 μM, with individual NNAL glucuronides detected by LC-MS as described previously.[299] Both L- and D-menthol showed some level of inhibition for the formation of each NNAL glucuronide product in HLM, with the strongest inhibition exhibited for NNAL-*N*-Gluc formation (IC_{50} values of 100 μM and 50 μM, respectively; Table 4.2). The IC_{50} values were 6.6- and 13.8-fold higher for (*S*)-NNAL-*O*-Gluc vs. NNAL-*N*-

Table 4.2. L- and D-menthol inhibition constants (IC50) for HLM and UGT-expressing cell microsomes for NNAL glucuronide formation.[a]

		NNAL-*N*-Gluc (μM)	**(*R*)-NNAL-*O*-Gluc** (μM)	**(*S*)-NNAL-*O*-Gluc** (μM)
L-menthol	HLM	100	750	660
	UGT1A9	NA	632	689
	UGT1A10	NA	2309	>2500
	UGT2B7	NA	NA	163
	UGT2B10	236	NA	NA
	UGT2B17	NA	927	NA
D-menthol	HLM	50	1,265	690
	UGT1A9	NA	1480	1215
	UGT1A10	NA	1419	>2500
	UGT2B7	NA	NA	343
	UGT2B10	202	NA	NA
	UGT2B17	NA	995	NA

[a] Data are expressed as the mean of three independent experiments.
NA, not applicable reaction not expected to produce the product.

Gluc formation, and 7.5- and 25.4-fold higher for (*R*)-NNAL-*O*-Gluc vs. NNAL-*N*-Gluc formation, for L- and D-menthol, respectively, in HLM. While the IC_{50} value was 2-fold higher for L- vs. D-menthol for NNAL-*N*-Gluc formation, D-menthol exhibited a 1.7-fold higher IC_{50} value as compared to L-menthol for (*R*)-NNAL-*O*-Gluc formation; no difference was observed between L- and D-menthol for the formation of (*S*)-NNAL-*O*-Gluc (IC_{50} values = 660 and 690 μM, respectively).

Table 4.3. Study subject demographics.

Subject Demographics	
Menthol smokers	50%
Age, mean	49 y
Age, range	40 – 66 y
Sex	56% female
Race/ethnicity	34% white
	60% black
	1% Hispanic
	5% mixed race
Cig per day, mean	15
Cig per day, range	3 – 40
Pack years, mean	25
Pack years, range	1 – 98

The formation of NNAL-*N*-Gluc by UGT2B10 was similarly inhibited by both L- and D-menthol (IC_{50} values = 236 and 202 μM, respectively); consistent with that observed in previous studies,[276] no NNAL-*N*-Gluc formation was detected for cell microsomes expressing UGTs 1A9, 1A10, 2B7 and 2B17 (with or without the addition of D- or L-menthol). The highest levels of inhibition of NNAL-*O*-Gluc formation by menthol enantiomers was observed for UGT2B7 for (*S*)-NNAL-*O*-Gluc (IC_{50} values = 163 and 343 μM for L- and D-menthol, respectively). Less inhibition was observed for menthol enantiomers of UGT1A9- and

UGT2B17-induced NNAL-*O*-Gluc formation; neither menthol enantiomer exhibited strong inhibition of the extra-hepatic UGT1A10.

The formation of NNAL-*N*-Gluc by UGT2B10 was similarly inhibited by both L- and D-menthol (IC_{50} values = 236 and 202 μM, respectively); consistent with that observed in previous studies,[276] no NNAL-*N*-Gluc formation was detected for cell microsomes expressing UGTs 1A9, 1A10, 2B7 and 2B17 (with or without the addition of D- or L-menthol). The highest levels of inhibition of NNAL-*O*-Gluc formation by menthol enantiomers was observed for UGT2B7 for (*S*)-NNAL-*O*-Gluc (IC_{50} values = 163 and 343 μM for L- and D-menthol, respectively). Less inhibition was observed for menthol enantiomers of UGT1A9- and UGT2B17-induced NNAL-*O*-Gluc formation; neither menthol enantiomer exhibited strong inhibition of the extra-hepatic UGT1A10.

To examine the potential effect of menthol inhibition on NNAL-Gluc formation *in vivo*, a panel of 100 urine specimens were examined from smokers recruited into the Southern Community Cohort Study. As shown in Table 4.3, 50% of the subjects indicated that they were smokers of mentholated cigarettes with subjects smoking an average of 15 cigarettes/day.

Each specimen was analyzed for levels of D-MG, L-MG, (*R*)-NNAL-*O*-Gluc, (*S*)-NNAL-*O*-Gluc, NNAL-*N*-Gluc, and free NNAL. NNAL metabolites were detectable in all of the urine specimens analyzed, with one specimen falling below the limit of quantification for (*R*)-NNAL-*O*-Gluc. L-MG was the most prevalent menthol metabolite in these urine specimens (Figure 4.2, panel A). Urinary L-MG and D-MG were detected in 97 and 44 of the subjects, respectively, with L-MG detectable in 50 menthol smokers and 47 non-menthol smokers and D-MG detectable in 18 menthol smokers and 26 non-menthol smokers. In only 3 non-menthol smokers was no MG (L- or D-) detected. When detectable (n=44), urinary D-MG comprised an average of 2.8% of total MG

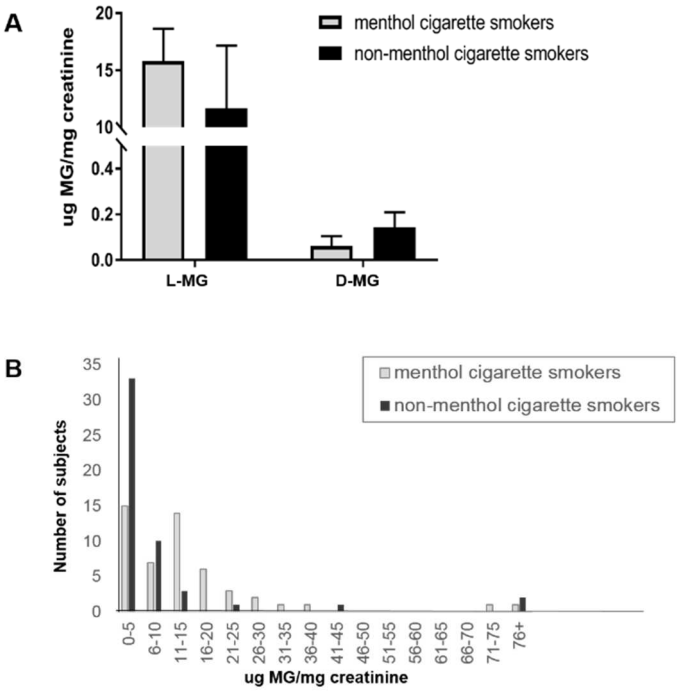

Figure 4.2. Levels of menthol glucuronides stratified by menthol and non-menthol cigarette smokers. Levels of L- and D-menthol glucuronides were quantified in the urine of smokers from menthol (n=50) and non-menthol (n=50) cigarette smokers. Menthol glucuronides were analyzed by liquid chromatography-mass spectrometry and were normalized to levels of creatinine. Subjects were stratified by menthol vs. non-menthol smoker groups based on cigarette brand labelling. Panel **A**, menthol and non-menthol branded smoking groups were analyzed for levels of urinary L- and D-menthol glucuronide. Bars represent mean (± SEM). Panel **B**, histogram showing the number of menthol vs. non-menthol smoking subjects (based on cigarette branding) at different total urinary menthol glucuronide levels. Subjects (non-menthol, n=3) with menthol glucuronide concentrations below the limit of quantification are included in the 0-5 ug/mg creatinine bar. Bars represent the number of subjects in each category. MG, menthol glucuronide.

and comprised an average of 1.3% among the specimens with detectable total MG (n=97); the range in the ratio of D-MG:total MG in the 44 specimens with detectable D-MG was 0.001-0.197. No significant differences in MG levels were observed for smokers who self-reported being menthol vs. non-menthol smokers (Figure 4.2, panel A). In addition, there were no significant differences in MG levels between white vs. black menthol smokers (p=0.25) or white and black non-menthol smokers (p=0.51; data not shown). When stratifying subjects based on levels of total urinary menthol (Figure 4.2, panel B), there were more non-menthol smokers vs. menthol smokers in the two lowest groups (0-5 and 6-10 µg MG/mg creatinine) but also in the highest group (76+ µg MG/mg creatinine). While levels of MG in menthol smokers had a wider distribution, the curve was skewed to the lower MG levels, with a small number of subjects exhibiting high MG levels. A large gap in distribution was observed with no subjects within the MG levels ranging from 46-70 µg MG/mg creatinine.

To better assess the potential interaction between menthol and NNAL detoxification, NNAL and its glucuronides were measured in all 100 urine specimens (Table 4.4). NNAL metabolites were detectable in all of the urine specimens analyzed, with one specimen falling below the limit of quantification for (*R*)-NNAL-*O*-Gluc. There were no significant differences between white and black smokers for (S)-NNAL-O-Gluc (p=0.28), (R)-NNAL-O-Gluc (p=0.51), NNAL-N-Gluc (p=0.82), or free NNAL (p=0.77; data not shown), suggesting that race was not a factor when assessing the levels of these urinary metabolites.

Table 4.4. Urinary NNAL and NNAL glucuronide levels in menthol and non-menthol smokers.[a]

	(S)-NNAL-O-Gluc	(R)-NNAL-O-Gluc	NNAL-N-Gluc	free NNAL
		White Smokers		
mean	0.64 ± 0.062	0.18 ± 0.020	0.29 ± 0.026	0.16 ± 0.020
range	0.074-1.66	0.22-0.47	0.076-0.69	0.050-0.51
		Black Smokers		
mean	0.50 ± 0.11	0.15 ± 0.040	0.26 ± 0.11	0.18 ± 0.070
range	0.051-8.90	0-3.2	0.017-8.5	0.009-5.6
		All Smokers		
mean	0.56 ± 0.090	0.16 ± 0.033	0.29 ± 0.085	0.19 ± 0.056
range	0.051-8.90	0-3.2	0.017-8.5	0.009-5.6

[a] Mean values are expressed as ng/mg creatinine ± SE

Negative Spearman correlation coefficients were observed for each NNAL-Gluc when compared with total MG (data not shown). These values were small and non-significant, likely due to the leveling out of NNAL-Glucs with higher levels of MG. Specimens were then stratified by tertiles based on levels of total urinary MG (termed ‘low’, ‘intermediate’ and ‘high’) and are

shown in Figure 4.3. While the intermediate and high MG levels exhibited similar NNAL-*N*-Gluc levels, significantly lower levels of urinary NNAL-*N*-Gluc (as a ratio with free NNAL) was observed in both the intermediate ($p<0.01$) and high ($p<0.05$) urinary MG groups as compared to the low urinary MG group (Figure 4.3). No significant difference was observed for (*R*)-NNAL-*O*-Gluc or (*S*)-NNAL-*O*-Gluc between different urinary MG groups.

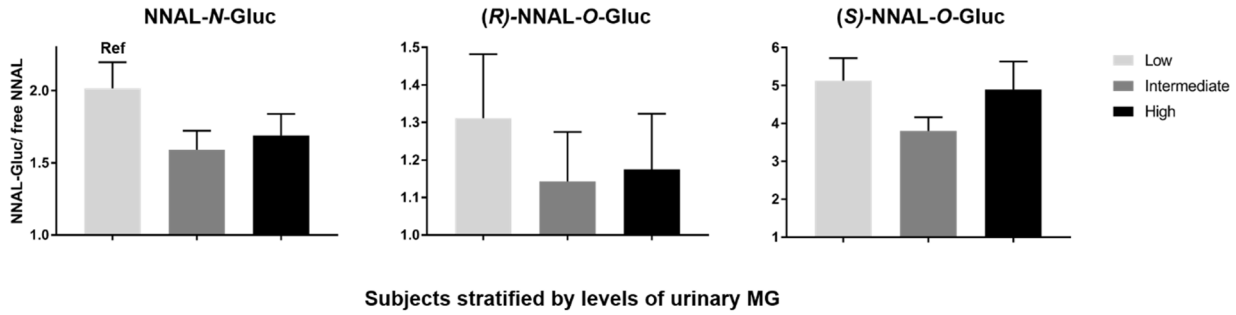

Figure 4.3. Levels of NNAL glucuronides stratified by levels of urinary menthol glucuronides. Shown are the urinary levels of NNAL-*N*-gluc:free NNAL, (*R*)-NNAL-*O*-Gluc:free NNAL, and (*S*)-NNAL-*O*-Gluc:free NNAL in subjects placed into tertiles of low (n=33), intermediate (n=33), and high (n=34) levels of total urinary MG. Total menthol glucuronides (MG), NNAL-*N*-gluc, (*R*)-NNAL-*O*-Gluc, (*S*)-NNAL-*O*-Gluc and free NNAL were analyzed by liquid chromatography-mass spectrometry as described in the Methods. The ratio of each NNAL glucuronide to free NNAL was compared with a Kruskal-Wallis (NNAL-*N*-Gluc, $p<0.01$) and a Dunn's posttest comparison of the intermediate and high MG groups vs the low MG group. Bars represent mean (± SEM). * $p < 0.05$, ** $p < 0.01$.

Discussion

In the present study, the metabolism of menthol was explored by utilizing a panel of 18 human UGTs screened for MG formation activity. UGTs 1A9, 1A10, 2A1, 2B7, and 2B17 all exhibited relatively high glucuronidation activity against both L- and D-menthol, with K_M values that were similar to those observed in HLM and HIM. The activity observed for UGT2B7 in the present study (K_M = 0.35 μM) is consistent with that observed previously for UGT2B7 against L-menthol.[328] The fact that UGT1A3 exhibited no activity against menthol enantiomers in the present study is also consistent with the lack of activity against menthol shown in previous studies.[329]

UGTs 2A1 and 1A10 are extra-hepatic enzymes that are expressed in digestive tract tissues [202, 219, 285] and are likely contributing to the MG formation observed in HIM. UGTs 1A9, 2B7, and 2B17 are hepatically-expressed enzymes [202, 208] that could all be playing a role in MG formation in HLM. UGTs 2A1 and 2B7 exhibited the highest affinity for D-menthol while UGTs 2B7 and 2B17 exhibited the highest affinity for L-menthol. While previous studies suggested that UGT1A4 exhibited glucuronidation activity against menthol enantiomers,[329] no detectable activity was observed for this enzyme in the current study. This difference in activity may be due to differences in assay sensitivity between studies.

Racemic, DL-menthol was previously shown to inhibit the formation of both NNAL-*N*-Gluc and NNAL-*O*-Gluc formation in HLM.[276] NNAL-*O*-Gluc formation is catalyzed by several of the same UGTs (1A9, 1A10, 2B7, and 2B17)[299, 300] that are also most active against menthol enantiomers. In the current study, the individual L- and D-menthol enantiomers were further studied as potential inhibitors of these UGTs as well as UGT2B10, which is known to be the primary enzyme involved in NNAL-*N*-Gluc formation.[3, 256, 299] While L- and D-menthol exhibited the strongest inhibition potential for formation of NNAL-*N*-Gluc in HLM, each enantiomer also exhibited some level of inhibition for HLM formation of (*R*)- and (*S*)-NNAL-*O*-Gluc. When each UGT enzyme was individually assayed for inhibition, both menthol enantiomers exhibited high inhibition potential for UGT2B7-mediated formation of (*S*)-NNAL-*O*-Gluc. These data are similar to other studies where menthol and other mercaptoid alcohols have been associated with the inhibition of UGT2B7 activity.[330] A similarly high inhibition potential was observed for UGT2B10-mediated formation of NNAL-*N*-Gluc. This inhibition of the hepatically-expressed UGT2B7 and UGT2B10 is consistent with the inhibition of NNAL-*O*-Gluc and NNAL-*N*-Gluc observed previously in HLM.[276]

Many studies have examined menthol vs non-menthol smokers in an attempt to determine the impact of menthol on tobacco-related diseases, with several studies measuring MG as a potential biomarker for identification of menthol or non-menthol cigarettes smokers. For example, one study indicated that the levels of urinary menthol (measured as MG) were not correlated with the use of menthol vs non-menthol cigarettes, while another study found significantly higher MG levels in the blood of menthol vs non-menthol smokers.[331] Consistent with these studies, results from the present study indicated that the levels of urinary MG were not correlated with subjects self-identifying as menthol or non-menthol cigarette smokers. These studies are consistent with the hypothesis that menthol branding is not an accurate method of examining the effects of menthol on tobacco-induced diseases.

Therefore, in the present study, the analysis of potential menthol-induced inhibition of NNAL-Gluc formation *in vivo* was performed by stratifying smokers into groups based on quantified levels of urinary MG rather than by menthol vs non-menthol cigarette branding type. Interestingly, the levels of urinary D-MG were relatively low as compared to the levels of urinary L-menthol, comprising, on average, 1.3% of the total menthol exposure for smokers with detectable urinary menthol. The group with the lowest urinary MG levels exhibited the highest levels of urinary NNAL-*N*-Gluc, suggesting a potential interaction between menthol and NNAL-*N*-Gluc formation, likely mediated by UGT2B10 based on the inhibition of UGT2B10 by menthol enantiomers *in vitro*. These data are consistent with the inhibitory effects observed with DL-menthol in HLM in previous studies.[276] A similar but non-significant trend was observed for (*R*)-NNAL-*O*-Gluc formation, an effect potentially due to menthol inhibition of the (*R*)-NNAL-*O*-Gluc forming enzyme, UGT2B17. The inter-individual variability in (*R*)-NNAL-*O*-Gluc formation was high within all of the urinary menthol groups (low vs. intermediate vs. high)

examined in this study. A possible confounder was that UGT2B17, which plays an important role in (*R*)-NNAL-*O*-Gluc formation,[3, 299] has a prevalent copy number variant (minor allele frequency = 0.30 in Caucasians)[332] that was not examined in this population. To better examine the potential inhibitory effects of menthol on (*R*)-NNAL-*O*-Gluc formation, a larger smoking population will be required.

Interestingly, the inhibition of (*S*)-NNAL-*O*-Gluc formation was observed for menthol enantiomers using UGT2B7-expressed cell microsomes in the current study, yet significant decreases in the levels of urinary (*S*)-NNAL-*O*-Gluc were not observed in smokers with high urinary MG. While this could in part be due to the large variability in (*S*)-NNAL-*O*-Gluc formation observed between subjects, it is also likely that, consistent with other studies,[3, 299] other UGTs involved in (*S*)-NNAL-*O*-Gluc formation that are not as inhibited by menthol, including UGT1A9, may be more important in hepatic (*S*)-NNAL-*O*-Gluc formation than UGT2B7.

While at lower levels than in menthol-branded cigarettes, menthol is also present in cigarettes classified as 'non-menthol'.[40] Based on the data from the current study, the levels of menthol in non-menthol cigarettes may still be at levels which could inhibit NNAL detoxification, especially in cases where the levels of menthol in non-menthol cigarettes still far exceed the levels of NNK per cigarette. Non-menthol cigarettes can contain up to 0.07 mg menthol per cigarette [333] while NNK levels are over 10-fold lower.[334, 335] Therefore, menthol content in non-menthol cigarettes could have been important confounders in previous epidemiologic studies examining the role of menthol as a factor in lung cancer risk (comparing 'menthol' vs 'non-menthol' smokers). However, menthol is an additive in many edible and topical products and may have been consumed by some of the non-menthol (as well as menthol) cigarette smoking subjects for whom

urines were analyzed in this study, potentially affecting the levels of urinary MG detected in these subjects. A limitation of the present study was that no information regarding very recent menthol consumption or exposure from other sources was collected from recruited subjects at the time of urine collection.

In summary, both menthol and NNAL are metabolized by some of the same UGT enzymes. Higher levels of urinary MG were shown to be correlated with decreases in urinary NNAL-*N*-Gluc in smokers, indicating that the presence of menthol could lead to NNAL being retained in the body longer, which could increase the opportunity for NNAL to result in increased DNA damage and increase the potential of tobacco-related cancers. The data presented in this study suggests that additional studies are required to better delineate the relationship between menthol, tobacco carcinogen detoxification, and cancer risk.

CHAPTER FIVE

DISCUSSION AND CONCLUSION

Summary

The studies described in this dissertation add to the growing body of knowledge of the role of UGTs in the detoxification of tobacco carcinogens. They include the first study to identify the UGT isoforms with a stereo-preference for either (*R*)- or (*S*)-NNAL, the first study to determine the percent contribution of UGT2B17 to the hepatic formation of (*R*)-NNAL-*O*-Gluc, the first study to examine stereospecific NNAL glucuronidation in head and neck tissues, and the first study to identify the impact of menthol on the clearance of tobacco carcinogens regardless of the source of menthol. The goal of these studies were to better understand the detoxification pathway for the potent tobacco carcinogen, NNK, and to identify genotypes and biomarkers that could eventually be used to identify tobacco users at the highest risk for the development of tobacco-related cancers.

Stereospecificity of UGT Enzymes

Stereospecific clearance and biological reactivity of endogenous compounds and xenobiotics has played an important role in the understanding of biochemical function for decades. The century of research into tobacco constituents had, until recently, largely overlooked the important role stereo-isomers may play in tobacco carcinogenesis. NNAL, a potent tobacco carcinogen, has been shown to exhibit a different carcinogenic potential for each of the enantiomers, (*R*)- and (*S*)-NNAL in rodents. While it is yet to be determined which of these enantiomers is more carcinogenic to humans, these studies have clearly outlined the differences in

detoxification for each NNAL enantiomer. As outlined in Chapters 2-3, each of the six UGTs that form an NNAL-Gluc have different, and distinct, stereospecific activity for the formation of NNAL-Gluc. UGT2B7 was the only enzyme to solely form (*S*)-NNAL-*O*-Gluc, while both UGT2B17 and UGT1A10 were shown to form primarily (*R*)-NNAL-*O*-Gluc. UGT1A9 was the only enzyme to exhibit a fairly equal formation of both (*R*)- and (*S*)-NNAL-*O*-Gluc. In addition, UGT2B10 and UGT1A4 were shown to exhibit a preference for (*R*)- and (*S*)-NNAL-*O*-Gluc formation, respectively.

The differences in stereo-preferences for the formation of each NNAL-*O*-Gluc diastereomer were used to narrow down the UGTs likely to play an important role in the detoxification of NNAL within head and neck tissues. Tissue specimens from human oral cavity, tongue, tonsil, and larynx were shown to only produce detectable levels of (*R*)-NNAL-*O*-Gluc formation. This observed stereoselectivity indicated that the stereospecificity observed should be mediated primarily by UGT2B17 and/or UGT1A10. Kinetic parameters for UGT2B17 and UGT1A10 with (R)-NNAL as a substrate indicated that UGT2B17 had a greater affinity for the substrate, with UGT2B17 exhibiting a far lower K_M value than UGT1A10. These data indicated that UGT2B17 would be the likely driver of NNAL clearance in any tissue of expression. However, UGT1A10 is likely to be the UGT driving NNAL clearance in most H&N tissues due to the large difference in tissue expression observed between UGT1A10 and UGT2B17, with UGT1A10 comprising close to half of the total UGT expression in each tissue type analyzed and UGT2B17 comprising closer to 10% of the total UGTs analyzed. Similar activity studies, with *rac*-NNAL as a substrate, could be used in the future to identify probable expression of certain UGTs in different tissue types throughout the entire human body.

Additionally, the identification of stereospecificity in the formation of menthol glucuronides was determined. It was interesting to discover that all of the UGTs that formed MG, with the exception of UGT2B7, exhibited a preference for the formation of D-MG over L-MG. These data are especially interesting in that D-menthol is not a naturally occurring compound. The striking differences between the extreme stereo-preference UGT2B7 exhibited for the formation of (*S*)-NNAL-*O*-Gluc while having no preference for the formation of D- vs. L-MG may be attributed to the differences the structure of each compound. NNAL has a chiral alcohol on a carbon adjacent to the pyridine ring while menthol contains the chiral alcohol on a carbon within the ring structure. The lack of a complete crystal structure of a mammalian UGT means that determination of the active site amino acids have largely been determined by changing individual amino acids within the UGT structure and measuring changes in activity. These types of stereo-preference differences could be used to determine substrate docking amino acids which could further be used in predictive enzyme folding computational analysis to narrow down the predicted race-mate activity when designing future drugs. Many drugs now rely on stereo-chemistry to manage the bioavailability parameters during the drug design phase. The more we know about form specific stereospecificity, the better the drug design predictions become. While the studies in this body of work were focused on tobacco constituents, the data has the ability to impact many scientific fields.

Detoxification of NNAL

The study of carcinogen activation pathways informs us on the mechanism of action that leads to the formation of DNA adducts that lead to the development of cancer. The studies within

this work focused on the identification of genotypes and tobacco additives that slow down the detoxification/clearance of tobacco carcinogens in humans. Studies into clearance rate manipulation can identify mechanisms with the potential to increase the concentration of carcinogens as well as the length of time the body is exposed to carcinogens. The focus on genotypes identified to decrease the clearance of tobacco carcinogens could inform clinical practice of smoking cessation by identifying genotypes that could be considered high risk for developing a tobacco-related cancer and targeting them for more aggressive smoking cessation therapies. A focus on the identification of tobacco additives known to decrease the clearance of tobacco carcinogens could identify urinary levels of specific additives that could be used as a biomarkers to identify individuals who may be at higher risks for certain types of tobacco-related cancers.

In Chapter 2, the absence of UGT2B17 was shown to reduce the formation of (*R*)-NNAL-*O*-Gluc by ~80% in human liver microsomes in relation to the formation of (*S*)-NNAL-*O*-Gluc. These data indicate the importance of UGT2B17 within the systemic clearance and detoxification of NNAL, and were further verified by an additional project analyzing the urinary metabolites

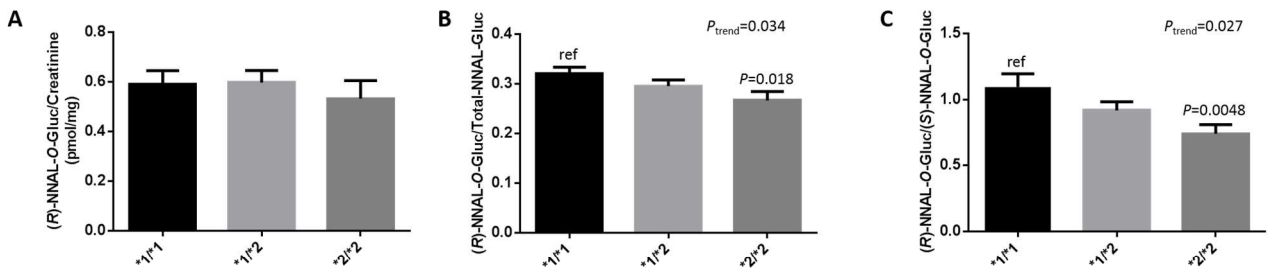

Figure 5.1. Effect of *UGT2B17* deletion polymorphism on urinary (*R*)-NNAL-*O*-Gluc levels in smokers. Subjects were stratified by *UGT2B17* copy number variant (CNV) genotypes, with the *UGT2B17**1 allele corresponding to the wild-type single-gene copy number and the *UGT2B17**2 allele corresponding to the *UGT2B17* gene deletion variant. **A**, *UGT2B17* CNV genotypes versus (*R*)-NNAL-*O*-Gluc/Creatinine (nmol/mg); **B**, *UGT2B17* CNV genotypes versus the ratio of (*R*)-NNAL-*O*-Gluc/total-NNAL-Gluc; and **C**, *UGT2B17* CNV genotypes versus the ratio of (*R*)-NNAL-*O*-Gluc/(*S*)-NNAL-*O*-Gluc. All values are expressed as the mean ± SEM for 180 genotype-informative subjects. Figure from ref [3]

from groups of smokers with known UGT2B17 genotypes.[3] The genotype/phenotype correlation study analyzed NNAL metabolites in the urine of smokers with known UGT2B17 and UGT2B10 genotypes. The *UGT2B17 *2/*2* copy number variation, in which a subset of the population does not contain a single copy of the *UGT2B17* gene, was shown to reduce the (*R*)-NNAL-*O*-Gluc by ~30% in relation to the formation of (S)-NNAL-O-Gluc systemically (Figure 5.1).[3] While the data from Chapter 3 indicate that UGT1A10 may be driving the tissue-specific detoxification of NNAL from head and neck tissues, UGT2B17 is still expressed in all the tissue types analyzed. Determination of the percent contribution of UGT2B17 to the detoxification of NNAL in tissues with direct tobacco exposure would require much larger sample sizes than those analyzed within this body of work. In addition, these data indicate the need for case control studies that look at the correlation between UGT2B17 copy number variations and specific types of tobacco-related cancers. Additionally, levels of NNAL-*N*-Gluc and the *UGT2B10*2* genotype, known to produce a non-functional UGT2B10 enzyme, were analyzed and discovered that in the absence of UGT2B10 activity, NNAL-N-Gluc formation is reduced by ~95% (Figure 5.2).[3]

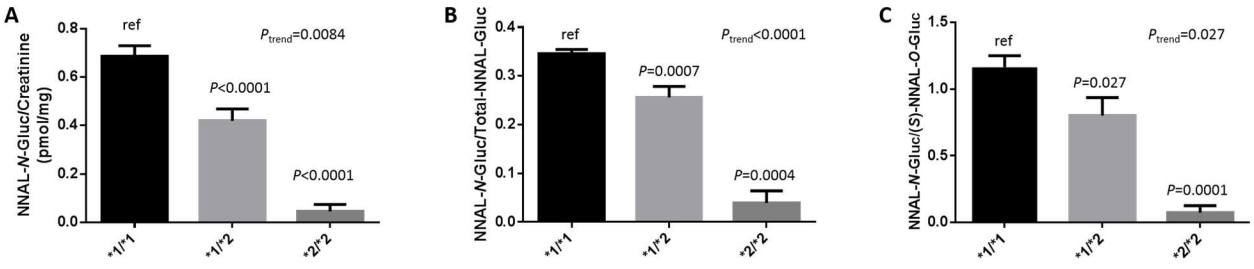

Figure 5.2. Effect of the *UGT2B10* codon 67 polymorphism on urinary NNAL-*N*-Gluc levels in smokers. Subjects were stratified by UGT2B10 codon 67 Asp>Tyr genotype, with the UGT2B10*1 allele corresponding to the wild-type UGT2B10^{67Asp} and the UGT2B10*2 allele corresponding to the UGT2B10^{67Tyr} variant. **A**, *UGT2B10* genotypes versus NNAL-*N*-Gluc/Creatinine (pmol/mg); **B**, *UGT2B10* genotypes versus the ratio of NNAL-*N*-Gluc/total-NNAL-Gluc; and **C**, *UGT2B10* genotypes versus the ratio of NNAL-*N*-Gluc/(*S*)-NNAL-*O*-Gluc. All values are expressed as the mean ± SEM for 174 genotype-informative subjects. For comparative analysis between genotypes, the Students t-test was performed on squared-root transformed data for panel A only; non-transformed data were used for panels B and C. Figure from ref [3]

While menthol is the most ubiquitous and well known tobacco additive in US tobacco products, little has been studied on its impact within the tobacco carcinogen pathway. Chapter 4 outlined the enzymes involved in the clearance of menthol from the human body and identified that both menthol and NNAL are both substrates for 4 UGTs (1A9, 1A10, 2B7, and 2B17). Furthermore, the presence of menthol was shown to slow down the formation of both NNAL-N- and NNAL-O-Gluc in human liver microsomes. When 100 urine samples from smokers were screened for levels of MG as well as NNAL-Glucs, high levels of menthol metabolites were associated with significantly lower levels of NNAL-N-Gluc, indicating potent enough inhibition of UGT2B10 to detect systemically. These data were analyzed by levels of urinary menthol instead of menthol cigarette branding and indicate that, regardless of source, the presence of menthol decreases the detoxification of NNAL. This may be an important mechanism by which menthol increases cancer risk in certain tobacco smokers. Additional data would be needed to establish this causal mechanism by including a larger sample size, and executing a case-control study where menthol levels per-cigarette and/or urinary menthol metabolite levels were studied for an association with lung cancer incidents.

Tobacco Regulation

Menthol is discussed in a variety of ways in the tobacco field. First, there is menthol as a characterizing flavor; which means menthol is added in high enough levels to produce the smell, taste, and cooling sensation associated with menthol. Then there is the menthol added to non-menthol cigarettes; this includes menthol that is an additive in levels low enough that the specific taste and smell cannot be identified. Currently, the FDA is considering a ban on menthol as a

characterizing flavor due to the recommendation from the Tobacco Products Scientific Advisory Committee report on menthol from 2011. This report recommended a ban on menthol as a characterizing flavor based on the fact that a majority of young and first-time smokers enter into nicotine addiction through mentholated cigarettes. The studies in Chapter 4 indicate that menthol slows down the ability of the human body to remove or detoxify the potent tobacco carcinogen, NNAL. In addition, this study shows that menthol likely does this even at the menthol levels reported to be in non-menthol cigarettes. Therefore, simply banning the cigarettes the tobacco companies label as menthol ("characterizing flavors") while leaving it as an approved additive in other tobacco products will not remove the harm menthol may be causing because this harm occurs even at the (relatively) low menthol levels in products that are not identified as containing menthol as a characterizing flavor. Canada recently passed a national ban on menthol as an additive to any tobacco product. In light of the findings from these studies, the FDA should take a close look at the example Canada has set for tobacco regulation and tobacco harm reduction.

Future Directions

These works, in true science fashion, have produced more questions than answers. It is imperative that work continue in discovering which NNAL enantiomer is the stronger carcinogen. This piece of data would provide a vital piece of the tobacco carcinogen detoxification puzzle; it would assist in determining the extent of harm menthol adds to tobacco products, since we already know which detoxification enzymes menthol inhibits. Both the tissue work and the urinary analysis need to be expanded into larger sample sizes to answer several questions: (i) what is the % contribution of UGT2B17 to the detoxification of NNAL in tissues susceptible to tobacco-

related cancers and how does this impact NNAL detoxification within direct tobacco exposure tissues, (ii) can menthol inhibition of NNAL-O-Gluc formation be detected within a larger population, (iii) which NNAL enantiomer is formed into an NNAL-N-Gluc at a higher rate, and finally (iiii) what is the urinary menthol level that causes the rapid decrease in NNAL-N-Gluc formation. The development of cut-off points are requirements to identify biomarkers of any kind. This is no different when it comes to tobacco constituents. There are published levels of urinary nicotine that differentiate between smokers and non-smokers, levels of total NNAL that differentiate between frequent and infrequent smokers as well as differentiate between smokers and smokeless tobacco users, and levels of PAHs that indicate smoke exposure. Menthol is not currently used as a biomarker to differentiate between smokers of menthol and non-menthol cigarette brands because, as seen in chapter 4, there is no clear difference in urinary levels of menthol from these two groups. However, studies could be performed to compare levels of menthol extracted from a cigarette and levels of urinary menthol metabolites to see if there is a correlation between urinary menthol and menthol per-cigarette regardless of tobacco branding.

Conclusions

While there are substantial amounts of data characterizing tobacco addiction and tobacco carcinogenesis, there is still a lot of work needed to fully characterize the clearance and detoxification of NNK. These data, summarized in Figure 5.3, may provide information that can be applied to the development of larger studies aimed at identifying genotypes and/or biomarkers to identify tobacco users at the highest risk for developing tobacco-related cancers. Both *in vitro* and *in vivo* studies indicate that there are distinct genotypes and tobacco additives that slow down

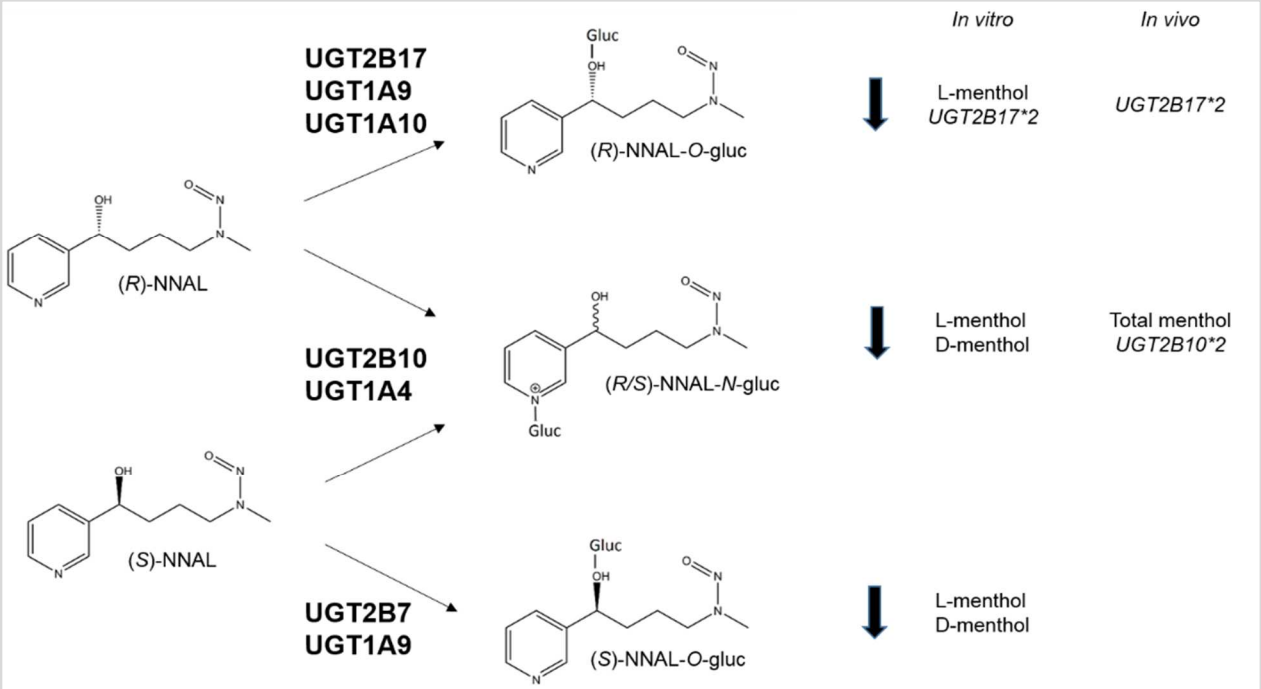

Figure 5.3. Schematic of stereospecificity and detoxification inhibition within the NNAL to NNAL-Gluc

the detoxification of NNK. These data indicate that it is possible to identify tobacco users by genotype who may have a slower tobacco carcinogen metabolism. Additionally, the data presented in this thesis suggest that menthol as a tobacco additive may be slowing down initial tobacco carcinogen detoxification at the site of exposure thus placing tobacco users at greater risk for the development of tobacco-related cancers. Having identified this mechanism of action should lend strength to efforts to regulate menthol addition to tobacco products. The introduction section summarized the current body of work regarding metabolism of TSNAs, but also highlighted the current state of tobacco regulation and health disparities in the United States. There is still much work that needs to be done to translate these findings into tobacco regulation or clinically relevant biomarkers. The *in vitro* and *in vivo* work described in this dissertation is necessary to understand the impact of slowing down the detoxification of tobacco carcinogens, and to identify tobacco additives that could be increasing the harm from tobacco use. This dissertation adds to the

accumulated knowledge of the metabolism of TSNAs and menthol and may build on the data necessary to move the United States regulatory agencies towards additional tobacco regulations.

REFERENCES

1. Mackenzie PI, Bock KW, Burchell B, Guillemette C, Ikushiro S, Iyanagi T, Miners JO, Owens IS, Nebert DW. Nomenclature update for the mammalian UDP glycosyltransferase (UGT) gene superfamily. Pharmacogenet Genomics. 2005;15(10):677-85. PubMed PMID: 16141793.

2. Lewis BC, Mackenzie PI, Miners JO. Homodimerization of UDP-glucuronosyltransferase 2B7 (UGT2B7) and identification of a putative dimerization domain by protein homology modeling. Biochem Pharmacol. 2011;82(12):2016-23. doi: 10.1016/j.bcp.2011.09.007. PubMed PMID: 21930117.

3. Chen G, Luo S, Kozlovich S, Lazarus P. Association between Glucuronidation Genotypes and Urinary NNAL Metabolic Phenotypes in Smokers. Cancer Epidemiol Biomarkers Prev. 2016;25(7):1175-84. doi: 10.1158/1055-9965.EPI-15-1245. PubMed PMID: 27197298.

4. Adler I. Primary malignant growths of the lungs and bronchi; a pathological and clinical study. London,: Longmans, Green; 1912. xii, 325 p.

5. Katanoda K, Yako-Suketomo H. Cancer mortality attributable to tobacco by selected countries based on the WHO Global Report. Jpn J Clin Oncol. 2012; 42(9):866. doi: 10.1093/jjco/hys134. PubMed PMID: 22918963.

6. Jha P, Ramasundarahettige C, Landsman V, Rostron B, Thun M, Anderson RN, McAfee T, Peto R. 21st-century hazards of smoking and benefits of cessation in the United States. N Engl J Med. 2013; 368(4):341-50. doi: 10.1056/NEJMsa1211128. PubMed PMID: 23343063.

7. Office of the Surgeon General. The health consequences of smoking--50 years of progress: a report of the Surgeon General. 2014.

8. Miners JO, Mackenzie PI. Drug glucuronidation in humans. Pharmacol Ther. 1991; 51(3):347-69. PubMed PMID: 1792239.

9. Miners JO, Mackenzie PI, Knights KM. The prediction of drug-glucuronidation parameters in humans: UDP-glucuronosyltransferase enzyme-selective substrate and inhibitor probes for reaction phenotyping and in vitro-in vivo extrapolation of drug clearance and drug-drug interaction potential. Drug Metab Rev. 2010;42(1):196-208. doi: 10.3109/03602530903210716. PubMed PMID: 19795925.

10. Centers for Disease Control and Prevention. Tobacco Product Use Among Adults — United States, 2017. In: Morbidity and Mortality Weekly Report. 2018.

11. Maxwell JC. The Maxwell report. Sales estimates for the cigarette industry. Richmond, VA. 2016.

12. Sharma A, Fix BV, Delnevo C, Cummings KM, O'Connor RJ. Trends in market share of leading cigarette brands in the USA: national survey on drug use and health 2002-2013. BMJ Open. 2016;6(1):e008813. doi: 10.1136/bmjopen-2015-008813. PubMed PMID: 26826144; PMCID: PMC4735173.

13. Delnevo CD, Wackowski OA, Giovenco DP, Manderski MT, Hrywna M, Ling PM. Examining market trends in the United States smokeless tobacco use: 2005-2011. Tob Control. 2014;23(2):107-12. doi: 10.1136/tobaccocontrol-2012-050739. PubMed PMID: 23117999; PMCID: PMC3604094.

14. Commission FT. Federal Trade Commission Smokeless Tobacco Report for 2016. Washington: Federal Trade Commission; 2018.

15. Commission FT. Federal Trade Commission Cigarette Report for 2016 Washington: Federal Trade Commission; 2018.

16. World Health Organization. Tobacco Trade. 2000.

17. International Agency for Research on Cancer. Personal habits and indoor combustions. Volume 100 E. A review of human carcinogens. IARC Monographs for Evaluation of Carcinogen Risks in Humans. 2012;100(Pt E):1-538. PubMed PMID: 23193840; PMCID: PMC4781577.

18. Piano MR, Benowitz NL, Fitzgerald GA, Corbridge S, Heath J, Hahn E, Pechacek TF, Howard G, American Heart Association Council on Cardiovascular N. Impact of smokeless tobacco products on cardiovascular disease: implications for policy, prevention, and treatment: a policy statement from the American Heart Association. Circulation. 2010;122(15):1520-44. doi: 10.1161/CIR.0b013e3181f432c3. PubMed PMID: 20837898.

19. Villanti AC, Richardson A, Vallone DM, Rath JM. Flavored tobacco product use among U.S. young adults. Am J Prev Med. 2013;44(4):388-91. Epub 2013/03/19. doi: 10.1016/j.amepre.2012.11.031. PubMed PMID: 23498105.

20. Corey CG, Ambrose BK, Apelberg BJ, King BA. Flavored Tobacco Product Use Among Middle and High School Students--United States, 2014. MMWR Morb Mortal Wkly Rep. 2015;64(38):1066-70. Epub 2015/10/01. doi: 10.15585/mmwr.mm6438a2. PubMed PMID: 26421418.

21. Henley SJ, Thun MJ, Chao A, Calle EE. Association between exclusive pipe smoking and mortality from cancer and other diseases. J Natl Cancer Inst. 2004;96(11):853-61. Epub 2004/06/03. PubMed PMID: 15173269.

22. Wyss A, Hashibe M, Chuang SC, Lee YC, Zhang ZF, Yu GP, Winn DM, Wei Q, Talamini R, Szeszenia-Dabrowska N, Sturgis EM, Smith E, Shangina O, Schwartz SM, Schantz S, Rudnai P, Purdue MP, Eluf-Neto J, Muscat J, Morgenstern H, Michaluart P, Jr., Menezes A, Matos E, Mates IN, Lissowska J, Levi F, Lazarus P, La Vecchia C, Koifman S, Herrero R, Hayes RB, Franceschi S, Wunsch-Filho V, Fernandez L, Fabianova E, Daudt AW, Dal Maso L, Curado MP, Chen C, Castellsague X, de Carvalho MB, Cadoni G, Boccia S, Brennan P, Boffetta P, Olshan AF. Cigarette, cigar, and pipe smoking and the risk of head and neck cancers: pooled analysis in the International Head and Neck Cancer Epidemiology Consortium. Am J Epidemiol. 2013;178(5):679-90. doi: 10.1093/aje/kwt029. PubMed PMID: 23817919; PMCID: 3755640.

23. Smith-Simone S, Maziak W, Ward KD, Eissenberg T. Waterpipe tobacco smoking: knowledge, attitudes, beliefs, and behavior in two U.S. samples. Nicotine Tob Res. 2008;10(2):393-8. Epub 2008/02/01. doi: 10.1080/14622200701825023. PubMed PMID: 18236304; PMCID: PMC3215239.

24. Cobb C, Ward KD, Maziak W, Shihadeh AL, Eissenberg T. Waterpipe tobacco smoking: an emerging health crisis in the United States. Am J Health Behav. 2010;34(3):275-85. Epub 2009/12/17. PubMed PMID: 20001185; PMCID: PMC3215592.

25. World Health Organization. Advisory Note. Waterpipe Tobacco Smoking: Health Effects, Research Needs and Recommended Actions for Regulators, 2nd edition. editor: World Health Organization; 2015.

26. Prignot JJ, Sasco AJ, Poulet E, Gupta PC, Aditama TY. Alternative forms of tobacco use. Int J Tuberc Lung Dis. 2008;12(7):718-27. Epub 2008/06/12. PubMed PMID: 18544194.

27. United States. Public Health Service. Office of the Surgeon General., National Heart Lung and Blood Institute. Chronic obstructive lung disease : summary of the health consequences of smoking : a report of the Surgeon General. Bethesda, Md.: U.S. Dept. of Health and Human Services, Public Health Service, National Institutes of Health, National Heart, Lung, and Blood Institute; 1984. 10 pages p.

28. Shopland DR, United States. Department of Health and Human Services., United States. Office on Smoking and Health., United States. Public Health Service. Office of the Surgeon General. The Health consequences of smoking: cancer: a report of the Surgeon General. Rockville, Md.: U.S. Dept. of Health and Human Services, Public Health Service; 1982. xix, 322 pages p.

29. Office of the Surgeon General. National Center for Chronic Disease Prevention and Health Promotion (U.S.). The health consequences of smoking: a report of the Surgeon General Atlanta, Ga.: U.S. Public Health Service, National Center for Chronic Disease Prevention and Health Promotion. 2004.

30. World Health Organization. IARC Monographs on the Evaluation of Carcinogenic Risks to Humans. Volume 89: Smokeless Tobacco and Some Tobacco-Specific N-Nitrosamines. In: IARC, editor. Lyon (France): World Health Organization; 2007.

31. Lund I, Scheffels J. Smoking and snus use onset: exploring the influence of snus debut age on the risk for smoking uptake with cross-sectional survey data. Nicotine Tob Res. 2014;16(6):815-9. doi: 10.1093/ntr/ntu001. PubMed PMID: 24500685.

32. Bonhomme MG, Holder-Hayes E, Ambrose BK, Tworek C, Feirman SP, King BA, Apelberg BJ. Flavoured non-cigarette tobacco product use among US adults: 2013-2014. Tob

Control. 2016;25(Suppl 2):ii4-ii13. Epub 2016/11/01. doi: 10.1136/tobaccocontrol-2016-053373. PubMed PMID: 27794065; PMCID: PMC5515238.

33. US Food and Drug Administration. Deeming Tobacco Products To Be Subject to the Federal Food, Drug, and Cosmetic Act, as Amended by the Family Smoking Prevention and Tobacco Control Act; Restrictions on the Sale and Distribution of Tobacco Products and Required Warning Statements for Tobacco Products. In: Health and Human Services, editor. Food and Drug Administration; 2016.

34. Cullen KA, Ambrose BK, Gentzke AS, Apelberg BJ, Jamal A, King BA. Notes from the Field: Use of Electronic Cigarettes and Any Tobacco Product Among Middle and High School Students - United States, 2011-2018. MMWR Morb Mortal Wkly Rep. 2018;67(45):1276-7. doi: 10.15585/mmwr.mm6745a5. PubMed PMID: 30439875; PMCID: PMC6290807 potential conflicts of interest. No potential conflicts of interest were disclosed.

35. Villanti AC, Johnson AL, Ambrose BK, Cummings KM, Stanton CA, Rose SW, Feirman SP, Tworek C, Glasser AM, Pearson JL, Cohn AM, Conway KP, Niaura RS, Bansal-Travers M, Hyland A. Flavored Tobacco Product Use in Youth and Adults: Findings From the First Wave of the PATH Study (2013-2014). Am J Prev Med. 2017;53(2):139-51. Epub 2017/03/21. doi: 10.1016/j.amepre.2017.01.026. PubMed PMID: 28318902; PMCID: PMC5522636.

36. Centers for Disease Control and Prevention. State Tobacco Activities Tracking and Evaluation. editor: Center for Disease Control and Prevention; 2017.

37. Fagan P, King G, Lawrence D, Petrucci SA, Robinson RG, Banks D, Marable S, Grana R. Eliminating tobacco-related health disparities: directions for future research. Am J Public Health. 2004;94(2):211-7. PubMed PMID: 14759929; PMCID: PMC1448230.

38. Giovino GA, Villanti AC, Mowery PD, Sevilimedu V, Niaura RS, Vallone DM, Abrams DB. Differential trends in cigarette smoking in the USA: is menthol slowing progress? Tob Control. 2015;24(1):28-37. doi: 10.1136/tobaccocontrol-2013-051159. PubMed PMID: 23997070.

39. Substance Abuse and Mental Health Services Administration. The NSDUH Report: Recent Trends in Menthol Cigarette Use. In: Office of Applied Studies, editor. Rockville (MD): Substance Abuse and Mental Health Services Administration; 2011.

40. Tobacco Products Scientific Advisory Committee. Menthol Cigarettes and Public Health: Review of the Scientific Evidence and Recommendations. Government Document Submitted to FDA. 2011.

41. Centers for Disease Control and Prevention. Results from the 2016 National Survey on Drug Use and Health. In: Substance Abuse and Mental Health Services Administration. Rockville, MD. 2017.

42. Maxwell J. The Maxwell Report: Cigar Industry in 2015. Richmond, VA: John C. Maxwell Jr.; 2016.

43. Akl EA, Gaddam S, Gunukula SK, Honeine R, Jaoude PA, Irani J. The effects of waterpipe tobacco smoking on health outcomes: a systematic review. Int J Epidemiol. 2010;39(3):834-57. doi: 10.1093/ije/dyq002. PubMed PMID: 20207606.

44. Waziry R, Jawad M, Ballout RA, Al Akel M, Akl EA. The effects of waterpipe tobacco smoking on health outcomes: an updated systematic review and meta-analysis. Int J Epidemiol. 2017;46(1):32-43. doi: 10.1093/ije/dyw021. PubMed PMID: 27075769.

45. Cobb CO, Shihadeh A, Weaver MF, Eissenberg T. Waterpipe tobacco smoking and cigarette smoking: a direct comparison of toxicant exposure and subjective effects. Nicotine Tob Res. 2011;13(2):78-87. doi: 10.1093/ntr/ntq212. PubMed PMID: 21127030; PMCID: PMC3107609.

46. US Department of Health and Human Services. Preventing Tobacco Use Among Youth and Young Adults: A Report of the Surgeon General. In: Department of Health and Human Services, Office on Smoking and Health, editor. Atlanta, GA2012.

47. Yen KL, Hechavarria E, Bostwick SB. Bidi cigarettes: An emerging threat to adolescent health. Arch Pediatr Adolesc Med. 2000;154(12):1187-9. PubMed PMID: 11115300.

48. Centers for Disease Control and Prevention. Bidi Use Among Urban Youth—Massachusetts, March–April 1999. In: Morbidity and Mortality Weekly Report, editor. 1999. p. 796-9.

49. Malson JL, Lee EM, Murty R, Moolchan ET, Pickworth WB. Clove cigarette smoking: biochemical, physiological, and subjective effects. Pharmacol Biochem Behav. 2003;74(3):739-45. PubMed PMID: 12543240.

50. Centers for Disease Control and Prevention. Tobacco Use Among Middle and High School Students—United States, 2011–2017. In: Morbidity and Mortality Weekly Report, editor. 2018. p. 629-33.

51. Office of the Surgeon General. Centers for Disease Control and Prevention (U.S.), National Center for Chronic Disease Prevention and Health Promotion (U.S.). Office on Smoking and Health. How tobacco smoke causes disease: the biology and behavioral basis for smoking-

attributable disease: a report of the Surgeon General. Rockville, MD; Washington, D.C.: U.S. Dept. of Health and Human Services, Public Health Service, Office of the Surgeon General; 2010.

52. Nash SH, Liao LM, Harris TB, Freedman ND. Cigarette Smoking and Mortality in Adults Aged 70 Years and Older: Results From the NIH-AARP Cohort. Am J Prev Med. 2017;52(3):276-83. doi: 10.1016/j.amepre.2016.09.036. PubMed PMID: 27914770; PMCID: PMC5318256.

53. Shopland DR, Eyre HJ, Pechacek TF. Smoking-attributable cancer mortality in 1991: is lung cancer now the leading cause of death among smokers in the United States? J Natl Cancer Inst. 1991;83(16):1142-8. PubMed PMID: 1886147.

54. National Toxicology P. Tobacco-related exposures: tobacco smoking. Rep Carcinog. 2011;12:408-10. PubMed PMID: 21863108.

55. National Toxicology P. Tobacco-related exposures: environmental tobacco smoke. Rep Carcinog. 2011;12:410-2. PubMed PMID: 21863109.

56. National Toxicology P. Tobacco-related exposures: smokeless tobacco. Rep Carcinog. 2011;12:412-4. PubMed PMID: 21863110.

57. Centers for Disease Control and Prevention. Sexual Orientation Information Background. In: National Center for Health Statistics, editor. 2016.

58. Murphy SE, Park SL, Balbo S, Haiman CA, Hatsukami DK, Patel Y, Peterson LA, Stepanov I, Stram DO, Tretyakova N, Hecht SS, Le Marchand L. Tobacco biomarkers and genetic/epigenetic analysis to investigate ethnic/racial differences in lung cancer risk among smokers. NPJ Precis Oncol. 2018;2:17. doi: 10.1038/s41698-018-0057-y. PubMed PMID: 30155522; PMCID: PMC6105591.

59. Xie SH, Rabbani S, Petrick JL, Cook MB, Lagergren J. Racial and Ethnic Disparities in the Incidence of Esophageal Cancer in the United States, 1992-2013. Am J Epidemiol. 2017;186(12):1341-51. doi: 10.1093/aje/kwx221. PubMed PMID: 28641390; PMCID: PMC5860465.

60. Daraei P, Moore CE. Racial Disparity Among the Head and Neck Cancer Population. J Cancer Educ. 2015;30(3):546-51. doi: 10.1007/s13187-014-0753-4. PubMed PMID: 25398667.

61. Baker MT, Bates JN, Van Dyke RA. Stabilization of the reduced halocarbon-cytochrome P-450 complex of halothane by N-alkanes. Biochem Pharmacol. 1987;36(7):1029-34. PubMed PMID: 3566799.

62. Rodgman A, Smith CJ, Perfetti TA. The composition of cigarette smoke: a retrospective, with emphasis on polycyclic components. Hum Exp Toxicol. 2000;19(10):573-95. doi: 10.1191/096032700701546514. PubMed PMID: 11211997.

63. Proctor RN. Tobacco and the global lung cancer epidemic. Nat Rev Cancer. 2001;1(1):82-6. doi: 10.1038/35094091. PubMed PMID: 11900255.

64. Wynder EL, Wright G, Lam J. A study of tobacco carcinogenesis. V. The role of pyrolysis. Cancer. 1958;11(6):1140-8. PubMed PMID: 13608415.

65. Kislov VV, Sadovnikov AI, Mebel AM. Formation mechanism of polycyclic aromatic hydrocarbons beyond the second aromatic ring. J Phys Chem A. 2013;117(23):4794-816. Epub 2013/05/16. doi: 10.1021/jp402481y. PubMed PMID: 23672431.

66. Schmeltz I, Schlotzhauer WS. Benzo(a)pyrene, phenols and other products from pyrolysis of the cigarette additive, (d,1)-menthol. Nature. 1968;219(5152):370-1. PubMed PMID: 5662150.

67. Smith LE, Denissenko MF, Bennett WP, Li H, Amin S, Tang M, Pfeifer GP. Targeting of lung cancer mutational hotspots by polycyclic aromatic hydrocarbons. J Natl Cancer Inst. 2000;92(10):803-11. PubMed PMID: 10814675.

68. McGrath TE, Wooten JB, Geoffrey Chan W, Hajaligol MR. Formation of polycyclic aromatic hydrocarbons from tobacco: the link between low temperature residual solid (char) and PAH formation. Food Chem Toxicol. 2007;45(6):1039-50. Epub 2007/02/17. doi: 10.1016/j.fct.2006.12.010. PubMed PMID: 17303297.

69. Smith CJ, Perfetti TA, Rumple MA, Rodgman A, Doolittle DJ. "IARC group 2A Carcinogens" reported in cigarette mainstream smoke. Food Chem Toxicol. 2000;38(4):371-83. PubMed PMID: 10722891.

70. Kim KH, Jahan SA, Kabir E, Brown RJ. A review of airborne polycyclic aromatic hydrocarbons (PAHs) and their human health effects. Environ Int. 2013;60:71-80. doi: 10.1016/j.envint.2013.07.019. PubMed PMID: 24013021.

71. Bach PB, Kattan MW, Thornquist MD, Kris MG, Tate RC, Barnett MJ, Hsieh LJ, Begg CB. Variations in lung cancer risk among smokers. J Natl Cancer Inst. 2003;95(6):470-8. PubMed PMID: 12644540.

72. Boffetta P, Jourenkova N, Gustavsson P. Cancer risk from occupational and environmental exposure to polycyclic aromatic hydrocarbons. Cancer Causes Control. 1997;8(3):444-72. PubMed PMID: 9498904.

73. Diggs DL, Huderson AC, Harris KL, Myers JN, Banks LD, Rekhadevi PV, Niaz MS, Ramesh A. Polycyclic aromatic hydrocarbons and digestive tract cancers: a perspective. J Environ

Sci Health C Environ Carcinog Ecotoxicol Rev. 2011;29(4):324-57. doi: 10.1080/10590501.2011.629974. PubMed PMID: 22107166; PMCID: PMC3247201.

74. Olsson AC, Fevotte J, Fletcher T, Cassidy A, t Mannetje A, Zaridze D, Szeszenia-Dabrowska N, Rudnai P, Lissowska J, Fabianova E, Mates D, Bencko V, Foretova L, Janout V, Brennan P, Boffetta P. Occupational exposure to polycyclic aromatic hydrocarbons and lung cancer risk: a multicenter study in Europe. Occup Environ Med. 2010;67(2):98-103. doi: 10.1136/oem.2009.046680. PubMed PMID: 19773276.

75. Wells PG, McCallum GP, Lam KC, Henderson JT, Ondovcik SL. Oxidative DNA damage and repair in teratogenesis and neurodevelopmental deficits. Birth Defects Res C Embryo Today. 2010;90(2):103-9. doi: 10.1002/bdrc.20177. PubMed PMID: 20544694.

76. Shimada T, Fujii-Kuriyama Y. Metabolic activation of polycyclic aromatic hydrocarbons to carcinogens by cytochromes P450 1A1 and 1B1. Cancer Sci. 2004;95(1):1-6. PubMed PMID: 14720319.

77. Billet S, Garcon G, Dagher Z, Verdin A, Ledoux F, Cazier F, Courcot D, Aboukais A, Shirali P. Ambient particulate matter (PM2.5): physicochemical characterization and metabolic activation of the organic fraction in human lung epithelial cells (A549). Environ Res. 2007;105(2):212-23. doi: 10.1016/j.envres.2007.03.001. PubMed PMID: 17462623.

78. Kiss I, Orsos Z, Gombos K, Bogner B, Csejtei A, Tibold A, Varga Z, Pazsit E, Magda I, Zolyomi A, Ember I. Association between allelic polymorphisms of metabolizing enzymes (CYP 1A1, CYP 1A2, CYP 2E1, mEH) and occurrence of colorectal cancer in Hungary. Anticancer Res. 2007;27(4C):2931-7. PubMed PMID: 17695473.

79. Moorthy B, Chu C, Carlin DJ. Polycyclic aromatic hydrocarbons: from metabolism to lung cancer. Toxicol Sci. 2015;145(1):5-15. doi: 10.1093/toxsci/kfv040. PubMed PMID: 25911656; PMCID: PMC4408964.

80. Xue W, Warshawsky D. Metabolic activation of polycyclic and heterocyclic aromatic hydrocarbons and DNA damage: a review. Toxicol Appl Pharmacol. 2005;206(1):73-93. doi: 10.1016/j.taap.2004.11.006. PubMed PMID: 15963346.

81. Nebert DW, Dalton TP, Okey AB, Gonzalez FJ. Role of aryl hydrocarbon receptor-mediated induction of the CYP1 enzymes in environmental toxicity and cancer. J Biol Chem. 2004;279(23):23847-50. doi: 10.1074/jbc.R400004200. PubMed PMID: 15028720.

82. MacDonald CJ, Ciolino HP, Yeh GC. Dibenzoylmethane modulates aryl hydrocarbon receptor function and expression of cytochromes P50 1A1, 1A2, and 1B1. Cancer Res. 2001;61(10):3919-24. PubMed PMID: 11358806.

83. Raunio H, Rautio A, Pelkonen O. The CYP2A subfamily: function, expression and genetic polymorphism. IARC Sci Publ. 1999(148):197-207. PubMed PMID: 10493259.

84. Piipari R, Savela K, Nurminen T, Hukkanen J, Raunio H, Hakkola J, Mantyla T, Beaune P, Edwards RJ, Boobis AR, Anttila S. Expression of CYP1A1, CYP1B1 and CYP3A, and polycyclic aromatic hydrocarbon-DNA adduct formation in bronchoalveolar macrophages of smokers and non-smokers. Int J Cancer. 2000;86(5):610-6. PubMed PMID: 10797280.

85. Heudorf U, Angerer J. Urinary monohydroxylated phenanthrenes and hydroxypyrene--the effects of smoking habits and changes induced by smoking on monooxygenase-mediated metabolism. Int Arch Occup Environ Health. 2001;74(3):177-83. PubMed PMID: 11355291.

86. Pelkonen O, Nebert DW. Metabolism of polycyclic aromatic hydrocarbons: etiologic role in carcinogenesis. Pharmacol Rev. 1982;34(2):189-222. PubMed PMID: 6287505.

87. Schmoldt A, Jacob J, Grimmer G. Dose-dependent induction of rat liver microsomal aryl hydrocarbon monooxygenase by benzo[k]fluoranthene. Cancer Lett. 1981;13(3):249-57. PubMed PMID: 7296534.

88. Courter LA, Pereira C, Baird WM. Diesel exhaust influences carcinogenic PAH-induced genotoxicity and gene expression in human breast epithelial cells in culture. Mutat Res. 2007;625(1-2):72-82. doi: 10.1016/j.mrfmmm.2007.05.005. PubMed PMID: 17612574; PMCID: PMC2815343.

89. Saint-Georges F, Abbas I, Billet S, Verdin A, Gosset P, Mulliez P, Shirali P, Garcon G. Gene expression induction of volatile organic compound and/or polycyclic aromatic hydrocarbon-metabolizing enzymes in isolated human alveolar macrophages in response to airborne particulate matter (PM2.5). Toxicology. 2008;244(2-3):220-30. doi: 10.1016/j.tox.2007.11.016. PubMed PMID: 18178302.

90. Misaki K, Matsui S, Matsuda T. Metabolic enzyme induction by HepG2 cells exposed to oxygenated and nonoxygenated polycyclic aromatic hydrocarbons. Chem Res Toxicol. 2007;20(2):277-83. doi: 10.1021/tx060197u. PubMed PMID: 17253728.

91. Palackal NT, Burczynski ME, Harvey RG, Penning TM. The ubiquitous aldehyde reductase (AKR1A1) oxidizes proximate carcinogen trans-dihydrodiols to o-quinones: potential role in polycyclic aromatic hydrocarbon activation. Biochemistry. 2001;40(36):10901-10. PubMed PMID: 11535067.

92. Penning TM. Aldo-keto reductases and formation of polycyclic aromatic hydrocarbon o-quinones. Methods Enzymol. 2004;378:31-67. doi: 10.1016/S0076-6879(04)78003-9. PubMed PMID: 15038957; PMCID: PMC2561330.

93. Quinn AM, Harvey RG, Penning TM. Oxidation of PAH trans-dihydrodiols by human aldo-keto reductase AKR1B10. Chem Res Toxicol. 2008;21(11):2207-15. doi: 10.1021/tx8002005. PubMed PMID: 18788756; PMCID: PMC2645959.

94. Burczynski ME, Lin HK, Penning TM. Isoform-specific induction of a human aldo-keto reductase by polycyclic aromatic hydrocarbons (PAHs), electrophiles, and oxidative stress: implications for the alternative pathway of PAH activation catalyzed by human dihydrodiol dehydrogenase. Cancer Res. 1999;59(3):607-14. PubMed PMID: 9973208.

95. Ozeki T, Takahashi Y, Kume T, Nakayama K, Yokoi T, Nunoya K, Hara A, Kamataki T. Co-operative regulation of the transcription of human dihydrodiol dehydrogenase (DD)4/aldo-keto reductase (AKR)1C4 gene by hepatocyte nuclear factor (HNF)-4alpha/gamma and HNF-1alpha. Biochem J. 2001;355(Pt 2):537-44. PubMed PMID: 11284743; PMCID: PMC1221767.

96. Marinkovic N, Pasalic D, Potocki S. Polymorphisms of genes involved in polycyclic aromatic hydrocarbons' biotransformation and atherosclerosis. Biochem Med (Zagreb). 2013;23(3):255-65. PubMed PMID: 24266295; PMCID: PMC3900076.

97. Rothman N, Shields PG, Poirier MC, Harrington AM, Ford DP, Strickland PT. The impact of glutathione s-transferase M1 and cytochrome P450 1A1 genotypes on white-blood-cell polycyclic aromatic hydrocarbon-DNA adduct levels in humans. Mol Carcinog. 1995;14(1):63-8. PubMed PMID: 7546226.

98. Butkiewicz D, Cole KJ, Phillips DH, Harris CC, Chorazy M. GSTM1, GSTP1, CYP1A1 and CYP2D6 polymorphisms in lung cancer patients from an environmentally polluted region of Poland: correlation with lung DNA adduct levels. Eur J Cancer Prev. 1999;8(4):315-23. PubMed PMID: 10493307.

99. Hessel S, John A, Seidel A, Lampen A. Multidrug resistance-associated proteins are involved in the transport of the glutathione conjugates of the ultimate carcinogen of benzo[a]pyrene in human Caco-2 cells. Arch Toxicol. 2013;87(2):269-80. doi: 10.1007/s00204-012-0917-0. PubMed PMID: 22899102.

100. Iwano S, Asanuma F, Nukaya M, Saito T, Kamataki T. CYP1A1-mediated mechanism for atherosclerosis induced by polycyclic aromatic hydrocarbons. Biochem Biophys Res Commun. 2005;337(2):708-12. doi: 10.1016/j.bbrc.2005.09.109. PubMed PMID: 16202979.

101. Luckert C, Ehlers A, Buhrke T, Seidel A, Lampen A, Hessel S. Polycyclic aromatic hydrocarbons stimulate human CYP3A4 promoter activity via PXR. Toxicol Lett. 2013;222(2):180-8. doi: 10.1016/j.toxlet.2013.06.243. PubMed PMID: 23845848.

102. Strassburg CP, Strassburg A, Nguyen N, Li Q, Manns MP, Tukey RH. Regulation and function of family 1 and family 2 UDP-glucuronosyltransferase genes (UGT1A, UGT2B) in human oesophagus. Biochem J. 1999;338 (Pt 2):489-98. Epub 1999/02/20. PubMed PMID: 10024527; PMCID: PMC1220077.

103. Zhang L, Huang M, Blair IA, Penning TM. Interception of benzo[a]pyrene-7,8-dione by UDP glucuronosyltransferases (UGTs) in human lung cells. Chem Res Toxicol. 2013;26(10):1570-8. doi: 10.1021/tx400268q. PubMed PMID: 24047243; PMCID: PMC3829198.

104. Grove AD, Kessler FK, Metz RP, Ritter JK. Identification of a rat oltipraz-inducible UDP-glucuronosyltransferase (UGT1A7) with activity towards benzo(a)pyrene-7,8-dihydrodiol. J Biol Chem. 1997;272(3):1621-7. Epub 1997/01/17. PubMed PMID: 8999837.

105. Guillemette C, Ritter JK, Auyeung DJ, Kessler FK, Housman DE. Structural heterogeneity at the UDP-glucuronosyltransferase 1 locus: functional consequences of three novel missense mutations in the human UGT1A7 gene. Pharmacogenetics. 2000;10(7):629-44. Epub 2000/10/19. PubMed PMID: 11037804.

106. Mojarrabi B, Mackenzie PI. Characterization of two UDP glucuronosyltransferases that are predominantly expressed in human colon. Biochem Biophys Res Commun. 1998;247(3):704-9. Epub 1998/07/02. doi: 10.1006/bbrc.1998.8843. PubMed PMID: 9647757.

107. Jin CJ, Miners JO, Burchell B, Mackenzie PI. The glucuronidation of hydroxylated metabolites of benzo[a]pyrene and 2-acetylaminofluorene by cDNA-expressed human UDP-glucuronosyltransferases. Carcinogenesis. 1993;14(12):2637-9. Epub 1993/12/01. PubMed PMID: 8269638.

108. Kondraganti SR, Fernandez-Salguero P, Gonzalez FJ, Ramos KS, Jiang W, Moorthy B. Polycyclic aromatic hydrocarbon-inducible DNA adducts: evidence by 32P-postlabeling and use of knockout mice for Ah receptor-independent mechanisms of metabolic activation in vivo. Int J Cancer. 2003;103(1):5-11. doi: 10.1002/ijc.10784. PubMed PMID: 12455047.

109. Nakatsuru Y, Wakabayashi K, Fujii-Kuriyama Y, Ishikawa T, Kusama K, Ide F. Dibenzo[A,L]pyrene-induced genotoxic and carcinogenic responses are dramatically suppressed in aryl hydrocarbon receptor-deficient mice. Int J Cancer. 2004;112(2):179-83. doi: 10.1002/ijc.20365. PubMed PMID: 15352028.

110. Mahesh K. Lakshman PLK, Surendrakumar Chaturved, Joseph H. Saugier, Herman J. C. Yeh, Jenny P. Glusker, H. L. Carrell, Amy K. Katz, Carol E. Afshar, Won-Mohaiza Dashwood, Gary Kenniston, and William M. Baird. Methyl Group-Induced Helicity in 1,4-Dimethylbenzo[c]phenanthrene and Its Metabolites: Synthesis, Physical, and Biological Properties. J Am Chem Soc. 2000;122(51):12629-36. doi: 10.1021/ja002072w.

111. Platt KL, Aderhold S, Kulpe K, Fickler M. Unexpected DNA damage caused by polycyclic aromatic hydrocarbons under standard laboratory conditions. Mutat Res. 2008;650(2):96-103. doi: 10.1016/j.mrgentox.2007.09.011. PubMed PMID: 18160334.

112. Ewa B, Danuta MS. Polycyclic aromatic hydrocarbons and PAH-related DNA adducts. J Appl Genet. 2017;58(3):321-30. doi: 10.1007/s13353-016-0380-3. PubMed PMID: 27943120; PMCID: PMC5509823.

113. Wood AW, Levin W, Lu AY, Ryan D, West SB, Lehr RE, Schaefer-Ridder M, Jerina DM, Conney AH. Mutagenicity of metabolically activated benzo[a]anthracene 3,4-dihydrodiol: evidence for bay region activation of carcinogenic polycyclic hydrocarbons. Biochem Biophys Res Commun. 1976;72(2):680-6. PubMed PMID: 791280.

114. Levin W, Wood AW, Yagi H, Jerina DM, Conney AH. (+/-)-trans-7,8-dihydroxy-7,8-dihydrobenzo (a)pyrene: a potent skin carcinogen when applied topically to mice. Proc Natl Acad Sci U S A. 1976;73(11):3867-71. PubMed PMID: 1069271; PMCID: PMC431245.

115. Levin W, Wood AW, Yagi H, Dansette PM, Jerina DM, Conney AH. Carcinogenicity of benzo[a]pyrene 4,5-, 7,8-, and 9,10-oxides on mouse skin. Proc Natl Acad Sci U S A. 1976;73(1):243-7. PubMed PMID: 1061121; PMCID: PMC335877.

116. Levin W, Wood AW, Chang RL, Ittah Y, Croisy-Delcey M, Yagi H, Jerina DM, Conney AH. Exceptionally high tumor-initiating activity of benzo(c)phenanthrene bay-region diol-epoxides on mouse skin. Cancer Res. 1980;40(11):3910-4. PubMed PMID: 7471042.

117. Denissenko MF, Pao A, Tang M, Pfeifer GP. Preferential formation of benzo[a]pyrene adducts at lung cancer mutational hotspots in P53. Science. 1996;274(5286):430-2. PubMed PMID: 8832894.

118. Denissenko MF, Venkatachalam S, Ma YH, Wani AA. Site-specific induction and repair of benzo[a]pyrene diol epoxide DNA damage in human H-ras protooncogene as revealed by restriction cleavage inhibition. Mutat Res. 1996;363(1):27-42. PubMed PMID: 8632776.

119. Jin CJ, Miners JO, Lillywhite KJ, Mackenzie PI. cDNA cloning and expression of two new members of the human liver UDP-glucuronosyltransferase 2B subfamily. Biochem Biophys Res Commun. 1993;194(1):496-503. Epub 1993/07/15. doi: 10.1006/bbrc.1993.1847. PubMed PMID: 8333863.

120. Raunio H, Hakkola J, Hukkanen J, Lassila A, Paivarinta K, Pelkonen O, Anttila S, Piipari R, Boobis A, Edwards RJ. Expression of xenobiotic-metabolizing CYPs in human pulmonary tissue. Exp Toxicol Pathol. 1999;51(4-5):412-7. doi: 10.1016/S0940-2993(99)80031-1. PubMed PMID: 10445407.

121. Zhang J, Ichiba M, Hara K, Zhang S, Hanaoka T, Pan G, Yamano Y, Takahashi K, Tomokuni K. Urinary 1-hydroxypyrene in coke oven workers relative to exposure, alcohol consumption, and metabolic enzymes. Occup Environ Med. 2001;58(11):716-21. PubMed PMID: 11600727; PMCID: PMC1740063.

122. Yang M, Jang JY, Kim S, Lee SM, Chang SS, Cheong HK, Lee E, Kang D, Kim H, Kawamoto T, Shin HD. Genetic effects on urinary 1-hydroxypyrene levels in a Korean population. Carcinogenesis. 2003;24(6):1085-9. doi: 10.1093/carcin/bgg054. PubMed PMID: 12807751.

123. McIlwain CC, Townsend DM, Tew KD. Glutathione S-transferase polymorphisms: cancer incidence and therapy. Oncogene. 2006;25(11):1639-48. doi: 10.1038/sj.onc.1209373. PubMed PMID: 16550164.

124. Hessel S, Lampen A, Seidel A. Polycyclic aromatic hydrocarbons in food--efflux of the conjugated biomarker 1-hydroxypyrene is mediated by Breast Cancer Resistance Protein (ABCG2) in human intestinal Caco-2 cells. Food Chem Toxicol. 2013;62:797-804. doi: 10.1016/j.fct.2013.10.007. PubMed PMID: 24140465.

125. Hoffmann D, Adams JD, Lisk D, Fisenne I, Brunnemann KD. Toxic and carcinogenic agents in dry and moist snuff. J Natl Cancer Inst. 1987;79:1281-6. Epub 12/01. PubMed PMID: 3480379.

126. Czoli CD, Hammond D. TSNA Exposure: Levels of NNAL Among Canadian Tobacco Users. Nicotine Tob Res. 2015;17(7):825-30. doi: 10.1093/ntr/ntu251. PubMed PMID: 25481919.

127. International Agency for Research on Cancer. Tobacco habits other than smoking; betel-quid and areca-nut chewing; and some related nitrosamines. IARC Working Group. Lyon, France. IARC Monographs Evaluation Carcinogen Risk Chem Hum. 1985;37:1-268. Epub 09/01. PubMed PMID: 3866741.

128. Hatsukami DK, Stepanov I, Severson H, Jensen JA, Lindgren BR, Horn K, Khariwala SS, Martin J, Carmella SG, Murphy SE, Hecht SS. Evidence supporting product standards for

carcinogens in smokeless tobacco products. Cancer Prev Res (Phila). 2015;8(1):20-6. doi: 10.1158/1940-6207.CAPR-14-0250. PubMed PMID: 25524878; PMCID: 4299753.

129. International Agency for Research on Cancer. Smokeless tobacco and some tobacco-specific N-nitrosamines. IARC Monogr Eval Carcinog Risks Hum. 2008/03/14 ed2007. p. 1-592.

130. Food and Drug Administration. Harmful and Potentially Harmful Constituents in Tobacco Products and Tobacco Smoke: Established List. 2012.

131. Burns DM, Dybing E, Gray N, Hecht S, Anderson C, Sanner T, O'Connor R, Djordjevic M, Dresler C, Hainaut P, Jarvis M, Opperhuizen A, Straif K. Mandated lowering of toxicants in cigarette smoke: a description of the World Health Organization TobReg proposal. Tob Control. 2008;17(2):132-41. doi: 10.1136/tc.2007.024158. PubMed PMID: 18375736; PMCID: PMC2569138.

132. Hoffmann D, Hoffmann I, El-Bayoumy K. The less harmful cigarette: a controversial issue. a tribute to Ernst L. Wynder. Chem Res Toxicol. 2001;14(7):767-90. PubMed PMID: 11453723.

133. Appleton S, Olegario RM, Lipowicz PJ. TSNA exposure from cigarette smoking: 18 years of urinary NNAL excretion data. Regul Toxicol Pharmacol. 2014;68(2):269-74. doi: 10.1016/j.yrtph.2013.07.013. PubMed PMID: 23920111.

134. Hecht SS, Spratt TE, Trushin N. Absolute configuration of 4-(methylnitrosamino)-1-(3-pyridyl)-1-butanol formed metabolically from 4-(methylnitrosamino)-1-(3-pyridyl)-1-butanone. Carcinogenesis. 1997;18(9):1851-4. PubMed PMID: 9328186.

135. Stephen S.Hecht TESaNT. Corrigendum: Absolute configuration of 4-(methylnitrosamino)-1-(3-pyridyl)-1-butanol formed metabolically from4-(methylnitrosamino)-1-(3-pyridyl)-1-butanone. Carcinogenesis. 2000;21(4):850.

136. Hecht SS. Biochemistry, biology, and carcinogenicity of tobacco-specific N-nitrosamines. Chem Res Toxicol. 1998;11(6):559-603. doi: 10.1021/tx980005y. PubMed PMID: 9625726.

137. Rivenson A, Hoffmann D, Prokopczyk B, Amin S, Hecht SS. Induction of lung and exocrine pancreas tumors in F344 rats by tobacco-specific and Areca-derived N-nitrosamines. Cancer Res. 1988;48(23):6912-7. PubMed PMID: 3180100.

138. Upadhyaya P, Carmella SG, Guengerich FP, Hecht SS. Formation and metabolism of 4-(methylnitrosamino)-1-(3-pyridyl)-1-butanol enantiomers in vitro in mouse, rat and human tissues. Carcinogenesis. 2000;21(6):1233-8. PubMed PMID: 10837015.

139. Richter E, Engl J, Friesenegger S, Tricker AR. Biotransformation of 4-(methylnitrosamino)-1-(3-pyridyl)-1-butanone in lung tissue from mouse, rat, hamster, and man. Chem Res Toxicol. 2009;22(6):1008-17. doi: 10.1021/tx800461d. PubMed PMID: 19408892.

140. Carmella SG, Akerkar S, Hecht SS. Metabolites of the tobacco-specific nitrosamine 4-(methylnitrosamino)-1-(3-pyridyl)-1-butanone in smokers' urine. Cancer Res. 1993;53(4):721-4. PubMed PMID: 8428352.

141. Hecht SS, Carmella SG, Stepanov I, Jensen J, Anderson A, Hatsukami DK. Metabolism of the tobacco-specific carcinogen 4-(methylnitrosamino)-1-(3-pyridyl)-1-butanone to its biomarker total NNAL in smokeless tobacco users. Cancer Epidemiol Biomarkers Prev. 2008;17(3):732-5. doi: 10.1158/1055-9965.EPI-07-2843. PubMed PMID: 18349296.

142. Atalla A, Maser E. Characterization of enzymes participating in carbonyl reduction of 4-methylnitrosamino-1-(3-pyridyl)-1-butanone (NNK) in human placenta. Chem Biol Interact. 2001;130-132(1-3):737-48. PubMed PMID: 11306090.

143. Breyer-Pfaff U, Martin HJ, Ernst M, Maser E. Enantioselectivity of carbonyl reduction of 4-methylnitrosamino-1-(3-pyridyl)-1-butanone by tissue fractions from human and rat and by enzymes isolated from human liver. Drug Metab Dispos. 2004;32(9):915-22. PubMed PMID: 15319331.

144. Martin HJ, Breyer-Pfaff U, Wsol V, Venz S, Block S, Maser E. Purification and characterization of akr1b10 from human liver: role in carbonyl reduction of xenobiotics. Drug Metab Dispos. 2006;34(3):464-70. Epub 2005/12/31. doi: 10.1124/dmd.105.007971. PubMed PMID: 16381663.

145. Ashmore JH, Luo S, Watson CJW, Lazarus P. Carbonyl Reduction of NNK by Recombinant Human Lung Enzymes. Identification of HSD17beta12 as the Reductase important in (R)-NNAL formation in Human Lung. Carcinogenesis. 2018. Epub 2018/05/23. doi: 10.1093/carcin/bgy065. PubMed PMID: 29788210; PMCID: PMC6067128.

146. Kedderis GL. Biotransformation of Toxicants. In: McQueen CA, editor. Comprehensive Toxicology (Second Edition): Elsevier; 2010. p. 137-51.

147. Xue J, Yang S, Seng S. Mechanisms of Cancer Induction by Tobacco-Specific NNK and NNN. Cancers (Basel). 2014;6(2):1138-56. doi: 10.3390/cancers6021138. PubMed PMID: 24830349; PMCID: PMC4074821.

148. Khariwala SS, Ma B, Ruszczak C, Carmella SG, Lindgren B, Hatsukami DK, Hecht SS, Stepanov I. High Level of Tobacco Carcinogen-Derived DNA Damage in Oral Cells Is an Independent Predictor of Oral/Head and Neck Cancer Risk in Smokers. Cancer Prev Res (Phila). 2017;10(9):507-13. doi: 10.1158/1940-6207.CAPR-17-0140. PubMed PMID: 28679497; PMCID: PMC5712492.

149. Castonguay A, Lin D, Stoner GD, Radok P, Furuya K, Hecht SS, Schut HA, Klaunig JE. Comparative carcinogenicity in A/J mice and metabolism by cultured mouse peripheral lung of N'-nitrosonornicotine, 4-(methylnitrosamino)-1-(3-pyridyl)-1-butanone, and their analogues. Cancer Res. 1983;43:1223-9. Epub 03/01. PubMed PMID: 6825093.

150. Carmella SG, Borukhova A, Akerkar SA, Hecht SS. Analysis of human urine for pyridine-N-oxide metabolites of 4-(methylnitrosamino)-1-(3-pyridyl)-1-butanone, a tobacco-specific lung carcinogen. Cancer Epidemiol Biomarkers Prev. 1997;6(2):113-20. PubMed PMID: 9037562.

151. Hecht SS, Trushin N, Reid-Quinn CA, Burak ES, Jones AB, Southers JL, Gombar CT, Carmella SG, Anderson LM, Rice JM. Metabolism of the tobacco-specific nitrosamine 4-(methylnitrosamino)-1-(3-pyridyl)-1-butanone in the patas monkey: pharmacokinetics and characterization of glucuronide metabolites. Carcinogenesis. 1993;14(2):229-36. PubMed PMID: 8435864.

152. Morse MA, Eklind KI, Toussaint M, Amin SG, Chung FL. Characterization of a glucuronide metabolite of 4-(methyl-nitrosamino)-1-(3-pyridyl)-1-butanone (NNK) and its dose-dependent excretion in the urine of mice and rats. Carcinogenesis. 1990;11(10):1819-23. PubMed PMID: 2208595.

153. Ren Q, Murphy SE, Zheng Z, Lazarus P. O-Glucuronidation of the lung carcinogen 4-(methylnitrosamino)-1- (3-pyridyl)-1-butanol (NNAL) by human UDP-glucuronosyltransferases 2B7 and 1A9. Drug Metab Dispos. 2000;28(11):1352-60. PubMed PMID: 11038164.

154. Modesto JL, Hull A, Angstadt AY, Berg A, Gallagher CJ, Lazarus P, Muscat JE. NNK reduction pathway gene polymorphisms and risk of lung cancer. Mol Carcinog. 2014. doi: 10.1002/mc.22187. PubMed PMID: 24976539.

155. Hu CW, Hsu YW, Chen JL, Tam LM, Chao MR. Direct analysis of tobacco-specific nitrosamine NNK and its metabolite NNAL in human urine by LC-MS/MS: evidence of linkage to methylated DNA lesions. Arch Toxicol. 2014;88(2):291-9. doi: 10.1007/s00204-013-1137-y. PubMed PMID: 24057573.

156. Hecht SS, Carmella SG, Chen M, Dor Koch JF, Miller AT, Murphy SE, Jensen JA, Zimmerman CL, Hatsukami DK. Quantitation of urinary metabolites of a tobacco-specific lung carcinogen after smoking cessation. Cancer Res. 1999;59(3):590-6. PubMed PMID: 9973205.

157. Park SL, Carmella SG, Ming X, Vielguth E, Stram DO, Le Marchand L, Hecht SS. Variation in levels of the lung carcinogen NNAL and its glucuronides in the urine of cigarette smokers from five ethnic groups with differing risks for lung cancer. Cancer Epidemiol Biomarkers Prev. 2015;24(3):561-9. doi: 10.1158/1055-9965.EPI-14-1054. PubMed PMID: 25542827; PMCID: 4355389.

158. Wei B, Blount BC, Xia B, Wang L. Assessing exposure to tobacco-specific carcinogen NNK using its urinary metabolite NNAL measured in US population: 2011-2012. J Expo Sci Environ Epidemiol. 2015. doi: 10.1038/jes.2014.88. PubMed PMID: 25564369.

159. Carmella SG, Ming X, Olvera N, Brookmeyer C, Yoder A, Hecht SS. High throughput liquid and gas chromatography-tandem mass spectrometry assays for tobacco-specific nitrosamine and polycyclic aromatic hydrocarbon metabolites associated with lung cancer in smokers. Chem Res Toxicol. 2013;26(8):1209-17. doi: 10.1021/tx400121n. PubMed PMID: 23837805; PMCID: 3803150.

160. Yuan JM, Knezevich AD, Wang R, Gao YT, Hecht SS, Stepanov I. Urinary levels of the tobacco-specific carcinogen N'-nitrosonornicotine and its glucuronide are strongly associated with esophageal cancer risk in smokers. Carcinogenesis. 2011;32(9):1366-71. doi: 10.1093/carcin/bgr125. PubMed PMID: 21734256; PMCID: 3202311.

161. Gallagher CJ, Muscat JE, Hicks AN, Zheng Y, Dyer AM, Chase GA, Richie J, Lazarus P. The UDP-glucuronosyltransferase 2B17 gene deletion polymorphism: sex-specific association with urinary 4-(methylnitrosamino)-1-(3-pyridyl)-1-butanol glucuronidation phenotype and risk for lung cancer. Cancer Epidemiol Biomarkers Prev. 2007;16(4):823-8. doi: 10.1158/1055-9965.EPI-06-0823. PubMed PMID: 17416778.

162. Upadhyaya P, Kenney PM, Hochalter JB, Wang M, Hecht SS. Tumorigenicity and metabolism of 4-(methylnitrosamino)-1-(3-pyridyl)-1-butanol enantiomers and metabolites in the A/J mouse. Carcinogenesis. 1999;20(8):1577-82. PubMed PMID: 10426810.

163. Hecht SS, Carmella SG, Ye M, Le KA, Jensen JA, Zimmerman CL, Hatsukami DK. Quantitation of metabolites of 4-(methylnitrosamino)-1-(3-pyridyl)-1-butanone after cessation of smokeless tobacco use. Cancer Res. 2002;62(1):129-34. PubMed PMID: 11782369.

164. Burchell B, Brierley CH, Monaghan G, Clarke DJ. The structure and function of the UDP-glucuronosyltransferase gene family. Adv Pharmacol. 1998;42:335-8. PubMed PMID: 9327909.

165. Gong QH, Cho JW, Huang T, Potter C, Gholami N, Basu NK, Kubota S, Carvalho S, Pennington MW, Owens IS, Popescu NC. Thirteen UDPglucuronosyltransferase genes are encoded at the human UGT1 gene complex locus. Pharmacogenetics. 2001;11(4):357-68. PubMed PMID: 11434514.

166. Mackenzie PI, Owens IS, Burchell B, Bock KW, Bairoch A, Belanger A, Fournel-Gigleux S, Green M, Hum DW, Iyanagi T, Lancet D, Louisot P, Magdalou J, Chowdhury JR, Ritter JK, Schachter H, Tephly TR, Tipton KF, Nebert DW. The UDP glycosyltransferase gene superfamily: recommended nomenclature update based on evolutionary divergence. Pharmacogenetics. 1997;7(4):255-69. PubMed PMID: 9295054.

167. Fujiwara R, Yokoi T, Nakajima M. Structure and Protein-Protein Interactions of Human UDP-Glucuronosyltransferases. Front Pharmacol. 2016;7:388. doi: 10.3389/fphar.2016.00388. PubMed PMID: 27822186; PMCID: PMC5075577.

168. Miley MJ, Zielinska AK, Keenan JE, Bratton SM, Radominska-Pandya A, Redinbo MR. Crystal structure of the cofactor-binding domain of the human phase II drug-metabolism enzyme UDP-glucuronosyltransferase 2B7. J Mol Biol. 2007;369(2):498-511. doi: 10.1016/j.jmb.2007.03.066. PubMed PMID: 17442341; PMCID: PMC1976284.

169. Matern H, Matern S, Gerok W. Isolation and characterization of rat liver microsomal UDP-glucuronosyltransferase activity toward chenodeoxycholic acid and testosterone as a single form of enzyme. J Biol Chem. 1982;257(13):7422-9. PubMed PMID: 6806274.

170. Ikushiro S, Emi Y, Iyanagi T. Protein-protein interactions between UDP-glucuronosyltransferase isozymes in rat hepatic microsomes. Biochemistry. 1997;36(23):7154-61. doi: 10.1021/bi9702344. PubMed PMID: 9188715.

171. Ghosh SS, Sappal BS, Kalpana GV, Lee SW, Chowdhury JR, Chowdhury NR. Homodimerization of human bilirubin-uridine-diphosphoglucuronate glucuronosyltransferase-1 (UGT1A1) and its functional implications. J Biol Chem. 2001;276(45):42108-15. doi: 10.1074/jbc.M106742200. PubMed PMID: 11546782.

172. Radominska-Pandya A, Ouzzine M, Fournel-Gigleux S, Magdalou J. Structure of UDP-glucuronosyltransferases in membranes. Methods Enzymol. 2005;400:116-47. doi: 10.1016/S0076-6879(05)00008-X. PubMed PMID: 16399347.

173. Bosma PJ, Seppen J, Goldhoorn B, Bakker C, Oude Elferink RP, Chowdhury JR, Chowdhury NR, Jansen PL. Bilirubin UDP-glucuronosyltransferase 1 is the only relevant bilirubin glucuronidating isoform in man. J Biol Chem. 1994;269(27):17960-4. PubMed PMID: 8027054.

174. Watanabe Y, Nakajima M, Ohashi N, Kume T, Yokoi T. Glucuronidation of etoposide in human liver microsomes is specifically catalyzed by UDP-glucuronosyltransferase 1A1. Drug Metab Dispos. 2003;31(5):589-95. PubMed PMID: 12695347.

175. Mano Y, Usui T, Kamimura H. Effects of beta-estradiol and propofol on the 4-methylumbelliferone glucuronidation in recombinant human UGT isozymes 1A1, 1A8 and 1A9. Biopharm Drug Dispos. 2004;25(8):339-44. doi: 10.1002/bdd.418. PubMed PMID: 15378558.

176. Nishihara M, Hiura Y, Kawaguchi N, Takahashi J, Asahi S. UDP-glucuronosyltransferase 2B15 (UGT2B15) is the major enzyme responsible for sipoglitazar glucuronidation in humans: retrospective identification of the UGT isoform by in vitro analysis and the effect of UGT2B15*2 mutation. Drug Metab Pharmacokinet. 2013;28(6):475-84. PubMed PMID: 23648677.

177. Court MH. Isoform-selective probe substrates for in vitro studies of human UDP-glucuronosyltransferases. Methods Enzymol. 2005;400:104-16. doi: 10.1016/S0076-6879(05)00007-8. PubMed PMID: 16399346.

178. Krishnaswamy S, Duan SX, Von Moltke LL, Greenblatt DJ, Court MH. Validation of serotonin (5-hydroxtryptamine) as an in vitro substrate probe for human UDP-glucuronosyltransferase (UGT) 1A6. Drug Metab Dispos. 2003;31(1):133-9. PubMed PMID: 12485962.

179. Kato Y, Izukawa T, Oda S, Fukami T, Finel M, Yokoi T, Nakajima M. Human UDP-glucuronosyltransferase (UGT) 2B10 in drug N-glucuronidation: substrate screening and comparison with UGT1A3 and UGT1A4. Drug Metab Dispos. 2013;41(7):1389-97. doi: 10.1124/dmd.113.051565. PubMed PMID: 23611809.

180. Kuehl GE, Murphy SE. N-glucuronidation of nicotine and cotinine by human liver microsomes and heterologously expressed UDP-glucuronosyltransferases. Drug Metab Dispos. 2003;31(11):1361-8. doi: 10.1124/dmd.31.11.1361. PubMed PMID: 14570768.

181. Smith PA, Sorich MJ, McKinnon RA, Miners JO. Pharmacophore and quantitative structure-activity relationship modeling: complementary approaches for the rationalization and prediction of UDP-glucuronosyltransferase 1A4 substrate selectivity. J Med Chem. 2003;46(9):1617-26. doi: 10.1021/jm020397c. PubMed PMID: 12699380.

182. Rowland A, Elliot DJ, Williams JA, Mackenzie PI, Dickinson RG, Miners JO. In vitro characterization of lamotrigine N2-glucuronidation and the lamotrigine-valproic acid interaction. Drug Metab Dispos. 2006;34(6):1055-62. doi: 10.1124/dmd.106.009340. PubMed PMID: 16565174.

183. Barbier O, Turgeon D, Girard C, Green MD, Tephly TR, Hum DW, Belanger A. 3'-azido-3'-deoxythimidine (AZT) is glucuronidated by human UDP-glucuronosyltransferase 2B7 (UGT2B7). Drug Metab Dispos. 2000;28(5):497-502. PubMed PMID: 10772627.

184. Meech R, Mackenzie PI. UGT3A: novel UDP-glycosyltransferases of the UGT superfamily. Drug Metab Rev. 2010;42(1):45-54. doi: 10.3109/03602530903205823. PubMed PMID: 19814657.

185. Meech R, Rogers A, Zhuang L, Lewis BC, Miners JO, Mackenzie PI. Identification of residues that confer sugar selectivity to UDP-glycosyltransferase 3A (UGT3A) enzymes. J Biol Chem. 2012;287(29):24122-30. doi: 10.1074/jbc.M112.343608. PubMed PMID: 22621930; PMCID: PMC3397839.

186. Meech R, Miners JO, Lewis BC, Mackenzie PI. The glycosidation of xenobiotics and endogenous compounds: versatility and redundancy in the UDP glycosyltransferase superfamily. Pharmacol Ther. 2012;134(2):200-18. doi: 10.1016/j.pharmthera.2012.01.009. PubMed PMID: 22322248.

187. Al-Mahrouki A, Giles A, Hashim A, Kim HC, El-Falou A, Rowe-Magnus D, Farhat G, Czarnota GJ. Microbubble-based enhancement of radiation effect: Role of cell membrane ceramide metabolism. PLoS One. 2017;12(7):e0181951. doi: 10.1371/journal.pone.0181951. PubMed PMID: 28746357; PMCID: PMC5528834.

188. Park H, Lee S, Kim HJ, Ju YS, Shin JY, Hong D, von Grotthuss M, Lee DS, Park C, Kim JH, Kim B, Yoo YJ, Cho SI, Sung J, Lee C, Kim JI, Seo JS. Comprehensive genomic analyses associate UGT8 variants with musical ability in a Mongolian population. J Med Genet.

2012;49(12):747-52. doi: 10.1136/jmedgenet-2012-101209. PubMed PMID: 23118445; PMCID: PMC3512346.

189. Goodfellow JA, Willison HJ. Gangliosides and Autoimmune Peripheral Nerve Diseases. Prog Mol Biol Transl Sci. 2018;156:355-82. doi: 10.1016/bs.pmbts.2017.12.010. PubMed PMID: 29747820.

190. Astudillo L, Sabourdy F, Therville N, Bode H, Segui B, Andrieu-Abadie N, Hornemann T, Levade T. Human genetic disorders of sphingolipid biosynthesis. J Inherit Metab Dis. 2015;38(1):65-76. doi: 10.1007/s10545-014-9736-1. PubMed PMID: 25141825.

191. Itaaho K, Mackenzie PI, Ikushiro S, Miners JO, Finel M. The configuration of the 17-hydroxy group variably influences the glucuronidation of beta-estradiol and epiestradiol by human UDP-glucuronosyltransferases. Drug Metab Dispos. 2008;36(11):2307-15. doi: 10.1124/dmd.108.022731. PubMed PMID: 18719240.

192. Sneitz N, Krishnan K, Covey DF, Finel M. Glucuronidation of the steroid enantiomers ent-17beta-estradiol, ent-androsterone and ent-etiocholanolone by the human UDP-glucuronosyltransferases. J Steroid Biochem Mol Biol. 2011;127(3-5):282-8. doi: 10.1016/j.jsbmb.2011.08.008. PubMed PMID: 21899827; PMCID: PMC3234363.

193. Sneitz N, Vahermo M, Mosorin J, Laakkonen L, Poirier D, Finel M. Regiospecificity and stereospecificity of human UDP-glucuronosyltransferases in the glucuronidation of estriol, 16-epiestriol, 17-epiestriol, and 13-epiestradiol. Drug Metab Dispos. 2013;41(3):582-91. doi: 10.1124/dmd.112.049072. PubMed PMID: 23288867.

194. Court MH, Duan SX, Guillemette C, Journault K, Krishnaswamy S, Von Moltke LL, Greenblatt DJ. Stereoselective conjugation of oxazepam by human UDP-glucuronosyltransferases (UGTs): S-oxazepam is glucuronidated by UGT2B15, while R-oxazepam is glucuronidated by UGT2B7 and UGT1A9. Drug Metab Dispos. 2002;30(11):1257-65. PubMed PMID: 12386133.

195. Du J, You T, Chen X, Zhong D. Stereoselective glucuronidation of ornidazole in humans: predominant contribution of UDP-glucuronosyltransferases 1A9 and 2B7. Drug Metab Dispos. 2013;41(7):1306-18. doi: 10.1124/dmd.113.051235. PubMed PMID: 23571427.

196. Kim D, Zheng YF, Min JS, Park JB, Bae SH, Yoon KD, Chin YW, Oh E, Bae SK. In vitro stereoselective inhibition of ginsenosides toward UDP-glucuronosyltransferase (UGT) isoforms. Toxicol Lett. 2016;259:1-10. doi: 10.1016/j.toxlet.2016.07.108. PubMed PMID: 27462006.

197. Nakamura A, Nakajima M, Yamanaka H, Fujiwara R, Yokoi T. Expression of UGT1A and UGT2B mRNA in human normal tissues and various cell lines. Drug Metab Dispos. 2008;36(8):1461-4. doi: 10.1124/dmd.108.021428. PubMed PMID: 18480185.

198. Izukawa T, Nakajima M, Fujiwara R, Yamanaka H, Fukami T, Takamiya M, Aoki Y, Ikushiro S, Sakaki T, Yokoi T. Quantitative analysis of UDP-glucuronosyltransferase (UGT) 1A and UGT2B expression levels in human livers. Drug Metab Dispos. 2009;37(8):1759-68. doi: 10.1124/dmd.109.027227. PubMed PMID: 19439486.

199. Ohno S, Nakajin S. Determination of mRNA expression of human UDP-glucuronosyltransferases and application for localization in various human tissues by real-time reverse transcriptase-polymerase chain reaction. Drug Metab Dispos. 2009;37(1):32-40. doi: 10.1124/dmd.108.023598. PubMed PMID: 18838504.

200. Somers GI, Lindsay N, Lowdon BM, Jones AE, Freathy C, Ho S, Woodrooffe AJ, Bayliss MK, Manchee GR. A comparison of the expression and metabolizing activities of phase I and II enzymes in freshly isolated human lung parenchymal cells and cryopreserved human hepatocytes. Drug Metab Dispos. 2007;35(10):1797-805. doi: 10.1124/dmd.107.015966. PubMed PMID: 17627976.

201. Thum T, Erpenbeck VJ, Moeller J, Hohlfeld JM, Krug N, Borlak J. Expression of xenobiotic metabolizing enzymes in different lung compartments of smokers and nonsmokers. Environ Health Perspect. 2006;114(11):1655-61. doi: 10.1289/ehp.8861. PubMed PMID: 17107849; PMCID: PMC1665420.

202. Zheng Z, Fang JL, Lazarus P. Glucuronidation: an important mechanism for detoxification of benzo[a]pyrene metabolites in aerodigestive tract tissues. Drug Metab Dispos. 2002;30(4):397-403. PubMed PMID: 11901093.

203. Nishimura M, Naito S. Tissue-specific mRNA expression profiles of human phase I metabolizing enzymes except for cytochrome P450 and phase II metabolizing enzymes. Drug Metab Pharmacokinet. 2006;21(5):357-74. PubMed PMID: 17072089.

204. Bellemare J, Rouleau M, Harvey M, Tetu B, Guillemette C. Alternative-splicing forms of the major phase II conjugating UGT1A gene negatively regulate glucuronidation in human carcinoma cell lines. Pharmacogenomics J. 2010;10(5):431-41. doi: 10.1038/tpj.2009.64. PubMed PMID: 19997083.

205. Court MH, Zhang X, Ding X, Yee KK, Hesse LM, Finel M. Quantitative distribution of mRNAs encoding the 19 human UDP-glucuronosyltransferase enzymes in 26 adult and 3 fetal

tissues. Xenobiotica. 2012;42(3):266-77. doi: 10.3109/00498254.2011.618954. PubMed PMID: 21995321.

206. Harbourt DE, Fallon JK, Ito S, Baba T, Ritter JK, Glish GL, Smith PC. Quantification of human uridine-diphosphate glucuronosyl transferase 1A isoforms in liver, intestine, and kidney using nanobore liquid chromatography-tandem mass spectrometry. Anal Chem. 2012;84(1):98-105. doi: 10.1021/ac201704a. PubMed PMID: 22050083; PMCID: 3259189.

207. Ekstrom L, Johansson M, Rane A. Tissue distribution and relative gene expression of UDP-glucuronosyltransferases (2B7, 2B15, 2B17) in the human fetus. Drug Metab Dispos. 2013;41(2):291-5. doi: 10.1124/dmd.112.049197. PubMed PMID: 23223495.

208. Jones NR, Lazarus P. UGT2B gene expression analysis in multiple tobacco carcinogen-targeted tissues. Drug Metab Dispos. 2014;42(4):529-36. doi: 10.1124/dmd.113.054718. PubMed PMID: 24459179; PMCID: 3965906.

209. Nakamura K, Hirayama-Kurogi M, Ito S, Kuno T, Yoneyama T, Obuchi W, Terasaki T, Ohtsuki S. Large-scale multiplex absolute protein quantification of drug-metabolizing enzymes and transporters in human intestine, liver, and kidney microsomes by SWATH-MS: Comparison with MRM/SRM and HR-MRM/PRM. Proteomics. 2016;16(15-16):2106-17. doi: 10.1002/pmic.201500433. PubMed PMID: 27197958.

210. Neumann E, Mehboob H, Ramirez J, Mirkov S, Zhang M, Liu W. Age-Dependent Hepatic UDP-Glucuronosyltransferase Gene Expression and Activity in Children. Front Pharmacol. 2016;7:437. doi: 10.3389/fphar.2016.00437. PubMed PMID: 27899892; PMCID: PMC5110524.

211. Achour B, Dantonio A, Niosi M, Novak JJ, Fallon JK, Barber J, Smith PC, Rostami-Hodjegan A, Goosen TC. Quantitative Characterization of Major Hepatic UDP-Glucuronosyltransferase Enzymes in Human Liver Microsomes: Comparison of Two Proteomic Methods and Correlation with Catalytic Activity. Drug Metab Dispos. 2017;45(10):1102-12. doi: 10.1124/dmd.117.076703. PubMed PMID: 28768682.

212. Sundararaghavan VL, Sindhwani P, Hinds TD, Jr. Glucuronidation and UGT isozymes in bladder: new targets for the treatment of uroepithelial carcinomas? Oncotarget. 2017;8(2):3640-8. doi: 10.18632/oncotarget.12277. PubMed PMID: 27690298; PMCID: PMC5356909.

213. Meech R, Hu DG, McKinnon RA, Mubarokah SN, Haines AZ, Nair PC, Rowland A, Mackenzie PI. The UDP-Glycosyltransferase (UGT) Superfamily: New Members, New Functions, and Novel Paradigms. Physiol Rev. 2019;99(2):1153-222. doi: 10.1152/physrev.00058.2017. PubMed PMID: 30724669.

214. Strassburg CP, Nguyen N, Manns MP, Tukey RH. Polymorphic expression of the UDP-glucuronosyltransferase UGT1A gene locus in human gastric epithelium. Mol Pharmacol. 1998;54(4):647-54. PubMed PMID: 9765507.

215. Vogel A, Ockenga J, Ehmer U, Barut A, Kramer FJ, Tukey RH, Manns MP, Strassburg CP. Polymorphisms of the carcinogen detoxifying UDP-glucuronosyltransferase UGT1A7 in proximal digestive tract cancer. Z Gastroenterol. 2002;40(7):497-502. doi: 10.1055/s-2002-32805. PubMed PMID: 12122597.

216. Oda S, Fukami T, Yokoi T, Nakajima M. Epigenetic regulation of the tissue-specific expression of human UDP-glucuronosyltransferase (UGT) 1A10. Biochem Pharmacol. 2014;87(4):660-7. doi: 10.1016/j.bcp.2013.11.001. PubMed PMID: 24239897.

217. Miyauchi E, Tachikawa M, Decleves X, Uchida Y, Bouillot JL, Poitou C, Oppert JM, Mouly S, Bergmann JF, Terasaki T, Scherrmann JM, Lloret-Linares C. Quantitative Atlas of Cytochrome P450, UDP-Glucuronosyltransferase, and Transporter Proteins in Jejunum of Morbidly Obese Subjects. Mol Pharm. 2016;13(8):2631-40. doi: 10.1021/acs.molpharmaceut.6b00085. PubMed PMID: 27347605.

218. Mubarokah N, Hulin JA, Mackenzie PI, McKinnon RA, Haines AZ, Hu DG, Meech R. Cooperative Regulation of Intestinal UDP-Glucuronosyltransferases 1A8, -1A9, and 1A10 by CDX2 and HNF4alpha Is Mediated by a Novel Composite Regulatory Element. Mol Pharmacol. 2018;93(5):541-52. doi: 10.1124/mol.117.110619. PubMed PMID: 29519853.

219. Bushey RT, Chen G, Blevins-Primeau AS, Krzeminski J, Amin S, Lazarus P. Characterization of UDP-glucuronosyltransferase 2A1 (UGT2A1) variants and their potential role in tobacco carcinogenesis. Pharmacogenet Genomics. 2011;21(2):55-65. doi: 10.1097/FPC.0b013e328341db05. PubMed PMID: 21164388; PMCID: 3019304.

220. Thomas SS, Makar KW, Li L, Zheng Y, Yang P, Levy L, Rudolph RY, Lampe PD, Yan M, Markowitz SD, Bigler J, Lampe JW, Potter JD. Tissue-specific patterns of gene expression in the epithelium and stroma of normal colon in healthy individuals in an aspirin intervention trial. Genom Data. 2015;6:154-8. doi: 10.1016/j.gdata.2015.08.029. PubMed PMID: 26697360; PMCID: PMC4664722.

221. Giuliani L, Ciotti M, Stoppacciaro A, Pasquini A, Silvestri I, De Matteis A, Frati L, Agliano AM. UDP-glucuronosyltransferases 1A expression in human urinary bladder and colon cancer by immunohistochemistry. Oncol Rep. 2005;13(2):185-91. PubMed PMID: 15643497.

222. Jedlitschky G, Cassidy AJ, Sales M, Pratt N, Burchell B. Cloning and characterization of a novel human olfactory UDP-glucuronosyltransferase. Biochem J. 1999;340 (Pt 3):837-43. PubMed PMID: 10359671; PMCID: PMC1220318.

223. Oguri T, Takahashi T, Miyazaki M, Isobe T, Kohno N, Mackenzie PI, Fujiwara Y. UGT1A10 is responsible for SN-38 glucuronidation and its expression in human lung cancers. Anticancer Res. 2004;24(5A):2893-6. PubMed PMID: 15517893.

224. Strassburg CP, Oldhafer K, Manns MP, Tukey RH. Differential expression of the UGT1A locus in human liver, biliary, and gastric tissue: identification of UGT1A7 and UGT1A10 transcripts in extrahepatic tissue. Mol Pharmacol. 1997;52(2):212-20. PubMed PMID: 9271343.

225. Bellemare J, Rouleau M, Harvey M, Popa I, Pelletier G, Tetu B, Guillemette C. Immunohistochemical expression of conjugating UGT1A-derived isoforms in normal and tumoral drug-metabolizing tissues in humans. J Pathol. 2011;223(3):425-35. doi: 10.1002/path.2805. PubMed PMID: 21171088.

226. Sneitz N, Court MH, Zhang X, Laajanen K, Yee KK, Dalton P, Ding X, Finel M. Human UDP-glucuronosyltransferase UGT2A2: cDNA construction, expression, and functional characterization in comparison with UGT2A1 and UGT2A3. Pharmacogenet Genomics. 2009;19(12):923-34. doi: 10.1097/FPC.0b013e3283330767. PubMed PMID: 19858781; PMCID: PMC2928392.

227. Guillemette C, Levesque E, Rouleau M. Pharmacogenomics of human uridine diphospho-glucuronosyltransferases and clinical implications. Clin Pharmacol Ther. 2014;96(3):324-39. Epub 2014/06/13. doi: 10.1038/clpt.2014.126. PubMed PMID: 24922307.

228. Pan Q, Shai O, Lee LJ, Frey BJ, Blencowe BJ. Deep surveying of alternative splicing complexity in the human transcriptome by high-throughput sequencing. Nat Genet. 2008;40(12):1413-5. Epub 2008/11/04. doi: 10.1038/ng.259. PubMed PMID: 18978789.

229. Bushey RT, Lazarus P. Identification and functional characterization of a novel UDP-glucuronosyltransferase 2A1 splice variant: potential importance in tobacco-related cancer susceptibility. J Pharmacol Exp Ther. 2012;343(3):712-24. doi: 10.1124/jpet.112.198770. PubMed PMID: 22984225; PMCID: 3500542.

230. Bellemare J, Rouleau M, Girard H, Harvey M, Guillemette C. Alternatively spliced products of the UGT1A gene interact with the enzymatically active proteins to inhibit glucuronosyltransferase activity in vitro. Drug Metab Dispos. 2010;38(10):1785-9. doi: 10.1124/dmd.110.034835. PubMed PMID: 20610558.

231. Finel M, Kurkela M. The UDP-glucuronosyltransferases as oligomeric enzymes. Curr Drug Metab. 2008;9(1):70-6. Epub 2008/01/29. PubMed PMID: 18220573.

232. Zhang ZD, Frankish A, Hunt T, Harrow J, Gerstein M. Identification and analysis of unitary pseudogenes: historic and contemporary gene losses in humans and other primates. Genome Biol. 2010;11(3):R26. Epub 2010/03/10. doi: 10.1186/gb-2010-11-3-r26. PubMed PMID: 20210993; PMCID: PMC2864566.

233. Sasidharan R, Gerstein M. Genomics: protein fossils live on as RNA. Nature. 2008;453(7196):729-31. Epub 2008/06/06. doi: 10.1038/453729a. PubMed PMID: 18528383.

234. Kakehi M, Ikenaka Y, Nakayama SM, Kawai YK, Watanabe KP, Mizukawa H, Nomiyama K, Tanabe S, Ishizuka M. Uridine Diphosphate-Glucuronosyltransferase (UGT) Xenobiotic

Metabolizing Activity and Genetic Evolution in Pinniped Species. Toxicol Sci. 2015;147(2):360-9. doi: 10.1093/toxsci/kfv144. PubMed PMID: 26179383.

235. Heikkinen AT, Friedlein A, Matondo M, Hatley OJ, Petsalo A, Juvonen R, Galetin A, Rostami-Hodjegan A, Aebersold R, Lamerz J, Dunkley T, Cutler P, Parrott N. Quantitative ADME proteomics - CYP and UGT enzymes in the Beagle dog liver and intestine. Pharm Res. 2015;32(1):74-90. doi: 10.1007/s11095-014-1446-8. PubMed PMID: 25033762.

236. Bartel DP. MicroRNAs: genomics, biogenesis, mechanism, and function. Cell. 2004;116(2):281-97. Epub 2004/01/28. PubMed PMID: 14744438.

237. Carthew RW, Sontheimer EJ. Origins and Mechanisms of miRNAs and siRNAs. Cell. 2009;136(4):642-55. Epub 2009/02/26. doi: 10.1016/j.cell.2009.01.035. PubMed PMID: 19239886; PMCID: PMC2675692.

238. Gu W, Xu Y, Xie X, Wang T, Ko JH, Zhou T. The role of RNA structure at 5' untranslated region in microRNA-mediated gene regulation. RNA. 2014;20(9):1369-75. Epub 2014/07/09. doi: 10.1261/rna.044792.114. PubMed PMID: 25002673; PMCID: PMC4138320.

239. Fang Z, Rajewsky N. The impact of miRNA target sites in coding sequences and in 3'UTRs. PLoS One. 2011;6(3):e18067. Epub 2011/03/30. doi: 10.1371/journal.pone.0018067. PubMed PMID: 21445367; PMCID: PMC3062573.

240. Naguibneva I, Ameyar-Zazoua M, Polesskaya A, Ait-Si-Ali S, Groisman R, Souidi M, Cuvellier S, Harel-Bellan A. The microRNA miR-181 targets the homeobox protein Hox-A11 during mammalian myoblast differentiation. Nat Cell Biol. 2006;8(3):278-84. Epub 2006/02/21. doi: 10.1038/ncb1373. PubMed PMID: 16489342.

241. Dluzen DF, Sun D, Salzberg AC, Jones N, Bushey RT, Robertson GP, Lazarus P. Regulation of UDP-glucuronosyltransferase 1A1 expression and activity by microRNA 491-3p. J Pharmacol Exp Ther. 2014;348(3):465-77. doi: 10.1124/jpet.113.210658. PubMed PMID: 24399855; PMCID: 3935146.

242. Papageorgiou I, Freytsis M, Court MH. Transcriptome association analysis identifies miR-375 as a major determinant of variable acetaminophen glucuronidation by human liver. Biochem Pharmacol. 2016;117:78-87. Epub 2016/08/18. doi: 10.1016/j.bcp.2016.08.014. PubMed PMID: 27531059; PMCID: PMC5031542.

243. Papageorgiou I, Court MH. Identification and validation of microRNAs directly regulating the UDP-glucuronosyltransferase 1A subfamily enzymes by a functional genomics approach. Biochem Pharmacol. 2017;137:93-106. Epub 2017/04/24. doi: 10.1016/j.bcp.2017.04.017. PubMed PMID: 28433553; PMCID: PMC6179579.

244. Tatsumi N, Tokumitsu S, Nakano M, Fukami T, Nakajima M. miR-141-3p commonly regulates human UGT1A isoforms via different mechanisms. Drug Metab Pharmacokinet. 2018;33(4):203-10. Epub 2018/07/14. doi: 10.1016/j.dmpk.2018.05.002. PubMed PMID: 30001838.

245. Wijayakumara DD, Hu DG, Meech R, McKinnon RA, Mackenzie PI. Regulation of Human UGT2B15 and UGT2B17 by miR-376c in Prostate Cancer Cell Lines. J Pharmacol Exp Ther. 2015;354(3):417-25. Epub 2015/07/15. doi: 10.1124/jpet.115.226118. PubMed PMID: 26163549.

246. Margaillan G, Levesque E, Guillemette C. Epigenetic regulation of steroid inactivating UDP-glucuronosyltransferases by microRNAs in prostate cancer. J Steroid Biochem Mol Biol.

2016;155(Pt A):85-93. Epub 2015/09/20. doi: 10.1016/j.jsbmb.2015.09.021. PubMed PMID: 26385605.

247. Wijayakumara DD, Mackenzie PI, McKinnon RA, Hu DG, Meech R. Regulation of UDP-Glucuronosyltransferases UGT2B4 and UGT2B7 by MicroRNAs in Liver Cancer Cells. J Pharmacol Exp Ther. 2017;361(3):386-97. Epub 2017/04/09. doi: 10.1124/jpet.116.239707. PubMed PMID: 28389526.

248. Papageorgiou I, Court MH. Identification and validation of the microRNA response elements in the 3'-untranslated region of the UDP glucuronosyltransferase (UGT) 2B7 and 2B15 genes by a functional genomics approach. Biochem Pharmacol. 2017;146:199-213. Epub 2017/10/01. doi: 10.1016/j.bcp.2017.09.013. PubMed PMID: 28962835; PMCID: PMC6188638.

249. Dluzen DF, Sutliff AK, Chen G, Watson CJ, Ishmael FT, Lazarus P. Regulation of UGT2B Expression and Activity by miR-216b-5p in Liver Cancer Cell Lines. J Pharmacol Exp Ther. 2016;359(1):182-93. Epub 2016/07/31. doi: 10.1124/jpet.116.235044. PubMed PMID: 27474751; PMCID: PMC5034702.

250. Wiener D, Fang JL, Dossett N, Lazarus P. Correlation between UDP-glucuronosyltransferase genotypes and 4-(methylnitrosamino)-1-(3-pyridyl)-1-butanone glucuronidation phenotype in human liver microsomes. Cancer Res. 2004;64(3):1190-6. PubMed PMID: 14871856.

251. Wassenaar CA, Conti DV, Das S, Chen P, Cook EH, Ratain MJ, Benowitz NL, Tyndale RF. UGT1A and UGT2B genetic variation alters nicotine and nitrosamine glucuronidation in european and african american smokers. Cancer Epidemiol Biomarkers Prev. 2015;24(1):94-104. doi: 10.1158/1055-9965.EPI-14-0804. PubMed PMID: 25277794; PMCID: 4294984.

252. Chung CJ, Pu YS, Shiue HS, Lee HL, Lin P, Yang HY, Su CT, Hsueh YM. 4-(Methylnitrosamino)-1-(3-pyridyl)-1-butanone (NNK) metabolism-related enzymes gene polymorphisms, NNK metabolites levels and urothelial carcinoma. Toxicol Lett. 2013;216(1):16-22. doi: 10.1016/j.toxlet.2012.11.002. PubMed PMID: 23142425.

253. Lazarus P, Zheng Y, Runkle EA, Muscat JE, Wiener D. Genotype-phenotype correlation between the polymorphic UGT2B17 gene deletion and NNAL glucuronidation activities in human liver microsomes. Pharmacogenet Genomics. 2005;15(11):769-78. PubMed PMID: 16220109.

254. Gruber M, Le T, Filipits M, Gsur A, Mannhalter C, Jager U, Vanura K. UDP-glucuronosyltransferase 2B17 genotype and the risk of lung cancer among Austrian Caucasians. Cancer Epidemiol. 2013;37(5):625-8. doi: 10.1016/j.canep.2013.06.004. PubMed PMID: 23850147.

255. Wiener D, Doerge DR, Fang JL, Upadhyaya P, Lazarus P. Characterization of N-glucuronidation of the lung carcinogen 4-(methylnitrosamino)-1-(3-pyridyl)-1-butanol (NNAL) in human liver: importance of UDP-glucuronosyltransferase 1A4. Drug Metab Dispos. 2004;32(1):72-9. doi: 10.1124/dmd.32.1.72. PubMed PMID: 14709623.

256. Chen G, Dellinger RW, Sun D, Spratt TE, Lazarus P. Glucuronidation of tobacco-specific nitrosamines by UGT2B10. Drug Metab Dispos. 2008;36(5):824-30. doi: 10.1124/dmd.107.019406. PubMed PMID: 18238858; PMCID: 2714266.

257. Chen G, Dellinger RW, Gallagher CJ, Sun D, Lazarus P. Identification of a prevalent functional missense polymorphism in the UGT2B10 gene and its association with UGT2B10 inactivation against tobacco-specific nitrosamines. Pharmacogenet Genomics. 2008;18(3):181-91. doi: 10.1097/FPC.0b013e3282f4dbdd. PubMed PMID: 18300939.

258. Upadhyaya P, McIntee EJ, Hecht SS. Preparation of pyridine-N-glucuronides of tobacco-specific nitrosamines. Chem Res Toxicol. 2001;14(5):555-61. PubMed PMID: 11368554.

259. Carmella SG, Le Ka KA, Upadhyaya P, Hecht SS. Analysis of N- and O-glucuronides of 4-(methylnitrosamino)-1-(3-pyridyl)-1-butanol (NNAL) in human urine. Chem Res Toxicol. 2002;15(4):545-50. PubMed PMID: 11952341.

260. Carmella SG, Han S, Fristad A, Yang Y, Hecht SS. Analysis of total 4-(methylnitrosamino)-1-(3-pyridyl)-1-butanol (NNAL) in human urine. Cancer Epidemiol Biomarkers Prev. 2003;12(11 Pt 1):1257-61. PubMed PMID: 14652291.

261. Yao L, Zheng S, Guan Y, Yang J, Liu B, Wang W, Zhu X. Development of a rapid method for the simultaneous separation and determination of 4-(methylnitrosamino)-1-(3-pyridyl)-1-butanol and its N- and O-glucuronides in human urine by liquid chromatography-tandem mass spectrometry. Anal Chim Acta. 2013;788:61-7. doi: 10.1016/j.aca.2013.06.034. PubMed PMID: 23845482.

262. Murphy SE, von Weymarn LB, Parenteau M, Stepanov I, Tiirikainen M, LeMarchand L, Park SL. Influence of UGT2B10 Genotype on Urinary Excretion of 4-(Methylnitrosamino)-1-(3-pyridyl)-1-butanol- N-glucuronide by African American Smokers. Chem Res Toxicol. 2018;31(3):168-75. doi: 10.1021/acs.chemrestox.7b00264. PubMed PMID: 29460622; PMCID: PMC6058729.

263. Carmella SG, Akerkar SA, Richie JP, Jr., Hecht SS. Intraindividual and interindividual differences in metabolites of the tobacco-specific lung carcinogen 4-(methylnitrosamino)-1-(3-pyridyl)-1-butanone (NNK) in smokers' urine. Cancer Epidemiol Biomarkers Prev. 1995;4(6):635-42. PubMed PMID: 8547830.

264. Richie JP, Jr., Carmella SG, Muscat JE, Scott DG, Akerkar SA, Hecht SS. Differences in the urinary metabolites of the tobacco-specific lung carcinogen 4-(methylnitrosamino)-1-(3-pyridyl)-1-butanone in black and white smokers. Cancer Epidemiol Biomarkers Prev. 1997;6(10):783-90. PubMed PMID: 9332760.

265. Murata M, Warren EH, Riddell SR. A human minor histocompatibility antigen resulting from differential expression due to a gene deletion. J Exp Med. 2003;197(10):1279-89. doi: 10.1084/jem.20030044. PubMed PMID: 12743171; PMCID: 2193779.

266. Wilson W, 3rd, Pardo-Manuel de Villena F, Lyn-Cook BD, Chatterjee PK, Bell TA, Detwiler DA, Gilmore RC, Valladeras IC, Wright CC, Threadgill DW, Grant DJ. Characterization of a common deletion polymorphism of the UGT2B17 gene linked to UGT2B15. Genomics. 2004;84(4):707-14. doi: 10.1016/j.ygeno.2004.06.011. PubMed PMID: 15475248.

267. Gallagher CJ, Kadlubar FF, Muscat JE, Ambrosone CB, Lang NP, Lazarus P. The UGT2B17 gene deletion polymorphism and risk of prostate cancer. A case-control study in Caucasians. Cancer Detect Prev. 2007;31(4):310-5. doi: 10.1016/j.cdp.2007.07.005. PubMed PMID: 17935910; PMCID: 2096411.

268. Chen G, Blevins-Primeau AS, Dellinger RW, Muscat JE, Lazarus P. Glucuronidation of nicotine and cotinine by UGT2B10: loss of function by the UGT2B10 Codon 67 (Asp>Tyr) polymorphism. Cancer Res. 2007;67(19):9024-9. doi: 10.1158/0008-5472.CAN-07-2245. PubMed PMID: 17909004.

269. Stepanov I, Hecht SS. Tobacco-specific nitrosamines and their pyridine-N-glucuronides in the urine of smokers and smokeless tobacco users. Cancer Epidemiol Biomarkers Prev. 2005;14(4):885-91. doi: 10.1158/1055-9965.EPI-04-0753. PubMed PMID: 15824160.

270. Oertling H, Reckziegel A, Surburg H, Bertram HJ. Applications of menthol in synthetic chemistry. Chem Rev. 2007;107(5):2136-64. doi: 10.1021/cr068409f. PubMed PMID: 17488063.

271. Eccles R, Griffiths DH, Newton CG, Tolley NS. The effects of D and L isomers of menthol upon nasal sensation of airflow. J Laryngol Otol. 1988;102(6):506-8. PubMed PMID: 3397650.

272. Bhatia SP, McGinty D, Letizia CS, Api AM. Fragrance material review on d-menthol. Food Chem Toxicol. 2008;46 Suppl 11:S215-7. doi: 10.1016/j.fct.2008.06.039. PubMed PMID: 18640220.

273. Lawrence D, Cadman B, Hoffman AC. Sensory properties of menthol and smoking topography. Tob Induc Dis. 2011;9 Suppl 1:S3. doi: 10.1186/1617-9625-9-S1-S3. PubMed PMID: 21624149; PMCID: PMC3102902.

274. Celebucki CC, Wayne GF, Connolly GN, Pankow JF, Chang EI. Characterization of measured menthol in 48 U.S. cigarette sub-brands. Nicotine Tob Res. 2005;7(4):523-31. doi: 10.1080/14622200500186270. PubMed PMID: 16085523.

275. Giovino GA, Sidney S, Gfroerer JC, O'Malley PM, Allen JA, Richter PA, Cummings KM. Epidemiology of menthol cigarette use. Nicotine Tob Res. 2004;6 Suppl 1:S67-81. doi: 10.1080/14622203710001649696. PubMed PMID: 14982710.

276. Muscat JE, Chen G, Knipe A, Stellman SD, Lazarus P, Richie JP, Jr. Effects of menthol on tobacco smoke exposure, nicotine dependence, and NNAL glucuronidation. Cancer Epidemiol Biomarkers Prev. 2009;18(1):35-41. doi: 10.1158/1055-9965.EPI-08-0744. PubMed PMID: 19124478; PMCID: 2676921.

277. Kaffenberger RM, Doyle MJ. Determination of menthol and menthol glucuronide in human urine by gas chromatography using an enzyme-sensitive internal standard and flame ionization detection. J Chromatogr. 1990;527(1):59-66. PubMed PMID: 2365793.

278. Gelal A, Jacob P, 3rd, Yu L, Benowitz NL. Disposition kinetics and effects of menthol. Clin Pharmacol Ther. 1999;66(2):128-35. doi: 10.1053/cp.1999.v66.100455001. PubMed PMID: 10460066.

279. Appleton S, Olegario RM, Lipowicz PJ. TSNA levels in machine-generated mainstream cigarette smoke: 35 years of data. Regul Toxicol Pharmacol. 2013;66(2):197-207. doi: 10.1016/j.yrtph.2013.03.013. PubMed PMID: 23557986.

280. Hecht SS, Hoffmann D. The relevance of tobacco-specific nitrosamines to human cancer. Cancer Surv. 1989;8(2):273-94. PubMed PMID: 2696581.

281. Zimmerman CL, Wu Z, Upadhyaya P, Hecht SS. Stereoselective metabolism and tissue retention in rats of the individual enantiomers of 4-(methylnitrosamino)-1-(3-pyridyl)-1-butanol (NNAL), metabolites of the tobacco-specific nitrosamine, 4-(methylnitrosamino)-1-(3-pyridyl)-1-butanone (NNK). Carcinogenesis. 2004;25(7):1237-42. doi: 10.1093/carcin/bgh120. PubMed PMID: 14988218.

282. Lao Y, Yu N, Kassie F, Villalta PW, Hecht SS. Formation and accumulation of pyridyloxobutyl DNA adducts in F344 rats chronically treated with 4-(methylnitrosamino)-1-(3-pyridyl)-1-butanone and enantiomers of its metabolite, 4-(methylnitrosamino)-1-(3-pyridyl)-1-butanol. Chem Res Toxicol. 2007;20(2):235-45. doi: 10.1021/tx060207r. PubMed PMID: 17305407; PMCID: 2518979.

283. Zhang S, Wang M, Villalta PW, Lindgren BR, Upadhyaya P, Lao Y, Hecht SS. Analysis of pyridyloxobutyl and pyridylhydroxybutyl DNA adducts in extrahepatic tissues of F344 rats treated chronically with 4-(methylnitrosamino)-1-(3-pyridyl)-1-butanone and enantiomers of 4-(methylnitrosamino)-1-(3-pyridyl)-1-butanol. Chem Res Toxicol. 2009;22(5):926-36. doi: 10.1021/tx900015d. PubMed PMID: 19358518; PMCID: 2701567.

284. Coughtrie MW, Burchell B, Bend JR. Purification and properties of rat kidney UDP-glucuronosyltransferase. Biochem Pharmacol. 1987;36(2):245-51. PubMed PMID: 3101703.

285. Dellinger RW, Fang JL, Chen G, Weinberg R, Lazarus P. Importance of UDP-glucuronosyltransferase 1A10 (UGT1A10) in the detoxification of polycyclic aromatic hydrocarbons: decreased glucuronidative activity of the UGT1A10139Lys isoform. Drug Metab Dispos. 2006;34(6):943-9. doi: 10.1124/dmd.105.009100. PubMed PMID: 16510539.

286. Sun D, Chen G, Dellinger RW, Duncan K, Fang JL, Lazarus P. Characterization of tamoxifen and 4-hydroxytamoxifen glucuronidation by human UGT1A4 variants. Breast Cancer Res. 2006;8(4):R50. doi: 10.1186/bcr1539. PubMed PMID: 16884532; PMCID: 1779459.

287. Desai D, Krzeminski J, El-Bayoumy K, Amin S. Syntheses of isotope-labeled tobacco-specific nitrosamines and their metabolites Journal of Labelled Compounds and Radiopharmaceuticals Volume 51, Issue 5. J Labelled Compd Radiopharm [Internet]. 2008 01; 51 5:[226-30 pp.]. Available from: http://onlinelibrary.wiley.com/doi/10.1002/jlcr.1508/abstract.

288. Atalla A, Breyer-Pfaff U, Maser E. Purification and characterization of oxidoreductases-catalyzing carbonyl reduction of the tobacco-specific nitrosamine 4-methylnitrosamino-1-(3-pyridyl)-1-butanone (NNK) in human liver cytosol. Xenobiotica. 2000;30(8):755-69. doi: 10.1080/00498250050119826. PubMed PMID: 11037109.

289. Fallon JK, Neubert H, Hyland R, Goosen TC, Smith PC. Targeted quantitative proteomics for the analysis of 14 UGT1As and -2Bs in human liver using NanoUPLC-MS/MS with selected reaction monitoring. J Proteome Res. 2013;12(10):4402-13. doi: 10.1021/pr4004213. PubMed PMID: 23977844.

290. Carmella SG, Akerkar S, Hecht SS. Metabolites of the tobacco-specific nitrosamine 4-(methylnitrosamino)-1-(3-pyridyl)-1-butanone in smokers' urine. Cancer research. 1993;53:721-4. Epub 02/15. PubMed PMID: 8428352.

291. Hoffmann D, Raineri R, Hecht SS, Maronpot R, Wynder EL. A study of tobacco carcinogenesis. XIV. Effects of N'-nitrosonornicotine and N'-nitrosonanabasine in rats. J Natl Cancer Inst. 1975;55:977-81. Epub 10/01. PubMed PMID: 1237631.

292. Hecht SS. Biochemistry, biology, and carcinogenicity of tobacco-specific N-nitrosamines. Chemical research in toxicology. 1998;11:559-603. Epub 06/24. doi: 10.1021/tx980005y. PubMed PMID: 9625726.

293. Thomson NM, Kenney PM, Peterson LA. The pyridyloxobutyl DNA adduct, O6-[4-oxo-4-(3-pyridyl)butyl]guanine, is detected in tissues from 4-(methylnitrosamino)-1-(3-pyridyl)-1-butanone-treated A/J mice. Chem Res Toxicol. 2003;16:1-6. Epub 04/16. doi: 10.1021/tx025585k. PubMed PMID: 12693024.

294. Wang M, Cheng G, Sturla SJ, Shi Y, McIntee EJ, Villalta PW, Upadhyaya P, Hecht SS. Identification of adducts formed by pyridyloxobutylation of deoxyguanosine and DNA by 4-(acetoxymethylnitrosamino)-1-(3-pyridyl)-1-butanone, a chemically activated form of tobacco specific carcinogens. Chem Res Toxicol. 2003;16:616-26. Epub 05/21. doi: 10.1021/tx034003b. PubMed PMID: 12755591.

295. Hecht SS, Villalta PW, Sturla SJ, Cheng G, Yu N, Upadhyaya P, Wang M. Identification of O2-substituted pyrimidine adducts formed in reactions of 4-(acetoxymethylnitrosamino)- 1-(3-pyridyl)-1-butanone and 4-(acetoxymethylnitros- amino)-1-(3-pyridyl)-1-butanol with DNA. Chem Res Toxicol. 2004;17:588-97. Epub 05/18. doi: 10.1021/tx034263t. PubMed PMID: 15144215.

296. Hecht SS. Tobacco smoke carcinogens and lung cancer. J Natl Cancer Inst. 1999;91(14):1194-210. PubMed PMID: 10413421.

297. Nemzek WR, Hecht S, Gandour-Edwards R, Donald P, McKennan K. Perineural spread of head and neck tumors: how accurate is MR imaging? AJNR Am J Neuroradiol. 1998;19(4):701-6. PubMed PMID: 9576658.

298. Hecht SS. DNA adduct formation from tobacco-specific N-nitrosamines. Mutat Res. 1999;424(1-2):127-42. PubMed PMID: 10064856.

299. Kozlovich S, Chen G, Lazarus P. Stereospecific Metabolism of the Tobacco-Specific Nitrosamine, NNAL. Chem Res Toxicol. 2015. doi: 10.1021/acs.chemrestox.5b00278. PubMed PMID: 26452127.

300. Balliet RM, Chen G, Dellinger RW, Lazarus P. UDP-glucuronosyltransferase 1A10: activity against the tobacco-specific nitrosamine, 4-(methylnitrosamino)-1-(3-pyridyl)-1-butanol, and a potential role for a novel UGT1A10 promoter deletion polymorphism in cancer susceptibility. Drug Metab Dispos. 2010;38(3):484-90. doi: 10.1124/dmd.109.030569. PubMed PMID: 20007297; PMCID: 2835395.

301. Fang JL, Beland FA, Doerge DR, Wiener D, Guillemette C, Marques MM, Lazarus P. Characterization of benzo(a)pyrene-trans-7,8-dihydrodiol glucuronidation by human tissue microsomes and overexpressed UDP-glucuronosyltransferase enzymes. Cancer Res. 2002;62(7):1978-86. PubMed PMID: 11929814.

302. Elahi A, Bendaly J, Zheng Z, Muscat JE, Richie JP, Jr., Schantz SP, Lazarus P. Detection of UGT1A10 polymorphisms and their association with orolaryngeal carcinoma risk. Cancer. 2003;98(4):872-80. doi: 10.1002/cncr.11587. PubMed PMID: 12910533.

303. Saika K, Machii R. Cancer mortality attributable to tobacco by region based on the WHO Global Report. Jpn J Clin Oncol. 2012;42(8):771-2. doi: 10.1093/jjco/hys117. PubMed PMID: 22844131.

304. Goniewicz ML, Havel CM, Peng MW, Jacob P, 3rd, Dempsey D, Yu L, Zielinska-Danch W, Koszowski B, Czogala J, Sobczak A, Benowitz NL. Elimination kinetics of the tobacco-specific biomarker and lung carcinogen 4-(methylnitrosamino)-1-(3-pyridyl)-1-butanol. Cancer Epidemiol Biomarkers Prev. 2009;18(12):3421-5. doi: 10.1158/1055-9965.EPI-09-0874. PubMed PMID: 19959691; PMCID: 2804843.

305. Sidney S, Tekawa IS, Friedman GD, Sadler MC, Tashkin DP. Mentholated cigarette use and lung cancer. Arch Intern Med. 1995;155(7):727-32. PubMed PMID: 7695461.

306. Kabat GC, Hebert JR. Use of mentholated cigarettes and lung cancer risk. Cancer Res. 1991;51(24):6510-3. PubMed PMID: 1742723.

307. Carpenter CL, Jarvik ME, Morgenstern H, McCarthy WJ, London SJ. Mentholated cigarette smoking and lung-cancer risk. Ann Epidemiol. 1999;9(2):114-20. PubMed PMID: 10037555.

308. Stellman SD, Chen Y, Muscat JE, Djordjevic MV, Richie JP, Jr., Lazarus P, Thompson S, Altorki N, Berwick M, Citron ML, Harlap S, Kaur TB, Neugut AI, Olson S, Travaline JM, Witorsch P, Zhang ZF. Lung cancer risk in white and black Americans. Ann Epidemiol. 2003;13(4):294-302. PubMed PMID: 12684197.

309. Brooks DR, Palmer JR, Strom BL, Rosenberg L. Menthol cigarettes and risk of lung cancer. Am J Epidemiol. 2003;158(7):609-16; discussion 17-20. PubMed PMID: 14507595.

310. Murray RP, Connett JE, Skeans MA, Tashkin DP. Menthol cigarettes and health risks in Lung Health Study data. Nicotine Tob Res. 2007;9(1):101-7. doi: 10.1080/14622200601078418. PubMed PMID: 17365741.

311. Blot WJ, Cohen SS, Aldrich M, McLaughlin JK, Hargreaves MK, Signorello LB. Lung cancer risk among smokers of menthol cigarettes. J Natl Cancer Inst. 2011;103(10):810-6. doi: 10.1093/jnci/djr102. PubMed PMID: 21436064; PMCID: PMC3096798.

312. Rostron B. Lung cancer mortality risk for U.S. menthol cigarette smokers. Nicotine Tob Res. 2012;14(10):1140-4. doi: 10.1093/ntr/nts014. PubMed PMID: 22387991.

313. Munro HM, Tarone RE, Wang TJ, Blot WJ. Menthol and Nonmenthol Cigarette Smoking: All-Cause Deaths, Cardiovascular Disease Deaths, and Other Causes of Death Among Blacks and Whites. Circulation. 2016;133(19):1861-6. doi: 10.1161/CIRCULATIONAHA.115.020536. PubMed PMID: 27022064; PMCID: PMC4886344.

314. Lee PN. Systematic review of the epidemiological evidence comparing lung cancer risk in smokers of mentholated and unmentholated cigarettes. BMC Pulm Med. 2011;11:18. doi: 10.1186/1471-2466-11-18. PubMed PMID: 21501470; PMCID: PMC3103484.

315. Jones MR, Tellez-Plaza M, Navas-Acien A. Smoking, menthol cigarettes and all-cause, cancer and cardiovascular mortality: evidence from the National Health and Nutrition Examination Survey (NHANES) and a meta-analysis. PLoS One. 2013;8(10):e77941. doi: 10.1371/journal.pone.0077941. PubMed PMID: 24205038; PMCID: PMC3808303.

316. Benowitz NL, Dains KM, Dempsey D, Havel C, Wilson M, Jacob P, 3rd. Urine menthol as a biomarker of mentholated cigarette smoking. Cancer Epidemiol Biomarkers Prev. 2010;19(12):3013-9. doi: 10.1158/1055-9965.EPI-10-0706. PubMed PMID: 20962297; PMCID: PMC3005539.

317. Food and Drug Administration. Drugs for Human Use. In: Department of health and human Services, editor. April 2018 ed2018.

318. Haiman CA, Stram DO, Wilkens LR, Pike MC, Kolonel LN, Henderson BE, Le Marchand L. Ethnic and racial differences in the smoking-related risk of lung cancer. N Engl J Med. 2006;354(4):333-42. doi: 10.1056/NEJMoa033250. PubMed PMID: 16436765.

319. Coultas DB, Gong H, Jr., Grad R, Handler A, McCurdy SA, Player R, Rhoades ER, Samet JM, Thomas A, Westley M. Respiratory diseases in minorities of the United States. Am J Respir Crit Care Med. 1994;149(3 Pt 2):S93-131. doi: 10.1164/ajrccm/149.3_Pt_2.S93. PubMed PMID: 8118656.

320. Benowitz NL, Dains KM, Dempsey D, Wilson M, Jacob P. Racial differences in the relationship between number of cigarettes smoked and nicotine and carcinogen exposure. Nicotine Tob Res. 2011;13(9):772-83. doi: 10.1093/ntr/ntr072. PubMed PMID: 21546441; PMCID: 3168241.

321. Benowitz NL, Bernert JT, Caraballo RS, Holiday DB, Wang J. Optimal serum cotinine levels for distinguishing cigarette smokers and nonsmokers within different racial/ethnic groups in the United States between 1999 and 2004. Am J Epidemiol. 2009;169(2):236-48. doi: 10.1093/aje/kwn301. PubMed PMID: 19019851.

322. Caraballo RS, Giovino GA, Pechacek TF, Mowery PD, Richter PA, Strauss WJ, Sharp DJ, Eriksen MP, Pirkle JL, Maurer KR. Racial and ethnic differences in serum cotinine levels of cigarette smokers: Third National Health and Nutrition Examination Survey, 1988-1991. JAMA. 1998;280(2):135-9. PubMed PMID: 9669785.

323. Clark PI, Gautam S, Gerson LW. Effect of menthol cigarettes on biochemical markers of smoke exposure among black and white smokers. Chest. 1996;110(5):1194-8. PubMed PMID: 8915220.

324. Perez-Stable EJ, Herrera B, Jacob P, 3rd, Benowitz NL. Nicotine metabolism and intake in black and white smokers. JAMA. 1998;280(2):152-6. PubMed PMID: 9669788.

325. Park SL, Patel YM, Loo LWM, Mullen DJ, Offringa IA, Maunakea A, Stram DO, Siegmund K, Murphy SE, Tiirikainen M, Le Marchand L. Association of internal smoking dose with blood DNA methylation in three racial/ethnic populations. Clin Epigenetics. 2018;10(1):110. doi: 10.1186/s13148-018-0543-7. PubMed PMID: 30139389; PMCID: PMC6108111.

326. Kramlinger VM, von Weymarn LB, Murphy SE. Inhibition and inactivation of cytochrome P450 2A6 and cytochrome P450 2A13 by menthofuran, beta-nicotyrine and menthol. Chem Biol Interact. 2012;197(2-3):87-92. doi: 10.1016/j.cbi.2012.03.009. PubMed PMID: 22486895; PMCID: PMC3362486.

327. Signorello LB, Hargreaves MK, Blot WJ. The Southern Community Cohort Study: investigating health disparities. J Health Care Poor Underserved. 2010;21(1 Suppl):26-37. doi: 10.1353/hpu.0.0245. PubMed PMID: 20173283; PMCID: PMC2940058.

328. Bhasker CR, McKinnon W, Stone A, Lo AC, Kubota T, Ishizaki T, Miners JO. Genetic polymorphism of UDP-glucuronosyltransferase 2B7 (UGT2B7) at amino acid 268: ethnic diversity of alleles and potential clinical significance. Pharmacogenetics. 2000;10(8):679-85. PubMed PMID: 11186130.

329. Green MD, Tephly TR. Glucuronidation of amines and hydroxylated xenobiotics and endobiotics catalyzed by expressed human UGT1.4 protein. Drug Metab Dispos. 1996;24(3):356-63. PubMed PMID: 8820428.

330. Ishii Y, Iida N, Miyauchi Y, Mackenzie PI, Yamada H. Inhibition of morphine glucuronidation in the liver microsomes of rats and humans by monoterpenoid alcohols. Biol Pharm Bull. 2012;35(10):1811-7. PubMed PMID: 22878261.

331. Hsu PC, Lan RS, Brasky TM, Marian C, Cheema AK, Ressom HW, Loffredo CA, Pickworth WB, Shields PG. Metabolomic profiles of current cigarette smokers. Mol Carcinog. 2017;56(2):594-606. doi: 10.1002/mc.22519. PubMed PMID: 27341184; PMCID: PMC5646689.

332. Geer LY, Marchler-Bauer A, Geer RC, Han L, He J, He S, Liu C, Shi W, Bryant SH. The NCBI BioSystems database. Nucleic Acids Res. 2010;38(Database issue):D492-6. doi: 10.1093/nar/gkp858. PubMed PMID: 19854944; PMCID: PMC2808896.

333. Ai J, Taylor KM, Lisko JG, Tran H, Watson CH, Holman MR. Menthol Content in US Marketed Cigarettes. Nicotine Tob Res. 2016;18(7):1575-80. doi: 10.1093/ntr/ntv162. PubMed PMID: 26259988; PMCID: PMC4747842.

334. Rickert WS, Joza PJ, Sharifi M, Wu J, Lauterbach JH. Reductions in the tobacco specific nitrosamine (TSNA) content of tobaccos taken from commercial Canadian cigarettes and corresponding reductions in TSNA deliveries in mainstream smoke from such cigarettes. Regul Toxicol Pharmacol. 2008;51(3):306-10. doi: 10.1016/j.yrtph.2008.04.009. PubMed PMID: 18508168.

335. Ding YS, Zhang L, Jain RB, Jain N, Wang RY, Ashley DL, Watson CH. Levels of tobacco-specific nitrosamines and polycyclic aromatic hydrocarbons in mainstream smoke from different tobacco varieties. Cancer Epidemiol Biomarkers Prev. 2008;17(12):3366-71. doi: 10.1158/1055-9965.EPI-08-0320. PubMed PMID: 19064552.